Trinity College Dublin
Coláiste na Tríonóide, Baile Átha Cliath
The University of Dublin

Platinum Group Elements in Ireland and Northern Ireland: a regional survey of Palaeogene magmatism

Thesis Dissertation for Master of Science
School of Natural Sciences
Department of Geology

by

Anna Morrison

2025
Trinity College Dublin, the University of Dublin

Advisory Panel
Dr. Michael J. Stock, Supervisor

David Chew, Internal Panel Member
Jake Ciborowski, External Panel Member

Declaration

I declare that this thesis has not been submitted as an exercise for a degree at this or any other university and it is entirely my own work.

I agree to deposit this thesis in the University's open access institutional repository or allow the library to do so on my behalf, subject to Irish Copyright Legislation and Trinity College Library conditions of use and acknowledgement.

Anna Morrison

Acknowledgements

I would like to thank my supervisors, without whom this research would not have been possible. Firstly, I would like to thank Mike Stock for his guidance and mentoring throughout my time in Trinity. Mike has provided expert knowledge on the project as well as pushing me to develop the critical skills needed to transition to industry and grow as a researcher. His encouragement, patience, and insightful feedback have been invaluable throughout every stage of this project.

My co-supervisors, Mark Cooper and Jens Andersen have been extremely generous with their time and knowledge. Both dedicated significant efforts into training me on different aspects of the project, from fieldwork to lab work and all in between. Time in Camborne School of Mines with Jens really opened up my eyes to the world of exploration geology which was invaluable to my research. Additionally, thank you to all my other coauthors for their expertise and support throughout the project: Elliot, Hannah, Jack and Paul.

I would also like to thank the staff at the ESRL and the Geology technicians: Hilde, Clara, Sarah and Maura. They were extremely helpful in guiding me through different methods of sample preparation and analysis, and always patient and accommodating with my never-ending batch of samples.

A special thanks to the other PhD students in the Geology Department, who created a supportive and social atmosphere—one where ideas, emotions, and even the occasional gripe could be shared openly. It made the experience both productive and enjoyable.

Finally, I would like to acknowledge the support of my mum and dad, who throughout my time at Trinity were always there for me no matter how big or small the issue. Their unwavering belief in me carried me through the challenges and reminded me to find joy in the journey. Lastly, a big thank you to my girlfriend Bláithín, who played a vital role in my support system, always believing in me even when I was doubting myself.

FUNDING

This work was supported by a Masters by Research grant co-funded Geological Survey of Ireland and the Department for the Economy Northern Ireland, and a Trinity College Dublin Foundation Scholarship.

Abstract

Platinum Group Elements (PGE) play an essential role in green technologies, which are vital to achieving the Green Transition. They are currently classed as 'Critical Raw Materials' (CRM) due to concerns over the security of their continued supply. Therefore, innovative research is required to identify new deposits and fertile areas, strengthening Europe's endogenous supply of PGE.

Palaeogene igneous intrusions in the United Kingdom and Ireland have been identified as prospective areas for Ni-Cu-PGE exploration within Europe. Mafic Irish intrusions have been subject to PGE exploration since the ~1980s, but the fertility of the mantle feeding volcanism has not been directly verified. Their prospectivity is largely based on extrapolations from genetically related Scottish intrusions within the British and Irish Palaeogene Igneous Province (BIPIP).

This project will place the first direct constraints on PGE enrichment in the lithospheric mantle beneath Palaeogene mafic and ultramafic intrusions in Northern Ireland and Ireland. A key component of the study is the extension and refinement of digital maps of regional Palaeogene dyke swarms, which aids understanding of conduit networks and mineralisation potential. The results of this study will contribute to the understanding of mantle processes during Palaeogene North Atlantic rifting and produce a comprehensive, open-access geochemical data set of PGE abundances in Northern Irish and Irish mafic rocks. Integration of this dataset with other deposits within the North Atlantic Igneous Province (NAIP) will help to de-risk future Ni-Cu-PGE exploration efforts.

Initial findings confirm elevated PGE abundances (>MORB) and variable sulphide saturation histories, reflecting complex mantle processes within the proto-Icelandic plume. Variable Pt/Pd ratios provides evidence of the Northern Irish and Irish sector of the BIPIP as a transitional zone within the NAIP, reflecting changing geodynamic environments and plume conditions within a brief period. Our data also suggest the transitional geochemical signature within the BIPIP may be related to the cumulative effects of an evolving plume environment and proximity of melt generation to sub-continental lithospheric mantle. Extended dyke mapping enhanced understanding of the origins of radial swarms, with potential onshore and offshore origins in central igneous complexes.

This study presents a foundation for future PGE exploration in Northern Ireland and Ireland and contributes valuable data towards understanding plume dynamics and prospective mineralising zones.

TABLE OF CONTENTS

List of Abbreviations

ALG	Antrim Lava Group
BIPIP	British and Irish Igneous Province
IPGE	Iridium Group PGEs
LIP	Large Igneous Province
Ma	Million years
NAIP	North Atlantic Igneous Province
Ni-Cu-PGE	Nickel-Copper-Platinum Group Element
PGE	Platinum Group Elements
PPGE	Platinum Group PGEs
SCLM	Sub-Continental Lithospheric Mantle

List of Figures

Chapter 1

1. Introduction

1.1. Overview

The North Atlantic Igneous Province (NAIP) has been highlighted as one of the most prospective regions in Europe for Ni-Cu-PGE mineralisation. The British and Irish Paleogene Igneous Province (BIPIP) constitutes an early phase of magmatism within the NAIP. Recent studies have highlighted favourable conditions for PGE mineralisation within the BIPIP, however research has focused on the Hebridean portion of the BIPIP and extrapolated across to Ireland. No direct constrains on the fertility of the Irish mantle with respect to PGE have been made. This study addresses this critical knowledge gap, necessary to inform exploration strategies.

The aim of this research project was to produce a comprehensive geochemical survey of Irish and Northern Irish Palaeogene igneous rocks. It has placed the first direct constraints on the Platinum Group Element (PGE) abundance of the lithospheric mantle feeding intrusions between 61 and 55 million years ago (Ma). These constraints play a key role in guiding exploration efforts, evaluating the mineralisation potential of the region, and improving our understanding of mantle dynamics during this period. Producing an open-access geochemical dataset for Palaeogene deposits enables investigation of the spatiotemporal relationships within the BIPIP, and the wider NAIP. To complement the geochemical analyses, we extended previous digital maps of Palaeogene dyke swarms. These pervasive swarms, characteristic of magmatic activity in Northern Ireland and Ireland, are linked to the decompressional forces of the proto-Icelandic mantle plume. Seven radial dyke swarms have been mapped across the region, providing insight into their origins, propagation, and potential mineralisation pathways.

This study plays a part in the wider Critical Ireland research group—a Science Foundation Ireland-funded project focused on understanding Critical Raw Materials (CRM) in magmatic systems. Related projects examine crustal assimilation and its control on sulphide saturation in Irish intrusions, investigating the associated chemical processes. In contrast, this study centres on verifying the original PGE fertility of the mantle source feeding these intrusions. By addressing key geochemical questions, it contributes to the broader objectives of Critical Ireland and offers findings of direct relevance to its researchers.

The following chapters present the context and exploration history of PGE and their deposits (Chapter 2), research aims and objectives (Chapter 3), methods (Chapter 4), and summary and conclusions (Chapter 6). Chapter 5 comprises a manuscript under review for publication in *Lithos*, presenting original research on the geochemical characteristics of dykes, lava flows, and minor intrusions from the Northern Irish and Irish sectors of the BIPIP. The overarching aim of this work is to evaluate the PGE mineralisation potential, petrogenesis, and geodynamic setting of these magmatic systems.

CHAPTER 2

2. Literature Review

2.1. Platinum Group Elements

Platinum Group Elements are a commodity that is steadily increasing in demand, largely due to their use in novel 'Green Technologies', e.g., hydrogen fuel cells, catalytic converters and chemical process catalysts (Mudd, 2012b, Mudd et al., 2018). They are currently categorised as critical raw materials (CRM) due to the security of their supply and their high economic importance (Fig. 1; Moore et al., 2016, European Commission, 2017). Developing a sustainable supply of raw materials within the European Union (EU) has been emphasised to ensure the production of everyday goods and services, but also for the development of emerging technologies and innovations (European Commission, 2017). This would reduce Europe's reliance on mineral imports and help inform policies that safeguard economic growth and competitiveness from material shortages or supply bottlenecks. The EU *Critical Raw Materials Act* seeks (European Commission, 2020) to ensure that European markets can rely on strong, resilient, and sustainable value chains for CRM.

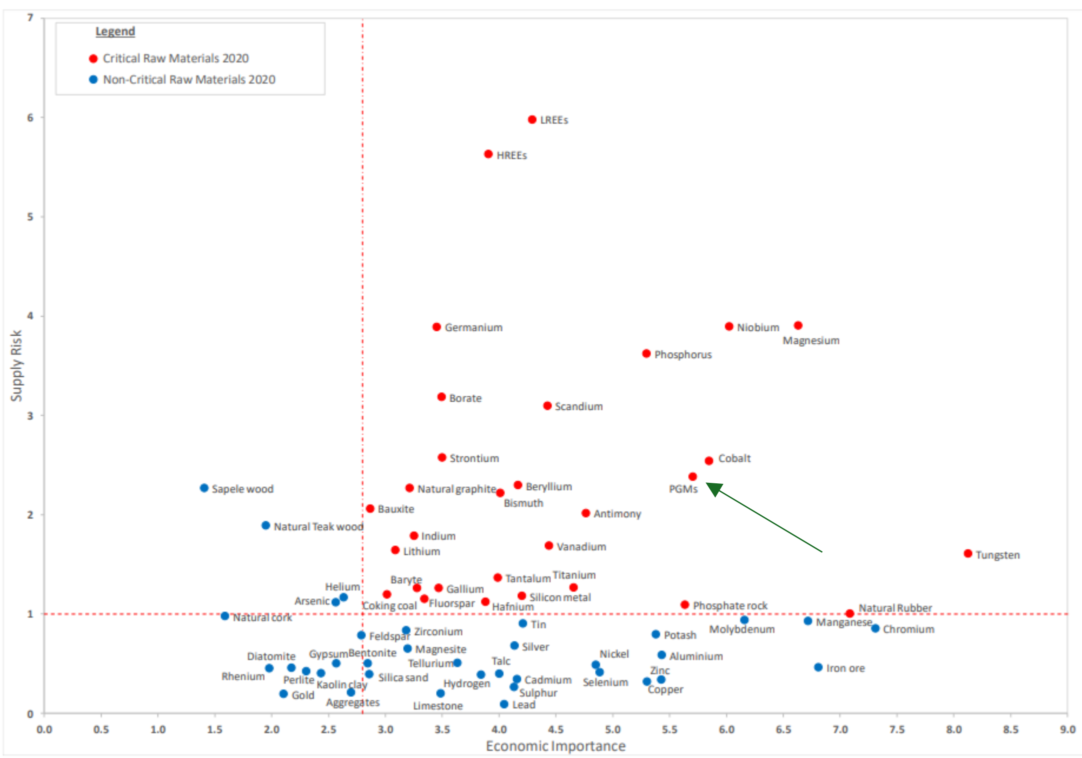

Figure 1 Results of the 2020 Criticality Assessment, highlighting economic importance and supply risk. Critical raw materials are designated by red dots and are located within the criticality zone (SR ≥ 1 and EI ≥ 2.8) of the graph. Blue dots represent the non-critical raw materials. PGE appears as PGM – Platinum Group Metals, ~5.75 Economic Importance and ~2.2 Supply risk (Green arrow points to PGM position). Figure from the European Commission (2020).

Within the *Critical Raw Materials Act,* measures are taken to improve the collection of CRM-rich waste and facilitate its recycling into secondary CRM. In Ireland, the importance of PGE (Pt, Pd, Rh, Ru, Ir, Os) was reiterated in the 2022 Policy statement on Mineral Exploration and Mining (Government of Ireland, 2022), where PGE are recognised as CRM and necessary for the transition to a circular economy. However, improving circularity and recycling efficiency will not be enough to sustain technological and population growth. Moore et al. (2016) emphasise that the shortage in CRM cannot fully be offset by recycling alone due to factors such as the dispersion of critical metals in the environment and manufacturing designs that inhibit separation, e.g., alloying. Therefore, we must continue to work strategically to diversify the EU's supplies.

2.1.1. Critical Raw Materials

Recent studies reveal that social, environmental, political, and economic factors will be the main drivers of mineral scarcity, supply bottlenecks, and economic criticality in the coming decade (Mudd 2012a; 2012b, Mudd et al., 2018). Studies suggest there are enough geological reserves and mineable quantities of PGE globally, to sustain a growing population (European Commission, 2024). Their classification as *Critical Metals* is related to supply chain reliability, not resource depletion. For example, Russia currently controls 46% of the global Pd supply; however, a history of geopolitical issues poses a threat to continued supply. Furthermore, South Africa dominates global Pt production (70%), but social challenges post-apartheid raises concerns about the sustainability and ethical integrity of extraction, which are essential to achieving the Sustainable Development Goals (SDGs) (Mudd, 2012a, White Paper, 2016, European Commission, 2017, Responsible Mining Foundation & Investment, 2020).

To secure a transition to a greener economy and effectively address climate change, research must focus on locating European deposits of CRM, particularly PGE. As demand for PGE continues to grow, it is essential to address the underlying challenges through improved exploration strategies—an area this work aims to support. CRM will be fundamental to the energy transition, and production from Ireland’s domestic resources could enhance supply security (Stephenson et al., 2023). Ireland’s diverse geology offers multiple environments where critical metals may be concentrated, making it essential to capitalise on these rich natural resources (Lusty, 2016, Gunn et al., 2020).

2.2.2. Indicators of Mantle Processes

Mantle-derived rocks preserve critical information on the behaviour of PGE during key processes such as melting, metasomatism, sulphide saturation, and fractionation (Maier et al., 2003, Maier and Groves, 2011, Barnes and Ripley, 2016, Singh et al., 2018). By applying PGE systematics, this study aims to enhance our understanding of mantle processes during the Palaeogene period.

PGE can be divided into two contrasting groups: the high-temperature Iridium group PGE (IPGE) (Ir, Os, Ru), which are primarily siderophile and refractory, while the lower temperature Platinum group PGE (PPGE) (Pt, Pd and Rh) are primarily chalcophile and volatile. These characteristics serve as effective geochemical tracers, making them ideal markers of magmatic processes and source dynamics (Hughes et al., 2015b, Singh et al., 2018, Lindsay et al., 2021). Significant fractionation between IPGE and PPGE can be used as a proxy for the extent of mantle melting. During partial melting, the first phases to melt include sulphides, garnet, and clinopyroxene. PPGEs are primarily hosted in Cu-rich and base metal sulphides, which are mobilised early in the melt. In contrast, IPGEs are commonly bound in Fe-rich monosulphide solid solution or refractory metal alloys, which are more stable at high temperatures and remain in the mantle residue until sulphides are fully exhausted (Maier, 2003, Barnes et al., 1985). As a result, the initial Pd/Ir ratio of the melt will be high. However, continued partial melting introduces IPGE-bearing alloys, lowering the Pd/Ir ratio of subsequent melts (Hughes et al., 2015b). Increasing concentrations of IPGE indicate higher degrees of partial melting have been achieved and have been linked to extensive magmatic volumes produced, such as those of the NAIP.

Furthermore, Barnes et al. (2015) stress a predominant control on the abundance of PGE in magmas is their interaction with these magmatic sulphide liquids. The partition coefficient of PGE from a silicate magma into a sulphide liquid is extremely high, meaning that the retention of sulphide liquids in the mantle source region exerts a critical control on the PGE concentration of resulting melts (Barnes et al., 2016). The *'All or Nothing'* model suggests that even the smallest concentration of residual sulphides in the melting region is sufficient to retain PGE at the source and produce a strong PGE depletion in ascending magmas (Barnes et al., 2015, 2016). Therefore, marked depletion of all PGE may result from the retention of PGE-hosting sulphides in the mantle, a consequence of limited or heterogeneous partial melting.

Additionally, studies have used Pt/Pd ratios to investigate the changing geodynamic environment over the lifetime of the proto-Icelandic mantle plume (Hughes et al., 2015b, Lindsay et al., 2021). A systematic change in the Pt/Pd ratios of otherwise equivalent flood basalts within the NAIP has sparked debate about the contribution of subcontinental lithospheric mantle (SCLM) on ascending plume magmas. Early formed deposits in West Greenland and the BIPIP exhibit higher Pt/Pd ratios, close to chondritic values (1.9), while later basalts of the seaward dipping reflector series (offshore East Greenland) and Iceland, and trend towards lower ratios (0.4-0.8; Hughes et al., 2015b, Lindsay et al., 2021).

Platinum and Pd have similar partition coefficients into sulphide liquids and therefore are not significantly fractionated during plume-driven magma ascent (Singh et al., 2018). The systematic change in Pt/Pd ratios has been evoked to represent the changing geodynamic environment of the plume throughout its lifetime and the contaminating effect of SCLM on early plume magmas (Griffin et al., 2013). The earliest magmas were generated from the inception of the plume at the base of the lithosphere, underneath the North Atlantic Craton. The theory suggests that parental magmas intruded at cratonic edge blocks could mobilise sulphides from enriched continental roots – preconditioned with elevated Pt concentrations by ancient metasomatic processes. The precious metal budget, specifically magmas enriched in Pt relative to Pd, may be linked to the contribution of, and proximity to, fusible SCLM interacting with plume-generated melts. Later flood basalts, formed during the opening of the North Atlantic, were generated from shallower plume material in cooling conditions, at diverging plate margins (Lindsay et al., 2021, Carter et al., 2024). They are associated with lower degrees of partial melting than deep, early formed melts within the plume head. The initial concentration of PGE in the source region is a key factor in where an orthomagmatic Ni-Cu-PGE deposit may form; therefore, deep plume sources, close to pre-conditioned SCLM impose a geochemical and geophysical constraint on the mineralisation potential of a plume across its lifespan.

This project presents an opportunity to further investigate Pt/Pd ratios within the NAIP and compare deposits within the BIPIP. Palaeogene igneous activity in Ireland spanned ~5 Ma (Cooper and Tapster, 2025), providing an exciting opportunity to examine the effects of changing plume dynamics on the precious metal budget of Irish and Northern Irish deposits.

2.2. Mineralisation and Exploration

Large Igneous Provinces (LIP) are increasingly reported as the choice environment for Ni-Cu-PGE mineralisation (Williamson and Saumur, 2019). Most of the world's Pt is supplied by the Bushveld Complex, which has a spatiotemporal link with the Phalaborwa carbonatite system (2.05 Ga; Chen et al., 2025). Additionally, the majority of Pd is produced in Norilsk, a conduit-hosted Ni-Cu-PGE mineralised system associated with the Siberian Traps (252 Ma; Barnes and Ripley, 2016, Barnes et al., 2019). Ore formation in Norilsk is coeval with LIP magmatism, and relatively early in the sequence (Barnes et al., 2016). This is encouraging for mineralisation within the NAIP and especially the BIPIP, as the bulk of BIPIP magmatism represents an early manifestation of LIP's formation. Nevertheless, currently all known economic PGE deposits were formed more than 1.8 Ga; only one potentially economic deposit is younger than this – Skaergaard (Maier and Groves, 2011). The Skaergaard complex, which formed in association with the opening of the North Atlantic (56.02 Ma; Holness et. al, 2024), presents an exciting opportunity for further mineralisation in the Palaeogene.

2.2.1. Deposit Formation

The origins of PGE mineralisation remain controversial as there is no universal model applicable to deposits, and diverse mineralisation styles and triggers have been found. Despite no unifying model, there is agreement that the overarching criteria for a mineralised PGE deposit to form is a mantle source that is enriched in PGE (Maier, 2005). Fertile mantle has approximately chondritic proportions of PGE (Lorand et al., 2008, Hughes et al., 2015b); however, for partial melts to become enriched in PGE, all sulphide phases at the source must be completely exhausted to ensure no PGE-bearing phases are retained in the residue. As noted earlier, PGE are chalcophile and partition strongly into sulphide phases over silicate magma. To concentrate PGE in the melt, melt fractions must continue to the point of sulphide exhaustion (F = ~13.5%). If partial melting in the magma source exceeds this threshold, PGE concentrations may become diluted due to the contribution of silicate melt, which offers little to no PGEs to the mantle-derived metal budget (Hughes et al., 2016b).

There are several mineralisation styles for PGE deposits, which makes the criteria for exploration difficult. Some models explain ore deposit formation via the entrainment of a PGE-rich immiscible sulphide liquid by the ascending mantle plume (Hughes et al., 2015a, Hughes et al., 2015b), via gravitational sinking and settling in a passive cooling or stationary environment, or when magma withdrawal is taking place (Hughes et al., 2016a). Another model explains the concentration of precious metals and PGE via extensive *in situ* fractionation of bulk melt. This is the model responsible for the Skaergaard deposit (Nielsen et al., 2015) - describing the transport of PGE through a migrating mush melt.

Another key requirement in the formation of mineralised deposits is a high R factor within the magmatic system. The R-factor is the mass ratio of silicate melt interacting with sulphide liquid – the mass of magma exchanging chalcophile elements with the sulphide liquid before emplacement. It is a significant constraint on the potential to produce mineralised economic deposits, especially in the sulphide sinking or entrainment models. They require large volumes of silicate magma to interact with immiscible sulphide liquid to upgrade the sulphide tenor. In contrast, *in situ* fractionation can generate PGE-rich sulphides with significantly lower R-factors, as enrichment occurs through progressive crystallisation and internal differentiation of sulphide liquid rather than extensive silicate–sulphide interaction (Nielsen et al., 2015).

The type of deposit investigated in this study is a magmatic Ni–Cu–PGE sulphide system, typically hosted within long-lived magma conduits fed by high-degree partial melts of the mantle (Barnes et al., 2016). In such deposits, PGE occur as accessory components concentrated within the sulphide assemblage associated with Ni–Cu mineralisation.

2.2.2. Exploration within Europe

Strategic exploration for PGE deposits in Europe has been ongoing over the decades; however, recent initiatives related to the EU *Critical Raw Materials* Act (European Commission, 2020) have incentivised increased efforts across the continent. Economic concentrations of PGE have been reported in the Skaergaard intrusion of East Greenland (Nielsen et al., 2015). The stratabound PGE-rich zone, known as the Platinova Reefs, is projected to contain over 280 million tonnes of Pd ore at 1.97 ppm and 91 million tonnes of Au ore at 1.8 ppm (Andersen et al., 2000). Furthermore, the Edvard Kap Holm complex in East Greenland also exhibits stratiform layering with PGE±Au mineralisation (Arnason and Bird, 2000, Andersen et al., 2000). In Russia, the Norilsk region dominates Pd production, as a byproduct of Ni mining. These Ni deposits occur in three sub-volcanic intrusions: Norilsk 1, Talnakh and Kharaelakh (Barnes and Ripley, 2016). Additionally, recent work by the Geological Survey of Finland (Makkonen et al., 2017) highlights the potential for Ni sulphide deposits as important sources of Cu, Co and PGE in mafic-ultramafic layered intrusions in north Finland. The Ni grade is expected to be too low for economic purposes; however, their main target within their exploration program is PGE.

Within the United Kingdom, PGE exploration is also associated with mafic-ultramafic central igneous complexes. Mineralisation associated with chromite layers within Mull, Rum and Skye has been documented, however, at sub-economic concentrations at present (Andersen et al., 2000, Hughes et al., 2016a). The Rum complex hosts the richest PGE occurrences in the province, particularly abundant in Eastern layered series. Additionally, evidence of sulphide-hosted PGE mineralisation has been documented in ultramafic plugs on the Isle of Rum and disseminated mineralisation in cross-cutting sulphide-rich dykes (Power et al., 2003).

Diverse PGE mineralisation styles within Europe represent a variety of mineralogical associations and highlight the importance of innovative approaches to exploration. The variety of mineralisation in Scotland has highlighted favourable conditions for PGE mineralisation in genetically related deposits in Ireland and Northern Ireland. This study surveys Palaeogene mafic intrusions to set a foundation for further strategic exploration for PGE.

2.2.3. Exploration within Ireland

Limited PGE exploration has taken place in the last decade in Ireland and Northern Ireland with varying degrees of success. The Carlingford complex was explored in the 1990s by BHP, sparked by the discovery of a 'float boulder' containing ~5 wt% Cu, 1.5 ppm Pt and 15.5 ppm Pd (Hurst, 1997). Following this, Irish Base Metal and Ennex conducted a magnetic survey and bore holes were drilled to target the base layer of mineralisation (Buchanan, 1985). The bore holes did not reach the target horizon at the base of the intrusion, and preliminary assay data suggested a low-grade PGE potential. Despite this, Hurst (1997) maintains there is still potential for further exploration. Recent exploration by Group Eleven (Group Eleven Corp., 2020) identified a sulphide-bearing dyke with anomalously high Pt, Pd and Rh. The dyke, which intersected drilling at Ballinalack Zinc Project, Co. Westmeath, is suggested to be laterally extensive. Group Eleven concluded the intercepts were likely 'rip-up' clasts from a larger sulphide body (Group Eleven Corp., 2020), but that the data is encouraging for future conduit exploration targets.

The Tellus geochemical and geophysical surveys (Geological Survey of Ireland (2022) and Geological Survey of Northern Ireland (2005)) have provided valuable data to supplement ongoing exploration activities. The Tellus survey has been integral in identifying potential mineralised areas; within Northern Ireland, the ALG and its associated feeder intrusions have been highlighted as one of the most prospective areas for PGE mineralisation based on Pd and Pt soil anomaly results (Lusty, 2016), and critical metal (REE, Nb, U) anomalies have been identified in the Mourne Mountains too (Moore et al., 2023).

This study presents a significant opportunity to evaluate mineralisation potential while also investigating potential mineralised regions using innovative monitoring techniques. Tellus data is utilised in this study to enhance regional mapping of Palaeogene dykes and intrusions, and to correlate PGE anomalies identified in soil and stream samples with lithological data from rock samples collected during the investigation.

CHAPTER 3

3. Research Objectives

3.1. Aims

The aim of this study is to produce the first comprehensive survey of PGE abundance in Palaeogene igneous intrusions across Northern Ireland and Ireland. The research also seeks to compare Northern Irish and Irish deposits with well-studied Scottish BIPIP intrusions, and the broader NAIP to better understand their geochemical and geodynamic relationships. In addition, the project aims to investigate regional dyke propagation networks to better understand conduit pathways and origin zones.

3.2. Objectives

The objectives of this research are:

1. Compile and analyse new and existing PGE data from Northern Irish and Irish Palaeogene deposits. Conduct whole-rock major and trace element geochemical analyses.

    Hypothesis (H)1: The PGE abundances in Northern Irish and Irish deposits will be elevated above mantle (MORB) concentrations.

    H2: The most mafic samples will have the highest PGE abundances.

    H3: Older deposits will have elevated Pt/Pd ratios compared to younger deposits.

2. Compare geochemical data from this study with published data on the NAIP to investigate the spatial and temporal relationship of plume-driven deposits.

    H4: Northern Irish and Irish deposits will be geochemically similar to Scottish deposits, as well as early formed Greenlandic volcanics.

    H5: The Pt/Pd ratios of Irish and Northern Irish deposits will be close to chondritic.

3. Digitally map and interpret the spatial distribution of Palaeogene dykes, using the updated Tellus geophysical survey data (2022).

H6: The origin of at least one of the dyke swarms emplaced in Northern Ireland and Ireland originates offshore.

H7: There will be a much greater density of dykes on the west Coast of Ireland than currently mapped.

CHAPTER 4

4. Materials and Methods

4.1. Sample Collection

Samples of putative magmatic 'liquids' (i.e. lavas and dykes, rather than cumulates) were collected from across Northern Ireland and Ireland for geochemical analysis, targeting finer grained doleritic or basaltic samples. In total, sixty-seven dyke and minor intrusion samples were collated for geochemical analysis, and fifty-five samples were analysed for PGE. Geochemical data from twenty-six samples of the Lower Basalt Formation (ALG) were also included in the compilation. The Northern Irish extrusive lava data complements the analysis of intrusive Irish and Northern Irish samples for PGE, and wider comparison with BIPIP and NAIP lavas.

4.1.1. Archival Samples

We compiled the majority of our samples from archival collections. Twenty-eight samples were provided by the Geological Survey of Northern Ireland (GSNI), courtesy of Dr Mark Cooper. Samples were collected across various field campaigns between 2013-2014. A representative subset of samples was chosen from the GSNI archive according to geochemical and spatial thresholds. Samples were selected based on mafic composition - containing 7–12 wt% MgO, to ensure representative mafic characteristics while minimizing the effects of olivine accumulation. Additionally, the selection included a representative spread from all mapped dyke swarms to ensure regional-scale compositional patterns were accounted for.

Furthermore, an archival collection in the University of Galway provided four samples from the west Connacht dyke system, originally collected in the 1980s. Samples were kindly provided by Dr Paul Mohr, whose original mapping of the west Connacht dyke systems informed most of our field strategy. These samples complemented our fieldwork by covering inaccessible regions and offshore localities beyond our reach. Three samples from exploration drill cores in Co. Monaghan and Co. Armagh were donated by Conroy Gold, collected from their drill store archive in 2023. These cores intersected mafic dykes within their licence area and served to supplement our dataset in the border region. Finally, three samples from the cone sheets in Carlingford, representing late-stage mafic injections within a central complex, were generously provided by Jack Beckwith, a PhD candidate at Trinity College, from his fieldwork in 2022. Basalt samples from the ALG were produced through a partnership between Cardiff University and Lonmin plc., as part of an exploration programme in 2013.

4.1.2. Fieldwork

To supplement our archival samples, most of which were in Northern Ireland, we carried out ten days of fieldwork along the west coast of Ireland. We collected over thirty-six samples from fieldwork and twenty-nine were used for geochemical analysis. Sample locations were planned and selected according to literature maps of Palaeogene dykes (Preston, 1967, Coe, 1969, Morris, 1974, Mohr, 1982, Mohr, 1987, Mohr, 1988, Pracht et al., 1996, Long et al., 1999, Kirstein and Timmerman, 2000, Mohr, 2000, Mohr et al., 2018). Field investigations spanned six counties: Cork, Kerry, Galway, Mayo, Sligo, and Donegal. Sample locations were chosen to ensure representative sampling according to published location and characteristics. At each sample location, approximately 500g of sample were removed, where possible, both margin and core samples were taken from the outcrop, with marginal samples considered for PGE analysis.

4.2. Dyke Mapping

An extended map of regional dyke swarms was produced following the methodology of Anderson et al. (2016), (2018). We used the updated database of the Tellus Geophysical survey (Geological Survey of Ireland, 2022). High concentrations of magnetic minerals, e.g., magnetite, in the igneous rocks produce strong magnetic susceptibility, evident in aeromagnetic surveys. The study applies a geoTIFF of First Vertical Derivative of the Reduced to Pole Total Magnetic Intensity anomaly field to constrain the locations of dyke-related features. Using QGIS, the dykes were digitised as polylines by tracing magnetic anomalies and ascribed a swarm according to orientation and location. This generated an extended database of georeferenced polylines, building upon the work in Anderson et al. (2016, 2018). At the current resolution, individual dyke-related anomalies may reflect the cumulative effect of multiple overlapping dykes rather than a single outcropping feature.

4.3. Geochemical Analysis

Weathered material was cut from each sample before being crushed to a fine gravel (2mm) and if present, amygdales and filled vesicles were hand-picked and removed from crushed samples. The samples were crushed in a Tungsten Carbide Jaw Crusher and milled in an Agate Powder Mill to 95% passing 105µm. Loss on Ignition (LOI) for all dykes and minor intrusions was determined gravimetrically by heating at 1000°C for one hour. For ALG samples, LOI was measured using ~1.5 ± 0.0001g of sample powder baked at 900°C in a Vecstar Furnace for 2 hours. Mg# was calculated following the method of Neave and Putirka (2017).

4.3.1. Major and Trace Elements

Total sulphur for west coast of Ireland samples was measured using an Analytik Jena multi-EA 40000 instrument (sample weight 0.25g. Accuracy and precision were constrained to -10% and 2% respectively, determined from repeat analysis of reference material 2648c (NIST, 2014).

The major and trace element compositions of west coast of Ireland dyke powders were analysed at the Earth Surface Research Laboratory, Trinity College Dublin, Ireland, using a Panalytical Zetium wavelength dispersive X-ray Fluorescence (XRF) spectrometer, on fused beads and pressed powder pellets, respectively. Sample preparation and analysis followed the method of Carter et al. (2024). For major elements, relative accuracy was -6.1% and precision <0.5%, constrained by analysis of the certified international reference materials GSJ JB-1b, JB-3a and JBb-1. For trace elements, relative accuracy was 19% and precision 17%, based on analysis of certified reference materials GSJ JA-1a, JA-2 and JB-2a.

Dyke samples collected by the Geological Survey of Northern Ireland were analysed by the Centre for Environmental Geochemistry, Nottingham, United Kingdom. Trace elements were analysed by sodium peroxide fusion and Inductively Coupled Plasma Mass Spectrometry (ICP-MS), and major elements analysed by Wavelength Dispersive-XRF on fused glass beads. For major element oxides, the analytical uncertainty over the full concentration range was estimated to be between 0.006% and 1.12% (relative uncertainty). Analytical accuracy for trace elements was assessed using BCR-2 certified reference material, for which expanded uncertainties (mg/kg, ppm) were supplied. For ALG samples, major and minor elements and Sc were measured at the School of Earth and Environmental Sciences, Cardiff, Wales, United Kingdom, using a JY-Horiba Ultima 2 Inductively Coupled Plasma Optical Emission Spectrometry (ICP-OES). Minor, trace and the rare earth elements were measured using a thermoelemental X series (X7) ICP-MS following methods described by McDonald and Viljoen (2006). Standard reference materials JB1a, JP1 and MRG1 were employed to constrain accuracy for majors, minor and trace elements.

4.3.2. Platinum Group Elements

Platinum group element and Au analyses for all dyke samples and minor intrusions were undertaken using Ni-S fire assay (sample weight 30g) with the sulphide residue dissolved, diluted, and analysed by ICP-MS. Analysis was carried out by Activation Laboratories Ltd., Canada, following the method of Hoffman and Dunn (2002). Analytical and preparation accuracy and reproducibility (including potential nugget effects) were assessed following the procedure of Passmore (2009). In general, accuracy was ~2% and precision was 5% based on repeat analysis of AMIS 0498 and OREAS 13b (AMIS, 2017; Ore Research & Exploration PTY Ltd, 2009), with potential nugget effects determined to be minor. Additionally, ALG samples were also analysed for PGE+Au by Fire Assay and ICP-MS, at the School of Earth and Environmental Sciences, Cardiff University, Wales, United Kingdom (sample weight 15g).

Chapter 5

5. Platinum Group Element Systematics in the North Atlantic Igneous Province: new insights from Northern Irish and Irish magmatism

This manuscript has been reviewed by Mike Stock and is intended to be submitted to *Lithos* for publication, following further review by coauthors.

Anna O. Morrison[1], Michael J. Stock[1 *], Mark R. Cooper[2], Jens C. Ø. Andersen [3], Hannah S.R. Hughes[3], Elliot J. Carter[4], Jack Beckwith[1], Andrew C. Kerr[5], Iain McDonald[5], Paul Mohr[6]

[1]Discipline of Geology, School of Natural Sciences, Trinity College Dublin, Dublin, Ireland

[2]Geological Survey of Northern Ireland, British Geological Survey, Belfast, UK

[3]Camborne School of Mines, University of Exeter, Falmouth, UK

[4]School of Geography, Geology and the Environment, Keele University, Keele, UK

[5]School of Earth and Environmental Sciences, Cardiff University, Cardiff, UK

[6] Department of Geology, University of Galway, Galway, Ireland

*Corresponding: Michael.Stock@tcd.ie

Key Words*:* North Atlantic Igneous Province, British and Irish Palaeogene Igneous Province, Icelandic plume, Platinum Group Elements, Dykes

5.1. Abstract

The North Atlantic Igneous Province (NAIP) is one of the most prospective regions for Ni-Cu-Platinum Group Element (PGE) mineralisation in Europe, and recent studies have found elevated PGE concentrations within its early lavas and minor intrusions comprising the British and Irish Palaeogene Igneous Province (BIPIP). This study presents an extended digital map of the regional mafic dyke swarms associated with the Northern Irish and Irish sector of the BIPIP and a comprehensive new geochemical dataset of these magma conduits, the Antrim Lava Group and associated minor intrusions, including PGE±Au analyses. Digital mapping using aerial electromagnetic data reveals a high density of dyke-related anomalies in the northwest and west of the island of Ireland. Dyke density and orientation point towards at least one swarm originating from an onshore Palaeogene igneous centre (Slieve Gullion, Carlingford, possibly Dromore High), with others likely propagate from submarine present-day igneous centres in the North Atlantic. The origins and evolution of dyke swarms provide context for interpreting variations in PGE abundances. Previous authors have highlighted that early NAIP magmatism (e.g., Greenland and Scotland) had high Pt/Pd ratios (~1.9), while younger sequences (e.g., Iceland) tend towards lower ratios (~0.4). Our data reveal Northern Irish and Irish BIPIP centres record this transition with an average Pt/Pd ratio of 1.6±0.8, reflecting an evolving geodynamic setting where the magmatic conditions transitioned from intra-plate volcanism through to the inception of continental rifting and ocean opening. A close spatiotemporal association between variable Pt/Pd Northern Irish and Irish BIPIP deposits and high Pt/Pd Scottish deposits suggests that the geodynamic transition occurred within a geologically short time interval (<1 Myr). Results from our samples attest to widespread sulphide saturation, supporting the potential for orthomagmatic Ni-Cu-PGE mineralisation within related central complexes or feeder networks.

5.2. Introduction

Platinum Group Elements (PGE) are useful proxies for mantle processes and geodynamic environment, in addition to being classed as critical raw materials, necessary to achieve climate mitigation goals (Mudd et al., 2018). They are ubiquitously siderophilic (Barnes and Ripley, 2016) but can be divided into two groups with different geochemical behaviours: the Platinum group PGEs (PPGE; Pt, Pd and Rh) are mainly hosted in base metal sulphides and the Iridium group PGEs (IPGE; Ir, Os, Ru) form alloys and monosulphide solid solutions (Barnes and Ripley, 2016). Recent studies have highlighted a close association between large igneous provinces (LIP) and PGE mineralisation (e.g., Norilsk-Talnakh, Bushveld; Maier, 2005; Barnes and Mansur, 2022) with LIP-related Ni-Cu-PGE deposits sharing geochemical characteristics that have been attributed to a metasomatic component from the sub-continental lithospheric mantle (SCLM; Griffin et al., 2013; Barnes et al., 2016). This has been suggested to result from parental magmas intruded at cratonic edge blocks mobilising sulphides from enriched continental roots (Chen et al., 2025).

Early NAIP magmatism occurred under conditions conducive to PGE mineralisation (Andersen et al., 2000) and has been subject to PGE exploration since the 1960s (e.g., Skaergaard, Kap Edvard Holm and Rum complex; Andersen et al., 2000; Hughes et al., 2015c; Andersen et al., 2017). Recent studies have shown that metal systematics in the British and Irish Palaeogene Igneous Province (BIPIP), an early manifestation of the NAIP, record contamination of plume-derived magmas by SCLM at margins of the North Atlantic Craton (Hughes et al., 2015b), resulting in enrichment of PPGEs. This pattern is consistent with major global PGE deposits where historic metasomatism during orogenic events can 'precondition' the cratonic SCLM, enriching it in Pt, and influencing the precious metal budget and Pt/Pd ratios of ascending magmas during LIP formation (Griffin et al., 2013). Furthermore, authors have suggested that the NAIP has an inherently high PGE concentration in the mantle source, which is a critical prerequisite to orthomagmatic Ni-Cu-PGE mineralisation (Andersen et al., 2000).

Despite extensive work on the PGE potential and geodynamic evolution of the BIPIP, previous studies have relied strongly on the Hebridean portion of province, extrapolating results to Northern Ireland and Ireland (Hughes, 2015 and references therein); while the major element, trace element and isotopic geochemical behaviour of Northern Irish and Irish BIPIP rocks have been extensively investigated (Mohr, 1988; Andersen et al., 2000; Carter et al., 2024), detailed studies of PGE systematics are sparse and largely limited to industry datasets (Hurst, 1997; Smyth, 2014). This study addresses this knowledge gap by first digitally Palaeogene regional dyke swarms on the island of Ireland using newly available aerial magnetic datasets and then presenting a new geochemical characterisation of these dykes, in addition to the Antrim Lava Group (ALG) and minor intrusions (sills and plugs), including PGE ± Au. We use this data, alongside a literature data compilation, to constrain the mantle petrogenesis, S-saturation processes and PGE mineralisation potential during the evolution of the NAIP.

5.3. Geological Setting

5.3.1. Overview of the North Atlantic Igneous Province

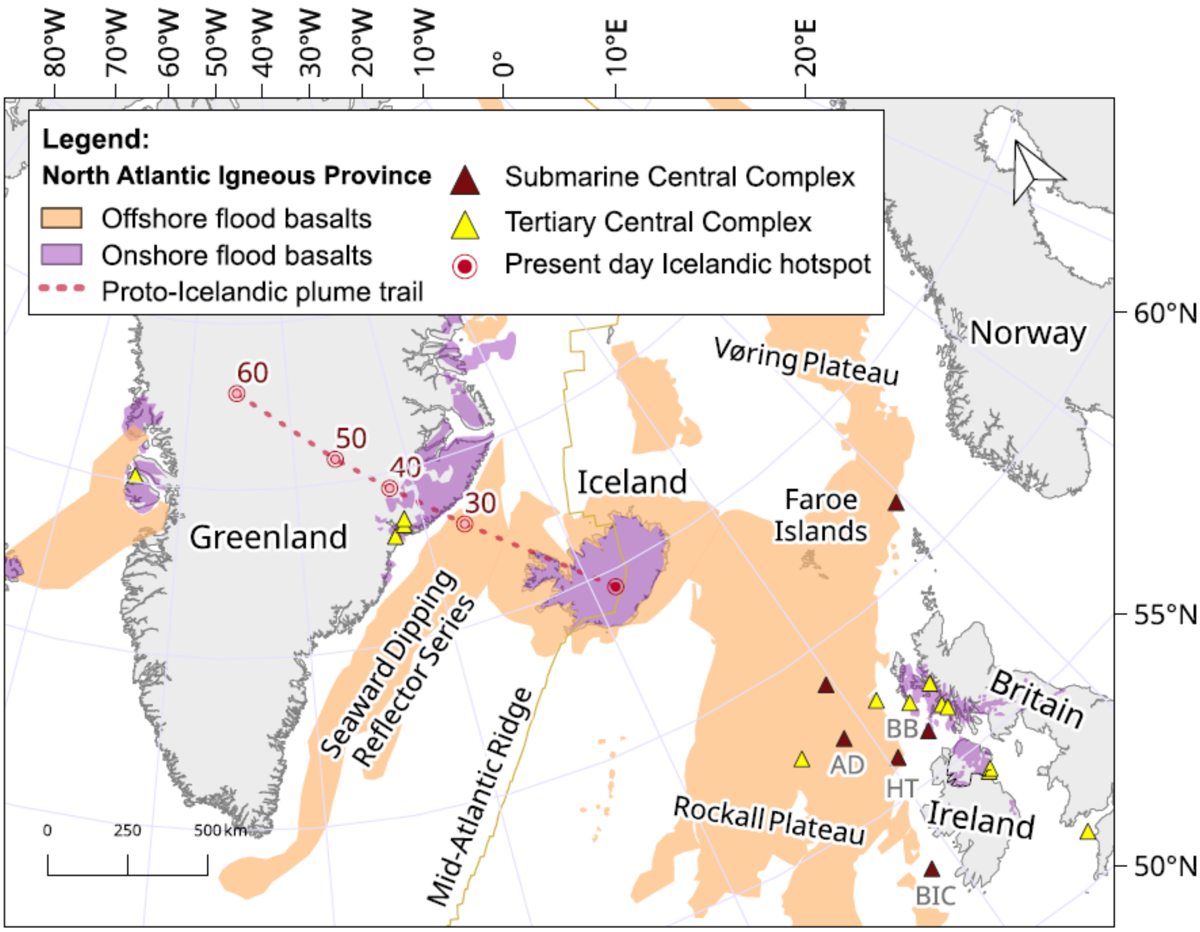

Figure 2 Simplified Geology of the NAIP, including onshore and offshore igneous centres and the hot-spot track of the proto-Icelandic mantle plume. Approximate ages of plume locations are given in red, leading to present-day Iceland. AD = Anton Dohrn, BB = Blackstones Bank, HT = Hebrides Terrace, BIC = Brendan Igneous Centre. Adapted from Mussett et al., 1988, Hughes et al., 2015c, Á Horni et al., 2017.

The NAIP includes volcanic and plutonic magmatism in Greenland, the Faeroe Islands, Britain, Ireland, Iceland and the surrounding offshore, which formed as a result of the (proto-) Icelandic plume impinging on the base of lithosphere (Fig. 2; Saunders et al., 1997), coupled with extension during North Atlantic rifting (Hansen et al., 2009; Wilkinson et al., 2016). Magmatic activity began in the Palaeogene in the present-day western (e.g. Greenland) and eastern (e.g. Britain, Ireland)

Atlantic, with ages broadly converging on modern day Iceland (Fig. 2). Palaeogene magmatism can be divided into two phases with a pre-rift phase at 62–58 Ma, followed by a hiatus at ~57 Ma. A subsequent voluminous syn- and post-rifting phase coincided with the opening of the North Atlantic at ~56–53 Ma (Saunders et al., 1997; Wilkinson et al., 2016). Plume-related volcanism has transitioned from continental to oceanic geodynamic settings throughout the last ~62 Myr (Hughes et al., 2015b).

5.3.2. The British and Irish Palaeogene Igneous Province

Palaeogene igneous rocks in Britain and Ireland comprise the BIPIP and include on- and offshore central igneous complexes, lava flows and regional dyke swarms (Andersen et al., 2000; Kent and Fitton, 2000). The first pulse of BIPIP magmatism occurred at ~61 Ma with the eruption of basaltic lavas into the Hebridean basin and the northeast of Ireland (Mussett et al., 1988; Cooper et al., 2012). The bulk of magmatic activity followed between ~61–59 Ma, marked by the emplacement of large mafic and silicic central complexes (e.g., Mull, Rum, Carlingford, and Slieve Gullion; Chambers and Pringle, 2001), widespread sills and dyke intrusion and effusive lava extrusions (e.g., Skye, Antrim). A second pulse of late-stage dyke emplacement continued until ~58 Ma (Mitchell, 2004). Recent work by Cooper et al. (2020) proposed a third pulse of activity at ~56–56.5 Ma, associated with emplacement of the Mourne Mountains. Analysing BIPIP samples, therefore, presents an opportunity to investigate petrogenetic changes through ~5.5 million years of geodynamically diverse magmatism (Fig. 4e) as the NAIP transitioned from a pre- to syn-rift phase (Saunders et al., 1997). Broadly contemporaneous to this onshore magmatism, offshore magmatism in the North Atlantic generated submarine igneous centres such as the Anton Dohrn, Hebrides Terrace and Blackstones Bank which have not been analysed extensively and are predominantly constrained by geophysical surveys or during dredging expeditions (Ritchie and Kitchen, 1996; O'Connor et al., 2000).

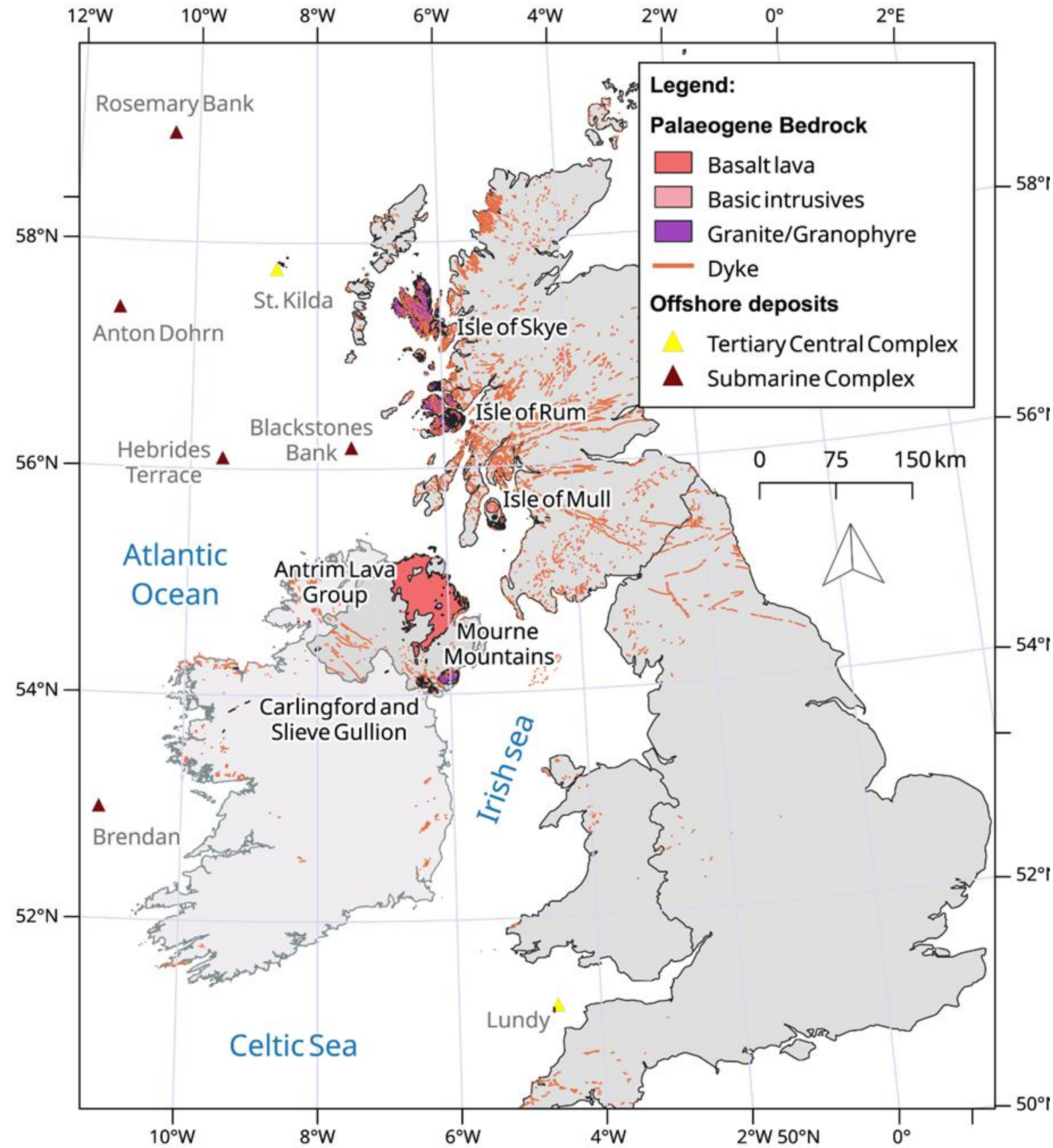

Figure 3 Simplified Regional Geology of the British and Irish Palaeogene Igneous Province. Dyke and igneous centre locations from Geological Survey Ireland (2021), British Geological Survey (2008), and offshore igneous centre locations from Mussett et al. (1988).

5.3.3. *The Antrim Lava Group*

The ALG is the largest extrusive suite in the BIPIP (59.4-61 Ma), comprising ~3,800 km^2 of flood basalts preserved in the northeast of Northern Ireland (Saunders et al., 1997). The lavas are separated into two stratigraphic sequences: the Upper and Lower Basalt Formations, which each represent ~0.5 Ma of activity, separated by ~0.5 Ma of quiescence (Mitchell, 2004; Carter et al., 2024). The quiescent (interbasaltic) period is marked by thick laterites and only minor eruptive activity, including the Causeway Tholeiite (Fig. 4e; Lyle and Preston, 1993; Wilkinson et al., 2016). Recent studies have found that mantle potential temperatures varied significantly during ALG emplacement as a result of thermal pulsing in the proto-Icelandic plume (Carter et al., 2024).

5.3.4. *Dyke Swarms*

The BIPIP contains characteristic NW-SE dykes formed as a result of NE-SW extension during Palaeogene mantle plume activity (Geoffroy et al., 1996). Five swarms traverse the island of Ireland (Anderson et al., 2018), relatively dated between ~61–56 Ma and hence spatially and temporally overlapping the emplacement of three exposed onshore central complexes (Mournes, Carlingford, Slieve Gullion) as well as the ALG and an enigmatic subsurface pluton. The Dromore High, is a positive gravity anomaly located within an area of low-density Devonian and Carboniferous bedrock (Reay, 2004), thought to represent dense magmatic material at depth. Several models have been proposed to account for this anomaly including it being: 1. a subsurface extension of the Ordovician Tyrone Igneous Complex (Cooper et al., 2011; Hollis et al, 2013); 2. a Late Caledonian igneous complex (Shaw et al., 2022); and 3. a Paleogene igneous complex similar to the Slieve Gullion Complex (Mitchell, 2004). All these scenarios are possible, with the potential for it having a Late Caledonian and Paleogene igneous history analogous to that recorded by the Slieve Gullion Complex and its surrounding Newry Igneous Complex Cloghoge pluton (Cooper et al. 2013; Anderson et al., 2016, 2017).

While only Erne and Killala dykes have absolute dates, relative age constraints exist for other swarms (Fig. 4e; Anderson et al., 2018; Cooper et al., 2025 (in review)). In decreasing age order: the oldest dykes comprise the Erne swarm (61.34 ± 0.11Ma) which is most abundant in the mid-west of the island, along the Irish–Northern Irish border. The swarm has a low dyke density with a general WNW-ESE strike (Mitchell, 2004). The second-oldest Donegal-Kingscourt swarm is a high-density swarm, emplaced across the northwest to the southeast of Ireland, with a NW-SE strike (Anderson et al., 2018). Both the Erne and Donegal-Kingscourt swarms are truncated by the Lower Basalt Formation, relatively indicating they predate the ALG (Anderson et al., 2016). Next, the Killala swarm (60.957 ±0.041 Ma) propagates across the northwest of Ireland with a W-E strike, contrasting with the general BIPIP dyke trend (NW-SE; Geoffroy et al., 1996). Killala dykes have a lower density than Donegal-Kingscourt but occur within a comparatively small area within the limits of the Tellus geophysical dataset at the time (Anderson et al., 2018). The NE-SW striking West Connacht (Mohr, 1988) and N-S striking Dingle dykes (Morris, 1974) outcrop with low densities on the west and southwest coast of Ireland, respectively, again contrasting with the general BIPIP dyke orientation; these have not previously been mapped using Tellus aeromagnetic data because prior studies were conducted before completion of the survey and therefore had an incomplete dataset (Anderson et al., 2016, 2018) but lithological and magnetic data support a Palaeogene age (Mussett et al., 1988). The Ardglass-Ballycastle swarm strikes NW-SE on the east coast and post-dates the Lower but not Upper Basalt Formation, providing a relative age constraint in the interbasaltic period between 59.9–60.5 Ma (Fig. 4e; Cooper et al., 2012; Anderson et al., 2018). Moreover, the high-density, NW–SE striking St. John’s Point Lisburn swarm also occurs on the east coast of the island and cuts both the lower and upper basalt formations, providing a relative age of intrusion after 59.4 Ma (Fig. 4e; Anderson et al., 2018).

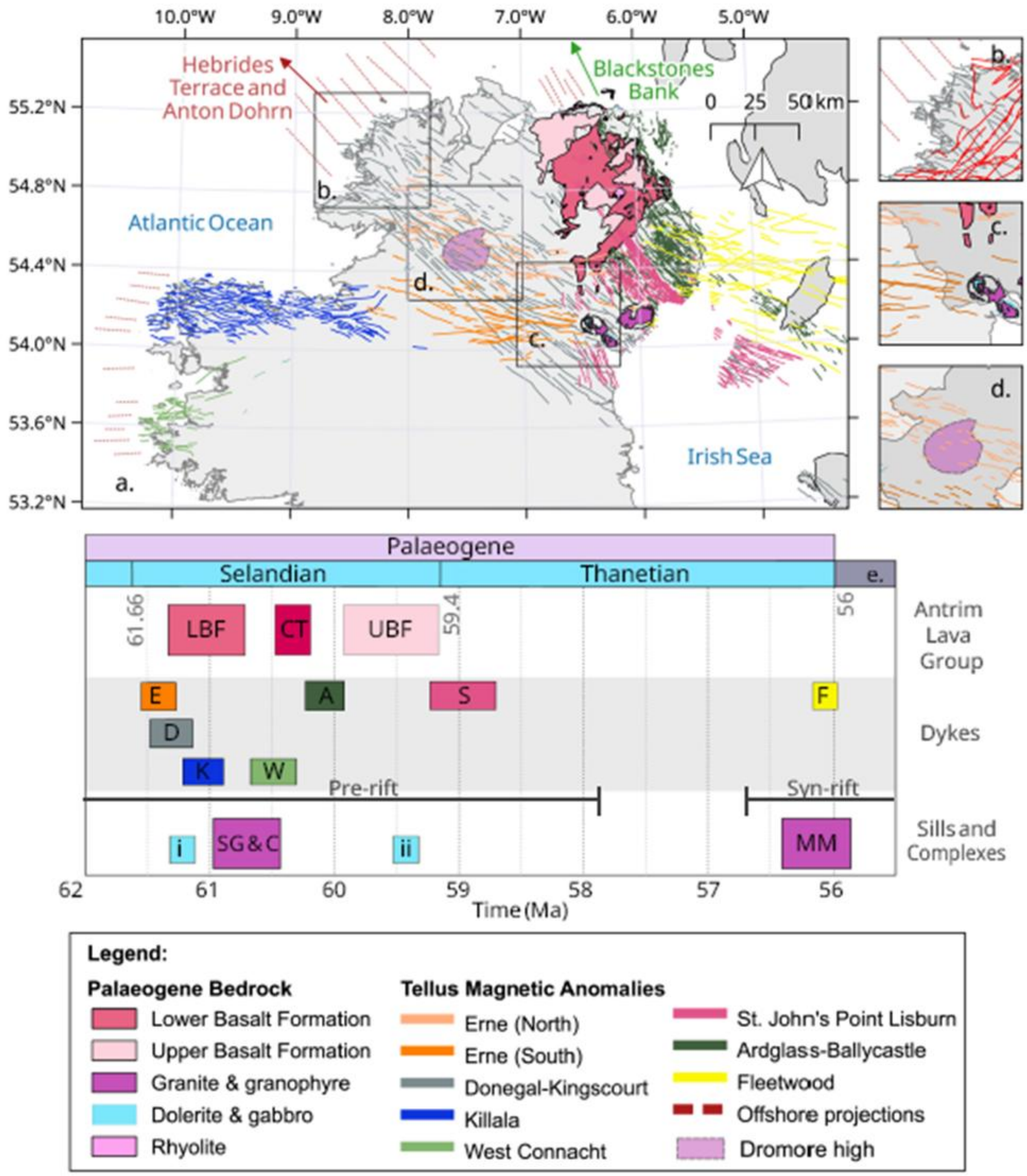

Figure 4 a) Results of extended dyke mapping of BIPIP regional swarms in Northern Ireland, Ireland and associated offshore areas. Includes data from Anderson et al. (2016, 2018) with newly interpolated dyke extents from Tellus aerial magnetic data (Geological Survey of Ireland ,2022), bedrock geology data from the British Geological Survey (2008) and Bouguer anomaly *from Mitchell (2004). Dashed lines indicate projected offshore dyke trajectories following onshore strikes. Arrows indicate direction of offshore seamounts (see Fig. 2). Red arrow = towards Anton Dohrn and Hebrides Terrace, Green arrow = towards Blackstones Bank. Boxes show detailed regions: b) the northwest coast of Ireland where the Donegal–Kingscourt swarm intersects heavily faulted terrane and reorientates along coastal fault structures (in red), c) the area around Slieve Gullion and Carlingford where the Southern Earne sub-swarm reorient towards/radiate from the central igneous complexes, and d) the high-density Northern Erne sub-swarm proximal to the Dromore High. e) Overview stratigraphy of relative Palaeogene activity in Northern Ireland and Ireland, including data from Cooper et al. (2012), Anderson et al. (2016), Anderson et al. (2018), Cooper et al. (2020), Cooper and Tapster (2025). LBF = Lower Basalt Formation, CTF = Causeway Tholeiite Formation, UBF = Upper Basalt Formation, E = Erne Swarm, D = Donegal-Kingscourt Swarm, K = Killala Swarm, W = West Connacht Swarm, A = Ardglass-Ballycastle Swarm, S = St. Johns Point-Lisburn Swarm, F = Fleetwood Swarm, i = Scrabo Sill, ii = Magilligan and Portrush Sills, SG & C = Slieve Gullion and Carlingford MM = Mourne Mountains.*

5.3.5. Sills and Plugs

Northern Ireland is host to many doleritic and gabbroic sills, with intrusions beneath and within the ALG (Mitchel, 2004). The north coast of the island features three large sills of comparable age (~58 Ma): the Portrush, Magilligan and Fairhead sills (Mitchell, 2004; Lindsay et al., 2018; Holness et al., 2015). In the northeast, the Scrabo Sill complex intrudes Triassic sandstones (61.318±0.026; Cooper et al., 2025 in review). Several doleritic plugs associated with the ALG represent sites of localised eruptive activity, with the Slemish plug representing the largest volcanic vent on the island of Ireland and outcropping on the Antrim Plateau. (Preston, 1963; Mitchell, 2004).

5.3.6. Platinum Group Exploration in Northern Ireland and Ireland

The Carlingford complex was subject to PGE exploration by BHP in the 1990s, sparked by the discovery of a 'float boulder' containing ~5 wt% Cu, 1.5 ppm Pt and 15.5 ppm Pd (Hurst, 1997). Following BHP's withdrawal from the area, Belmore Resources Ltd assumed the licence in 2005, finding further Pt mineralisation in dykes and several boulders containing mineralised PGE ± Au, Ni and Cu (Goodman and Slowley, 2005). Further potential for PGE mineralisation in Northern Ireland and Ireland was highlighted by the Tellus regional exploration programme (Geological Survey of Northern Ireland, 2005; Geological Survey of Ireland, 2022) which identified significant

Pt and Pd anomalies in stream and soil sediment samples, particularly in northwest and east County Antrim, associated with the Antrim Lava Group (ALG) and its feeder dykes (Lusty, 2016). These findings spurred exploration interest in the region, leading Lonmin Plc. to acquire exploration licences in the from 2008–2017 (Smyth, 2014; Lonmin Plc, 2018). More recently, Karelian Diamond Resources has expressed interest in Ni-Cu-PGE exploration in the southwest of Northern Ireland, following encouraging results from their stream sampling campaigns (Karelian Diamond Resources, 2025).

5.4. Materials and Methods

5.4.1. Digital Mapping

New digital maps of dyke-related anomalies across the island of Ireland were created following the method of Anderson *et al.* (2016, 2018) but using a more complete aerial magnetic dataset extending across most of the island (Geological Survey of Ireland, 2022) as opposed to only Northern Ireland and the border counties. Data from West Cork and Kerry are outstanding from our map as Tellus datasets were not available at the time of this study. We used a free-to-access, pre-processed geoTIFF of First Vertical Derivative of the Reduced to Pole Total Magnetic Intensity anomaly field (Geological Survey of Ireland, 2022) to constrain the locations of dyke-related features. Dyke-related anomalies were digitised in QGIS by tracing linear magnetic anomalies and classified into swarms based on orientation and location, creating an extended database of georeferenced polylines. At the current resolution, individual dyke-related anomalies may reflect the cumulative effect of multiple overlapping dykes rather than a single outcropping dyke; the magnetic anomalies have been interpreted to represent dyke features. This means that the number of intrusions is likely to be much greater than the number of mapped anomalies but may not reflect outcrop exposure. The digital mapping exercise has not yet been extensively ground truthed, however, some western dykes have been identified during fieldwork for sample collection.

5.4.2. Sample Collection and Preparation

Samples of putative magmatic 'liquids' (i.e. lavas and dykes, rather than cumulates) were collected from across the island of Ireland for geochemical analysis (Table 1). Dykes, sills and plugs were collected by the Geological Survey of Northern Ireland during multiple field campaigns in 2013–2014 study (subgroup A). Dyke samples from the west coast of Ireland and Carlingford cone sheets were collected during fieldwork in June 2024 and August 2022, respectively, specifically targeting finer-grained dyke margins (subgroup B). Samples from plutonic sills (e.g., Portrush, Magilligan), plugs (e.g., Slemish) and cone sheets comprise 'minor intrusions' within this study. All dykes, sills, plugs and cone sheets constitute intrusive samples. Antrim lava samples were collected from boreholes drilled by Lonmin Plc. across Northern Ireland in 2013 (subgroup C), focused on the bottom of drill cores (Lower Basalt Formation). Lavas constitute extrusive samples within this study. In hand specimen, samples were either crystal-free or porphyritic with a glassy or microcrystalline groundmass and occasional phenocrysts of olivine and/or clinopyroxene. Plagioclase was rarely present, and opaque (presumably oxide) phases were visible in thin section. Samples from subgroup B were prepared in the Discipline of Geology, Trinity College Dublin, first removing weathered material from the edge of each sample and washing in deionised water, before crushing in a tungsten carbide jaw crusher and grinding to a fine powder in an agate mill. If present, amygdales and filled vesicles were hand-picked and removed from crushed samples. Samples from subgroups A and C were similarly powdered at the Centre for Environmental

Geochemistry, Nottingham, and the School of Earth and Environmental Sciences, Cardiff University, respectively.

Table 1 Summary table of sample metadata

Sample	Swarm	Subgroup	Easting	Northing
A1007507	Erne	B	275396	329861
A1007505	Donegal-Kingscourt	B	287267	324574
A1007506	Donegal-Kingscourt	B	286630	324732
MRC404	Donegal-Kingscourt	A	219476	356499
MRC407	Erne	A	244329	354599
MRC462	St. John's Point Lisburn	A	323705	367595
MRC464	St. John's Point Lisburn	A	352760	333317
MRC467	Scrabo Sill	A	347890	372416
MRC471	Fairhead Sill	A	317616	442690
MRC472	Ardglass-Ballycastle	A	324243	425872
MRC475	Ardglass-Ballycastle	A	330388	377893
MRC482	Ardglass-Ballycastle	A	335617	381079
MRC483	Erne	A	244329	354599
MRC496	Fleetwood	A	336090	326710
MRC507	Donegal-Kingscourt	A	174979	373231
MRC510	Killala	A	111404	341170
MRC513	Killala	A	128560	330528
MRC517	Donegal-Kingscourt	A	305557	322080
MRC521	Portrush Sill	A	285600	441400
MRC523	Slemish Plug	A	322400	405700
MRC558	Donegal-Kingscourt	A	307017	339585
MRC574	St. John's Point Lisburn	A	315788	347482
MRC607	Magilligan Sill	A	268300	435300
MRC612	Slemish Plug	A	322099	405469
MRC613	Slemish Plug	A	321969	405488
22CCCI.35	Carlingford Cone Sheet	B	314162	307791
22CCI.23	Carlingford Cone Sheet	B	318325	309050
22CCI.6	Carlingford Cone Sheet	B	313032	313769
MRC622	Fleetwood	A	352405	371156
MRC490	Ardglass-Ballycastle	A	345600	402600
MRC552	Donegal-Kingscourt	A	306637	340314
24-PM-01	West Connacht	B	054400	267200
24-PM-02	West Connacht	B	054200	267400
24-PM-04	West Connacht	B	098200	281800
24-PM-05	West Connacht	B	081100	263500
24-WIT-01	Dingle	B	054237	0452370
24-WIT-02	Dingle	B	054237	0452370
24-WIT-04	Dingle	B	052447	042336
24-WIT-08	West Connacht	B	058805	253276
24-WIT-10	West Connacht	B	054285	257158
24-WIT-12	West Connacht	B	082549	272496

24-WIT-14	West Connacht	B	076934	268576
24-WIT-15	West Connacht	B	075542	267469
24-WIT-16	West Connacht	B	087842	277133
24-WIT-17	West Connacht	B	094896	280295
24-WIT-18	West Connacht	B	094893	280302
24-WIT-19	Killala	B	099368	341768
24-WIT-20	Killala	B	122313	333160
24-WIT-21	Killala	B	122321	333119
24-WIT-22	Killala	B	122335	332890
24-WIT-23	Killala	B	128609	330399
24-WIT-25	Killala	B	128584	330514
24-WIT-28	Killala	B	128522	331092
24-WIT-29	Killala	B	120449	338152
24-WIT-30d	Donegal-Kingscourt	B	180912	382130
24-WIT-32	Donegal-Kingscourt	B	184921	374462

5.4.3. Major and Trace Element Analysis

Loss on Ignition was measured gravimetrically for subgroups A and B by heating powders at 1000°C for one hour before determining their total sulphur and other major and trace element compositions. For subgroup C, loss on ignition (LOI) was measured using ~1.5 ± 0.0001g of sample powder baked at 900°C in a Vecstar Furnace for 2 hours. Total sulphur for subgroup B was then measured using an Analytik Jena multi-EA 40000 instrument in the Earth Surface Research Laboratory, Trinity College Dublin. Accuracy and precision were ~10% and ~2%, respectively, from repeat analysis of reference material 2648c (Supplementary Material Table S1; NIST, 2014). Samples from subgroup A were analysed in the Centre for Environmental Geochemistry, Nottingham (Table 2), with major element concentrations measured on fused beads by WD-XRF and trace elements by Agilent 7500 Ionising Coupled Plasma-Mass Spectroscopy (ICP-MS) following sodium peroxide fusion following Hollis et al. (2015). Analytical uncertainties for trace elements were assessed using BCR-2 certified reference material (USGS, 2022); while major elements uncertainties were monitored by repeat analysis of JG1a, JG3, BE-N, GXR-1 (Gouveia et al., 1994; SARM, 2022; GSJ, 2024). The major and trace element compositions of subgroup B were analysed using a Panalytical Zetium Wavelength Dispersive X-ray Fluorescence (WD-XRF) spectrometer in the Earth Surface Research Laboratory, Trinity College Dublin, on fused beads and pressed powder pellets, respectively. Samples were prepared and analysed following Carter et al. (2024). Analytical uncertainties were constrained using certified reference materials GSJ JB-1b, JB-3a and JBb-1 for major elements and GSJ JA-1a, JA-2 and JB-2 for trace elements (GSJ, 2024). Subgroup C was analysed in the School of Earth and Environmental Sciences, Cardiff University. Major elements, minor elements and Sc were measured using a JY-Horiba Ultima 2 Inductively Coupled Plasma Optical Emission Spectrometry and trace elements were measured using a thermoelemental X series (X7) ICP-MS, following McDonald and Viljoen (2006). Standard reference materials JB1a, JP1 and MRG1 were used to constrain uncertainties (GSJ, 2024; Gladney and Roelandts, 1988). Representative accuracy for major elements is typically 1–2%, except for Na_2O (3%) and P_2O_5 (4%). Representative accuracy for trace elements is typically 5–8%, except Zr (20%) and Ba (33%).

5.4.4. Platinum Group Element + Gold Fire Assay

Platinum group element and Au concentrations for subgroups A and B were analysed in Activation Laboratories Ltd, Canada, by Ni-sulphide fire assay followed by ICP-MS, following Hoffman and Dunn (2002). Subgroup C was also analysed for PGE + Au by Fire Assay and ICP-MS in the School of Earth and Environmental Sciences, Cardiff University, following Huber et al. (2001). Analytical and preparation accuracy and reproducibility (including potential nugget effects) were assessed following a validation approach similar to Passmore (2009; Supplementary Material Table S2). In general, representative accuracy PGE ± Au was between ~0.5– 9% (Pt – 4%, Pd 6%) and precision was better than 5%, based on repeat analysis of standards AMIS 0498 and

OREAS 13b (AMIS, 2017; Ore Research & Exploration PTY Ltd, 2009) and with potential nugget effects determined to be minor.

Table 2 Summary of analysis methods for samples within this study

Source	GSNI	Fieldwork	Cardiff Research Group
Subgroup	A	B	C
Sample Type	Dykes, sills, plugs	Dykes, cone sheets	Lavas
Location	Counties Antrim, Armagh, Derry, Donegal, Down, Fermanagh, Mayo, Sligo, Tyrone	Counties Cork, Donegal, Galway, Kerry, Louth, Mayo, Monaghan, Sligo	County Antrim
Preparation & analysis	Centre for Environmental Geochemistry, Nottingham	Discipline of Geology, Trinity College Dublin; Earth Surface Research Laboratory, Trinity College Dublin	School of Earth and Environmental Sciences, Cardiff University
Majors	WD-XRF	Panalytical Zetium Wavelength Dispersive X-ray Fluorescence (WD-XRF) spectrometer	JY-Horiba Ultima 2 Inductively Coupled Plasma Optical Emission Spectrometry
Trace	Agilent 7500 Ionising Coupled Plasma-Mass Spectroscopy (ICP-MS)		Thermoelemental X series (X7) ICP-MS
Standards	JG1a, JG3, BE-N, GXR-1, BCR-2, AMIS 0498, OREAS 13b	GSJ JB-1b, JB-3a, JBb-1, GSJ JA-1a, JA-2, JB-2, AMIS 0498, OREAS 13b	JB1a, JP1, MRG1
PGE+Au	Nickel sulphide fire assay followed by ICP-MS		
PGE analysis	Activation Laboratories Ltd, Canada		School of Earth and Environmental Sciences, Cardiff University
Methods	Hollis et al. (2015), Hoffman and Dunn (2002)	Carter et al. (2024), Hoffman and Dunn (2002)	McDonald and Viljoen (2006), Huber et al. (2001)

5.5. A Revised Palaeogene Dyke Map

Our enhanced digital mapping of regional dyke swarms reveals a greater density of dyke-related anomalies than previously identified in the northwest and west of the island and across the Irish

Sea (Fig. 4a). Specifically, our new results build on the mapping of Anderson et al. (2016, 2018), extending the mapped geographic coverage of the Donegal-Kingscourt, Killala and Erne swarms in the west and northwest. The Fleetwood dyke swarm, initially thought as an offshore component of the Donegal-Kingscourt swarm (Anderson et al., 2018), has been mapped to strike WNW-ESE, with a low onshore density in the east, extending to a high-density swarm across the Irish Sea Basin and outcropping on the Isle of Man; the dykes crosscut early granites of the Mournes relatively constraining its age to ~56–56.5 Ma (Cooper and Tapster, 2025). By mapping offshore continuations of the Donegal-Kingscourt, Ardglass-Ballycastle, St. John's Point, Lisburn and Fleetwood swarms, we provide new insights into the high density of dyke-related anomalies in the Irish Sea, demonstrating that the Fleetwood and Ardglass-Ballycastle swarms transect the Isle of Man.

In addition, we identify and map a dyke swarm which was not previously recognised in aerial magnetic studies by Anderson et al. (2016, 2018): the West Connacht dykes, originally mapped by Mohr (1988), comprise a high-density swarm with a NE-SW strike inland transitioning to more W-E on the western coast. They have a much higher density than previously identified in outcrop by Mohr (1988), occurring in clusters along the west coast, with fewer dykes inland. The West Connacht swarm shares orientation (W-E) with the Killala swarm on the northwest coast, however, their northern extent does not overlap inland with the Killala dykes. The Dingle syke swarm has not yet been resolved in our dataset due to outstanding Tellus survey data.

The orientation of dyke swarms across the island suggests a systematic regional variation, shifting from NW–SE in the north to predominantly W–E towards the southern extent of dyke propagation. Previous studies have suggested individual swarms have distinct strikes and that this shift in orientation reflects a temporal progression as a result of changing regional crustal stresses during north Atlantic opening (Anderson et al., 2018). However, our extended mapping demonstrates that some swarms are not continuous linear features with a constant strike but rather exhibit a pronounced curvature across their length, producing ‘hockey stick’ shaped regional features. This systematic change is exemplified by the St John’s Point Lisburn and Fleetwood dykes which have a NW–SE strike in the north but reorientate to a WNW–ESE and W-E strike in the south, across the Irish Sea and reach the Isle of Man, their, respectively. A similar re-orientation is observed in the West Connacht swarm, where more northernly dykes strike NE-SW while southern coastal dykes trend towards W-E. Given that extended mapping shows individual swarms changing orientation, differences in strike direction cannot reflect a temporal shift related to the relative timing of dyke emplacement.

5.6. Geochemical Results

For context, we compare our new geochemical results with those obtained for genetically related lava flows in Northern Ireland (Carter et al., 2024), the Scottish Hebrides (Hughes et al., 2015c), off- and on-shore East Greenland (Philip et al., 2001; Momme et al., 2002), West Greenland (Lightfoot et al., 1997; Keays and Lightfoot, 2007) and Iceland (Momme et al., 2003). This allows tracking North Atlantic plume dynamics from the Palaeogene to the present. Major and trace element results for all dykes, minor intrusions and lava flows are in Supplementary Material Table S3 and S4 and PGE+ Au results are in Table S5. Subgroups A and B comprise ‘Dykes and minor intrusions’ and subgroup C comprise ‘Antrim Lava Group (ALG)’

5.6.1. Major Elements

The major element compositions of our samples are broadly basaltic (Supplementary Material Fig.

S6; Alkali-subalkali basalts, tephrites), extending to highly primitive mantle-like compositions (>60 Mg#; Mg# = molar Mg/(Mg+Fe_t) x 100 where Fe_t = total Fe^{2+} + Fe^{3+}). Two samples from the Dingle dyke system are highly evolved (Dacite, Rhyolite; See S6), however contain PGEs below detection limits. The compositions of intrusives and ALG samples overlap, with dykes and minor intrusions extending to slightly more evolved compositions; individual dyke swarms do not exhibit any observable geochemical difference with broadly similar major and trace element signatures across all swarms (Supplementary Material Figs. S7 and S8). Compositional trends are consistent with fractional crystallisation of a mineral assemblage comprising predominantly olivine ± clinopyroxene ± minor plagioclase (Fig. 5a-d), consistent with other NAIP igneous centres (Lightfoot et al., 1997; Saunders et al., 1998; Tegner et al., 2023; Carter et al. 2024). While samples from Greenlandic centres have accumulated significant olivine (Fig. 5a) with high Mg content (>70 Mg#) and Fe_2O_3 concentrations (~13 wt%), our samples show less extensive olivine accumulation, extending to 50–70 Mg# and 10–14 wt% Fe_2O. Olivine is consistently the liquidus phase in our samples but the major element compositions indicate early clinopyroxene saturation (~60 Mg#), marked by an inflection in CaO concentrations with decreasing Mg#. None of our samples and a few NAIP literature analyses show evidence of plagioclase saturation (which would be manifest as a decrease in Al_2O_3 at low Mg#). Lithophile trace elements (Zr and Sr) further support lithophile major element trends, with concentrations of incompatible elements increasing with increasing Mg# (Supplementary Material Fig. S9). The total sulphur concentrations in our samples are low (average 0.13 wt%), consistent with an absence of visible sulphides in hand specimen (Supplementary Material Table S1).

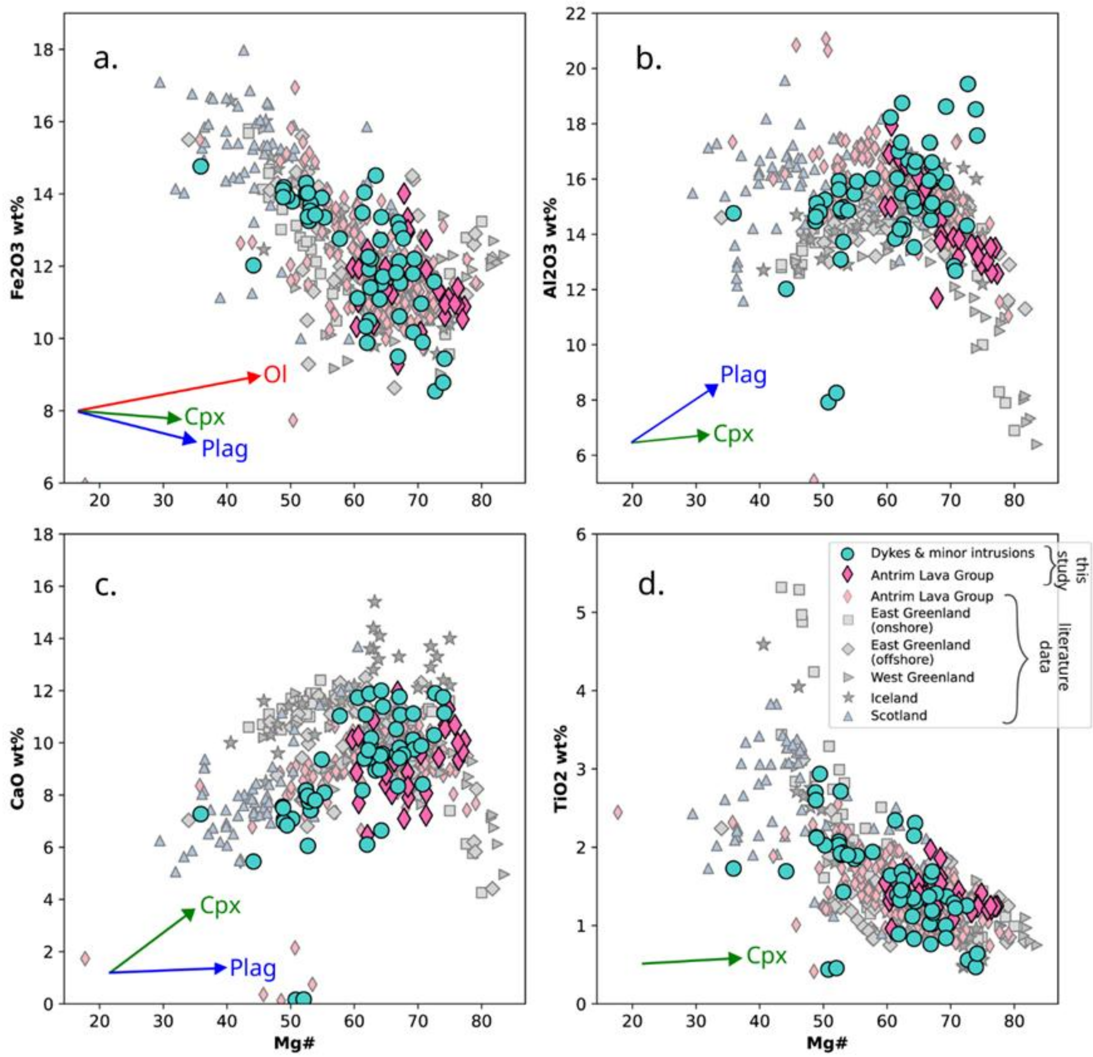

Figure 5 Binary plots showing Mg# versus major elements a) Fe_2O_3, b) Al_2O_3, c) CaO, d) TiO_2. New data in this study are coloured and literature data from the ALG and other NAIP centres are in grey (see legend). Arrows show trajectories towards mineral compositions from Pearson et al. (2003): Ol = olivine, Cpx = clinopyroxene, Plag = plagioclase. Contains data from genetically related lava flows in Northern Ireland (Carter et al., 2024), the Scottish Hebrides (Hughes et al., 2015c), East Greenland (Philip et al., 2001; Momme et al., 2002), West Greenland (Lightfoot et al., 1997; Keays and Lightfoot, 2007), and Iceland (Momme et al., 2003). Error bars are shown at 2σ or are less than the size of a data point.

5.6.2. Chalcophile Trace Elements

The highest Ni, Cr and Co concentrations in our dataset are associated with the most mafic samples, with concentrations in all dyke and minor intrusion samples and most ALG samples decreasing at lower Mg# (Fig. 6). This mirrors data from other NAIP centres and is consistent with the ‘incompatible fractionation’ trend of Hughes et al (2015b), reflecting Ni and Co partitioning into olivine during progressive crystallisation, and Cr into presumably minor amounts of spinel-group minerals which are not apparent from major element variations (Fig. 5). A subset of ALG samples have lower Ni than the general trend for their given Mg# (Fig. 6a), reflecting early sulphide depletion before extensive crystallisation and sulphur saturation, as identified in some samples from West Greenland (Hughes et al., 2015).

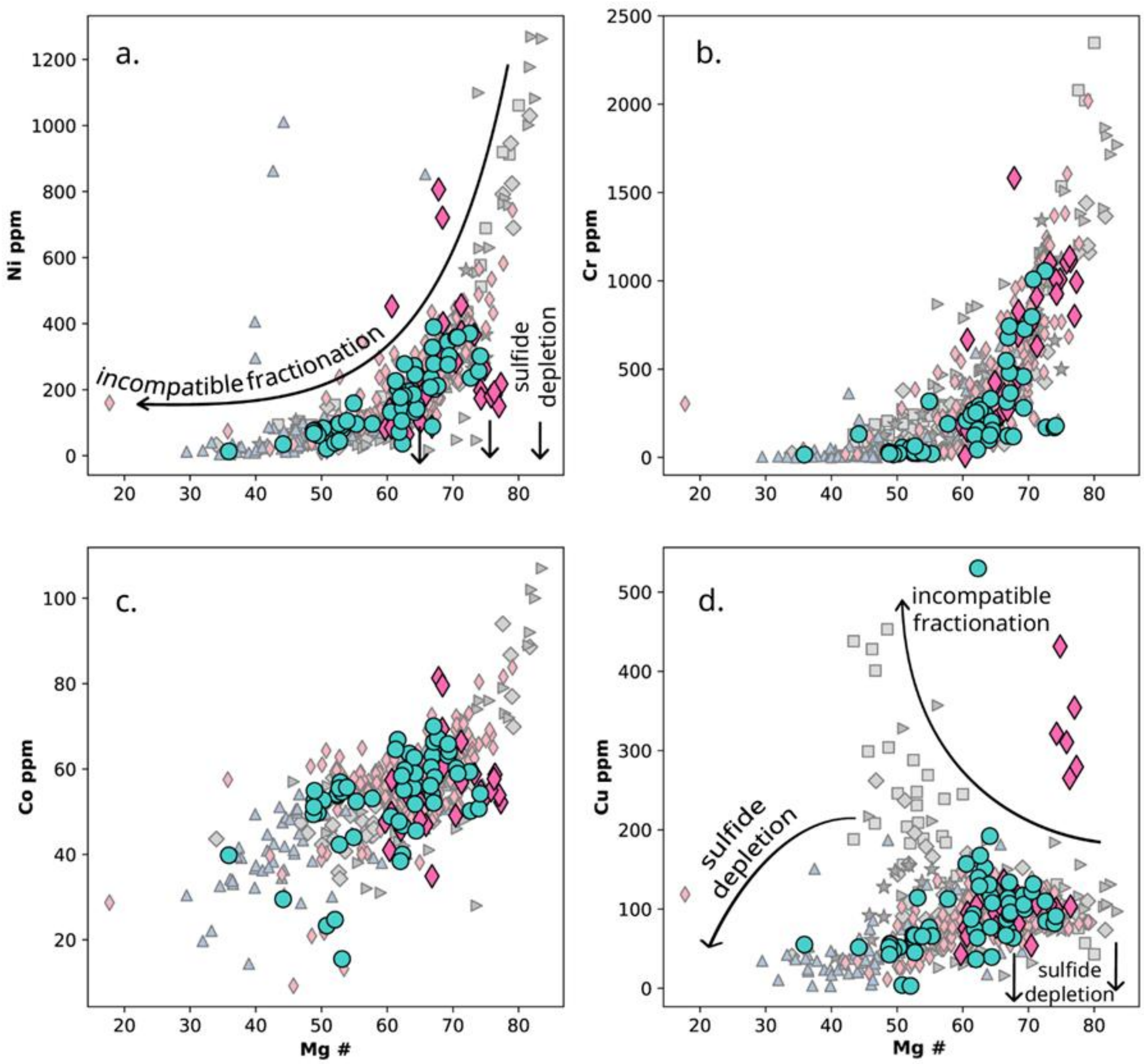

Figure 6 Binary plots for Chalcophile elements vs. Mg#. a) Ni, b) Co, c) Cr, d) Cu. Schematic Silicate fractionation and sulphide depletion trends adapted from Hughes et al. (2015c). New data in this study are coloured and literature data from the ALG and other NAIP centres are in grey (see legend in Fig. 5). Data sources as in Figure 5. Error bars are shown at 2σ or are less than the size of a data point.

As Cu is incompatible in common basaltic silicate minerals it increases in silicate melts as these phases crystallise (i.e. towards lower Mg#), unless a sulphide liquid exsolves in which case Cu partitions strongly into this phase and decreases during magmatic evolution. Both incompatible and compatible trends are seen in the NAIP with sulphide-undersaturated crystallisation apparent from some Greenlandic samples and sulphide-saturated crystallisation dominant elsewhere (Hughes et al., 2015; Fig. 6d). Most of our data show decreasing Cu abundance with decreasing Mg#, consistent with progressive sulphide exsolution during magmatic evolution (e.g. following trends in Scottish samples). However, a small number of our mafic ALG samples and one sill have anomalously high Cu relative to other samples at equivalent Mg#, '*high Cu group'*, recording sulphide-undersaturated crystallisation (e.g. mirroring trends in Greenland; Fig. 6d).

5.6.3. Platinum Group Elements + Au

Our samples contain negligible IPGE but PPGEs ± Au are generally above detection limit (>1 ppb; Supplementary Material Table S5). The highest total PGE concentration in our sample set is 34 ppb in an ALG sample, with the highest intrusive sample (a dyke from the Killala swarm) containing 28 ppb. The highest Pt concentration is 13 ppb and Pd 12 ppb, in the same dyke sample from the Killala swarm. The highest Au concentration is 26 ppb in an ALG sample. All other samples span these concentrations down to below detection limits. These concentrations are elevated relative to background mantle levels; average wholerock MORB contains 0.5 ppb Pt and 0.9 ppb Pd (Hao et al., 2021).

Our data correlate with the broader NAIP (Fig. 7a) with the highest and most variable Pt and Pd concentrations in the most mafic (highest Mg#) samples and lower concentrations in more evolved samples. Most of our samples have higher Pt than Pd concentrations. Only onshore East

Greenlandic samples significantly deviate from this relationship, with high Pd even at low Mg#. Ru concentrations are ubiquitously low both in our samples (<4 ppb) and other NAIP centres (Fig. 7c). Similarly, Au concentrations are close to the detection limit and show do not correlate with Mg#; only onshore East Greenlandic centres and one of our samples from ALG (26 ppb) have higher concentrations.

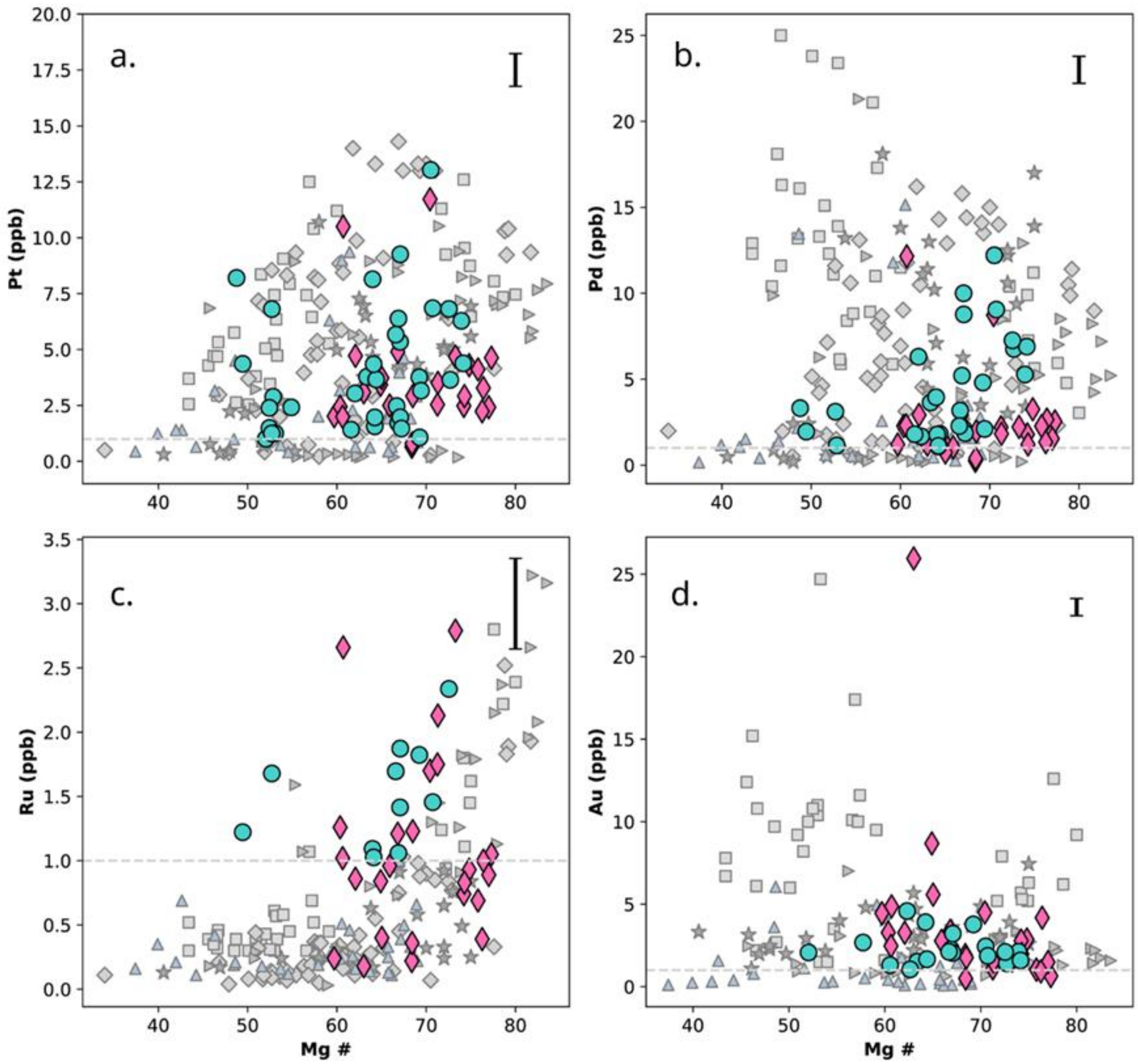

Figure 7 Binary plots for PGE vs. Mg#; a) Pt, b) Pd, c) Ru, d) Au. New data in this study are coloured and literature data from the ALG and other NAIP centres are in grey (see legend in Fig. 5). Data sources as in Figure 5. Error bars are shown at 2σ or are less than the size of a data point. The dashed grey line represents the detection limit for dykes and minor intrusions (1 ppb).

The relationship between PGEs and other chalcophile elements can be used to identify their partitioning into immiscible sulphide liquids. For example, Cu and Pd are both incompatible in silicate minerals but partition strongly into sulphide liquids when magmas become S-saturated. Our data show two trends in Cu versus Pd (Fig. 8a): one where Pd and Cu positively correlate up to ~15 ppb Pd and ~150 ppm Cu, and a second where Pd concentrations remain constantly low over a wide range of Cu abundances. The former trend is broadly consistent with other NAIP centre which show a general positive correlation between Cu and Pd, albeit extending to the highest values and most variable concentrations in onshore East Greenland, whereas the latter trend is most apparent in our samples from the ALG and a single sill sample. Gold shows only a weak correlation with Pd in the majority of our samples (Fig. 8b), with slightly diverse populations between the ALG and intrusive samples, again consistent with the general NAIP trend except East Greenland which has higher and more scattered Au and Pd abundances.

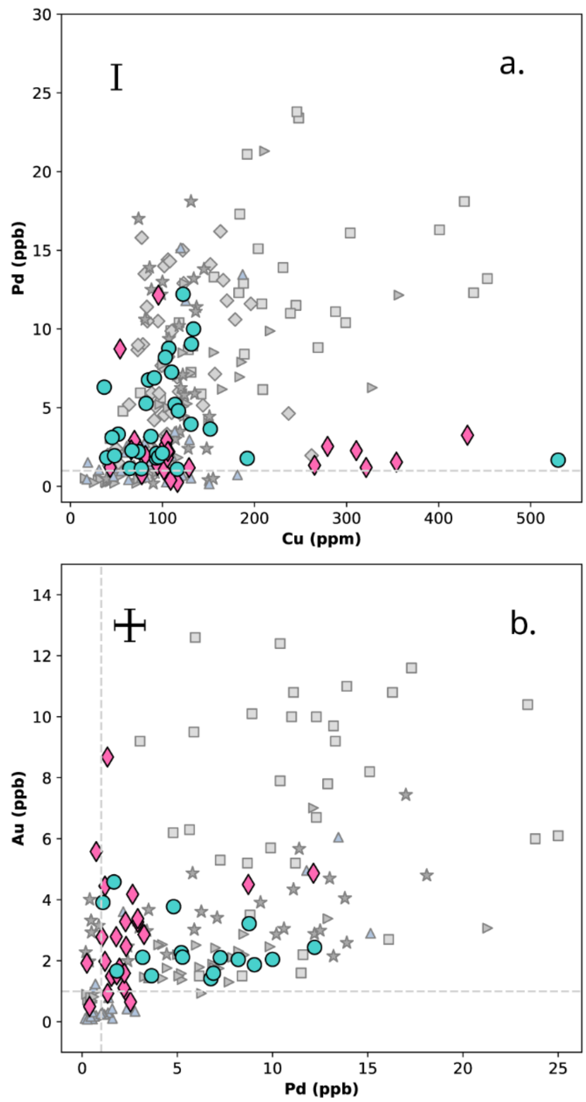

Figure 8 PGE + Au and chalcophile association: a) Pd and Cu, b) Au and Pd. New data in this study are coloured and literature data from the ALG and other NAIP centres are in grey (see legend in Fig. 5). Data sources as in Figure 5. Error bars are shown at 2σ or are less than the size of a data point. The dashed grey line represents the detection limit for dykes and minor intrusions (1 ppb).

While both Cu and Pd are chalcophilic, there is approximately an order of magnitude difference in their silicate melt–sulphide liquid partition coefficients, with Pd partitioning more strongly into the sulphide phase; Cu/Pd ratios of residual silicate melts therefore increase following S-saturation (Hughes et al., 2015c). The Cu/Pd ratios of mineralised PGE deposits tend to be lower than mantle values as they have not yet segregated sulphides and can concentrate PGE (Barnes et al., 1993, 2004, 2015); the extent of enrichment is enhanced through further silicate-magma interaction, with higher R-factors representing a greater volume of silicate magma interacting with sulphide, upgrading the sulphide tenor through additional PGE scavenging (Maier, 2005; Barnes et al., 2016; Lindsay et al., 2018). In contrast, magmas which have segregated sulphides have Cu/Pd ratios greater than mantle values as PGEs are preferentially lost (Barnes et al., 1993, 2004, 2015). The Cu/Pd ratios of our samples generally increase linearly with decreasing Pd concentration, plotting significantly above mantle values consistent with other NAIP centres (Fig. 9). Only the small '*high Cu group'* of samples with high Cu concentrations (principally from the ALG, plus one sill) plot slightly above the main data array.

As with major elements, there is little observable difference between our dyke and minor intrusion samples and the ALG samples (or between dyke swarms) in terms of chalcophile elements, PGEs and Au, except that ALG samples extend to the highest Cu/Pd ratios.

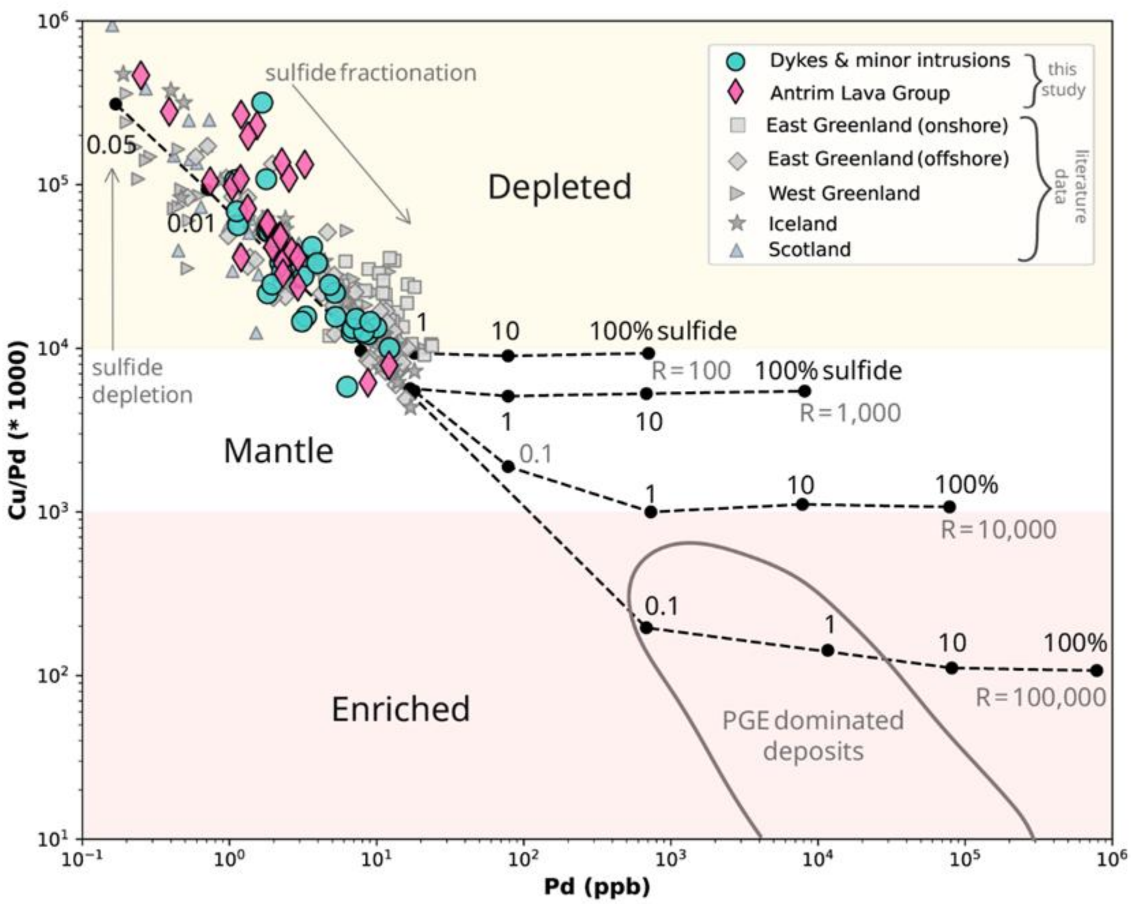

Figure 9 Binary plot showing Cu/Pd ratio versus Pd. The dashed line shows the composition of a modelled basalt melt when a sulphide liquid is added or removed in co-tectic proportions. Black dots represent 0.01, 1, 10% sulphide content, R factors describe the mass ratio of silicate melt interacting with a sulphide liquid, the black polygon shows the composition of PGE deposits (e.g. Merensky reef, Bushveld UG-2, Stillwater J-M reef). Adapted from Barnes et al. (1993) and Hughes et al. (2015c). The depleted field (yellow) represents magma compositions with Cu/Pd ratios higher than that of background mantle ratios, where Pd has been removed relative to Cu as sulphide liquids have been exsolved. The enriched field (pink) represents magma compositions with Cu/Pd ratios lower than that of background mantle ratios, with Pd enriched relative to Cu, concentrated within sulphides. Schematic sulphide fractionation and sulphide depletion trends adapted from Singh et al. (2018). New data in this study are coloured and literature data from the ALG and other NAIP centres are in grey (see legend). Data sources as in Figure 5.

5.7. Discussion

5.7.1. Dyke origins

Of the seven mapped swarms, six show no obvious association with the onshore Palaeogene central complexes of Slieve Gullion, Carlingford or the Mourne Mountains; they do not radiate from or curve towards these centres (e.g. as with the Mull swarm in England; MacDonald et al., 2018**)** and in some cases are reported to crosscut them (Baxter, 2008; Cooper and Tapster, 2025). Irish dykes are also too far south to have originated from Hebridean Palaeogene centres (Mull, Rum, Skye; Fig. 3); their NW-SE strike would not intersect these intrusions. Figure 4a projects the offshore trajectories of dyke swarms from the north and west coasts of the island, assuming a constant strike. Dykes extending off the north coast (St. John's Point Lisburn) trend towards the Blackstones Bank complex, while dykes extending off the northwest coast (Donegal-Kingscourt) strike towards Anton Dohrn and the Hebrides Terrace (as previously identified by Ritchie and Kitchen, 1996). At high spatial resolution, these dykes appear to deflect close to the northwest coast as they intersect strike-slip faults (Fig. 4b).Our new mapping of the Killala and West Connacht swarms indicates that the predominantly W-E orientation of the coastal dykes does not align well with any offshore centre, including the more southern Brendan Igneous Centre (Figs. 3, 4) which has previously been suggested as the source of the dykes (unless they reorientate dramatically offshore; Mohr 1982; Dewey 2000). Rather than originating from onshore

Palaeogene centres, we suggest that most Palaeogene dyke swarms transecting the island of Ireland originate from offshore centres in the North Atlantic.

Existing age constraints support most dykes originating from offshore centres. The Donegal-Kingscourt swarm are relatively dated as being older than 61.4 Ma (early Palaeogene) owing to their being unconformably overlain by the Lower Basalt Formation, with an extended period of episodic volcanism at Anton Dohrn and the Hebrides Terrace between 70.4 Ma and 42.0 Ma (O'Connor et al., 2000). The St. John's Point Lisburn swarm (56–58 Ma), agrees well with dating of the Blackstones Bank which returns an age of 58.6 ± 1 Ma (Dicken and Durant, 2002).

The Erne swarm is an exception, with an orientation that does not trend towards any known offshore centre. From a detailed analysis of our new aerial magnetic map, we suggest that these dykes, which have previously been grouped into a single swarm, in fact comprise two discrete populations: the Northern Erne sub-swarm with a NW-SE strike (similar to but slightly offset from the Donegal-Kingscourt dykes; light orange in Fig. 4a) and the Southern Erne sub-swarm with a more WNW-ESE strike (dark orange in Fig. 4a). There is a geographical gap between these two groups in the middle of the island. The Southern Erne sub-swarm extends across the width of the island but reorientates in the east, swinging towards and radiating from the Slieve Gullion and Carlingford central complexes (Fig. 4c) which have a near-contemporaneous age relationship with the Erne dykes (Cooper et al., 2012; Fig. 4e). In contrast, the Northern Erne sub-swarm has a notably high density proximal to the Dromore High gravity anomaly and do not extend very far southeast or northwest of this feature (Fig. 4d). While a component of the Dromore anomaly with relates to Northern Irish Caledonian magmatism, the possibility of a coincident Palaeogene central complex has not been discounted. The density of our mapped Southern Erne dykes supports the occurrence of Palaeogene magmatism in the Dromore area feeding these dykes. Hence, in contrast with other dykes which strike towards offshore NAIP igneous centres, we suggest that the Erne swarm may uniquely originate from onshore central complexes.

Previous authors have suggested that dyke swarms show a progressive temporal shift in orientation from broadly W-E to NW-SE, interpreted as reflecting successive phases of dyke emplacement with time (Anderson et al., 2018). However, our new maps show no such temporal trend with swarms showing a systematic spatial change in dyke emplacement orientation (the 'hockey stick' swing) from NW-SE in the north towards W-E in the southeast and southwest of the island. Hence, rather than reflecting a change in crustal stress state through time, we infer that propagating dykes simply realigned with crustal stresses as a function of distance from the plume: dykes on the north coast of the island were proximal to the proto-Icelandic plume and the plume controlled their oritentation radiating outwards, whereas dykes further south and east were distal from plume control and orientations were more susceptible to regional tectonic compression. Orientation patterns are further complicated by far-field Palaeogene alpine compression (Cooper et al., 2012) and dynamic topography generated by asymmetric impingement of the plume on the base of the lithosphere (Jones and White, 2003). Recent work has also suggested that the Irish Sea experienced significant lithospheric thinning during the Palaeogene through uplift and magmatism caused by magmatic underplating (Bonadio et al., 2025). A thinned lithosphere may have accomodated propagating dykes more easily owing to the high density of intrusion identified in the Irish Sea basin.

5.7.2. Crystallisation and Sulphur Saturation in Northern Irish and Irish Palaeogene Magmas

Our new geochemical results provide insights into Palaeogene magmatic processes during early lithospheric impingement of the proto-Icelandic plume and North Atlantic Rifting. Samples follow a typical tholeiitic fractional crystallisation trend with the liquid line of descent controlled predominantly by olivine ± clinopyroxene crystallisation with only minor late-stage plagioclase (Fig. 5a-d), consistent with previous studies of the BIPIP (e.g. Carter et al, 2024). Olivine crystallisation progressively depleted the residual melts in chalcophile Ni and Cr during magma evolution (Fig. 6a), with Co concentrations decreasing through the fractionation of spinel-group minerals.

The highest Pt, Pd and Ru concentrations are at high Mg# with lower concentrations in more evolved magmas, mirroring general trends in the NAIP and broadly consistent with PGE partitioning into sulphide liquids which progressively exsolve during magma evolution (Fig. 7a-c). However, there is a significant range in PGE concentrations at any given Mg# (Fig. 7a-d), suggesting that heterogeneity in S-saturation histories and varying degrees of PGE sequestration into segregated sulphides exerts a primary control on magma chalcophile budgets.

While whole-rock Ni concentrations have been suggested as a Ni-Cu-PGE exploration vector (Naldrett, 1999), Barnes et al. (1993) highlight that other chalcophiles (e.g. Cu, PGEs) have much higher partition coefficients into sulphide liquids and are therefore more sensitive to S-saturation. Copper, for example, shows a continuous depletion in most of our data, consistent with sulphide saturation early in magmatic evolution and mirroring trends in most other NAIP centres. Only samples within our '*high Cu group*' have higher Cu concentrations consistent with incompatible behaviour during crystallisation of silicate minerals in the absence of sulphides and recording an absence of S-saturation (Fig. 6d). These samples represent some of the oldest samples in this study; the sill has been dated to 61.318 ± 0.026 Ma (Fig. 4e; Scrabo Sill), and the ALG samples were extruded ~61 Ma (Fig. 4e; Lower Basalt Formation). A comparable geochemical trend is only observed in the onshore East Greenland samples from the Sortebre Plateau Basalts, associated with much younger magmatic activity (55.4 ± 0.14 Ma), coincident with the emplacement of the Skaergaard Intrusion (Momme et al., 2002). There, early fractionation of silicates and PGE prior to sulphide saturation has been proposed. A similar process in our older samples would imply that PGE concentrations are not primarily controlled by sulphide phases but were instead depleted through early crystallisation. The initially low Pd contents of the '*high Cu group'* may also reflect an early sulphide saturation event which removed PGEs from the system. However, subsequent evolution appears to have continued under sulphide-undersaturated conditions, such that the samples do not follow a typical sulphide-depletion trend (Fig. 6d)

The sulphur saturation history of a magma is critical to determining its orthomagmatic Ni-Cu-PGE sulphide mineralisation potential; the timing and mechanism of S-saturation are critical for deposit formation. Cu/Pd ratios demonstrate that all our samples have undergone sulphide saturation and are chalcophile depleted, comparable with other NAIP centres (Fig. 9). As these sulphides are no longer associated with the magma (i.e. our samples are not sulphide-rich), they must have segregated from the melt, either within central complexes (e.g., Bushveld; Barnes et al., 2004) or conduit systems during crustal magma transport (e.g., Norilsk; Barnes et al., 2016), and this is conduicive to deposit formation. Mineralisation has previously been identified in Carlingford, both within the central layered complex and associated dykes, and positive mienralisation indicators have been identified in Northern Irish and Palaeogene dykes (Lusty, 2016; Group Eleven Corp., 2020). A key exploration challenge will be identifying any zones of localised sulphide accumulation, for example fluid dynamical traps (Barnes et al., 2016; Hughes et al., 2016) within the dyke systems which extend across the island of Ireland (Dewey, 2000; Cooper et al., 2012; Anderson et al., 2016, 2018). Zones where dykes deflect across major faults (Fig. 4b) could provide such traps, as could areas proximal to the Dromore High, where conduits appear to be ascending near-vertically towards the surface; this is corroborated by soil compositions analysed in the Tellus geochemical survey which show elevated PGE concentrations associated with heavily faulted terranes and surrounding the Dromore High and along the northwest coast (Fig. 10; Geological Survey of Northern Ireland, 2016; Geological Survey of Ireland 2021).

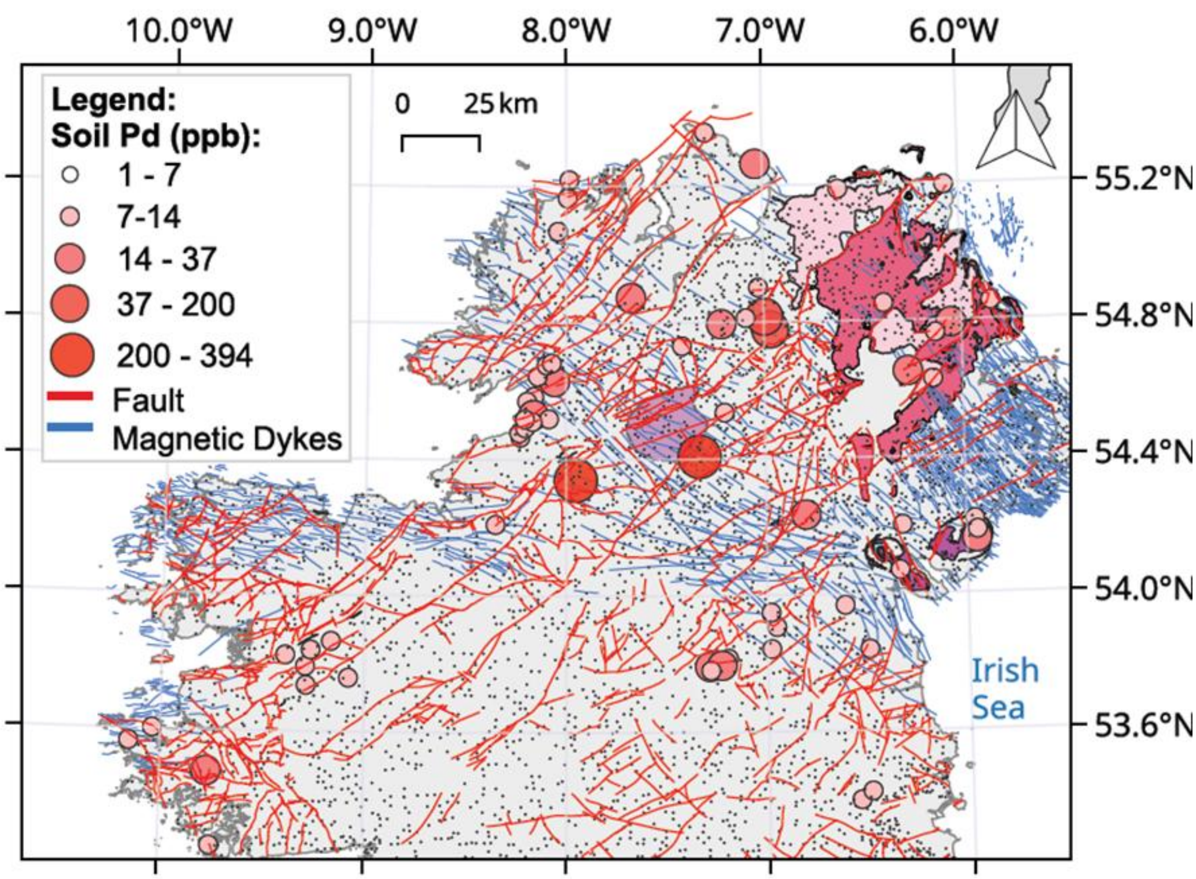

Figure 10 Pd concentrations in deeper topsoils in the Tellus geochemical survey (Geological Survey Ireland, 2021 and Geological Survey of Northern Ireland, 2005). All dykes are depicted as blue lines; swarm categories can be seen in Fig. 4a. Red lines represent geological faults. Bedrock geology (ALG, Slieve Gullion, Carlingford, Mourne Mountains, Dromore High) as in Figure 4a.

5.7.3. Mantle Dynamics Recorded in the Northern Irish and Irish North Atlantic Igneous Province

Almost all our samples only contain detectable PPGEs, with IPGEs largely below detection limit. This may reflect insufficient melting temperatures in the mantle source region required to liberate IPGEs monosulphide solid solutions (Singh et al., 2018). If the degrees of partial melting is low overall, residual sulphides can retain a significant proportion of PGE in the source region (Barnes et al., 2015) and hence the limited PGE concentrations in our samples (maximum Σ34 ppb PGE) may be a result of incomplete melting of mantle sulphides.

The Pt/Pd ratios of mafic melts preserve a record of geodynamic environment and mantle source conditions during magma generation (Hughes et al., 2015c; Lindsay et al., 2021). In the NAIP, Pt/Pd ratios generally decrease from high, near chondritic values in older igneous centres (~1.9; West Greenland ~63 Ma and Scotland ~61 Ma) to lower values in younger centres (~0.4; Iceland <50 Ma; Fig. 11a; Lindsay et al., 2021). This variation has been attributed to transient mantle conditions associated with the opening of the North Atlantic. Higher Pt/Pd ratios are interpreted to reflect pre-rift, intraplate magmatism at the inception of the proto-Icelandic mantle plume and proximity to the North Atlantic Craton, whereas lower Pt/Pd ratios are suggested to record contributions from shallower mantle sources and declining temperatures syn- and post-rifting of the Eurasian and North American plates (Griffin et al., 2013; Hughes et al., 2014).

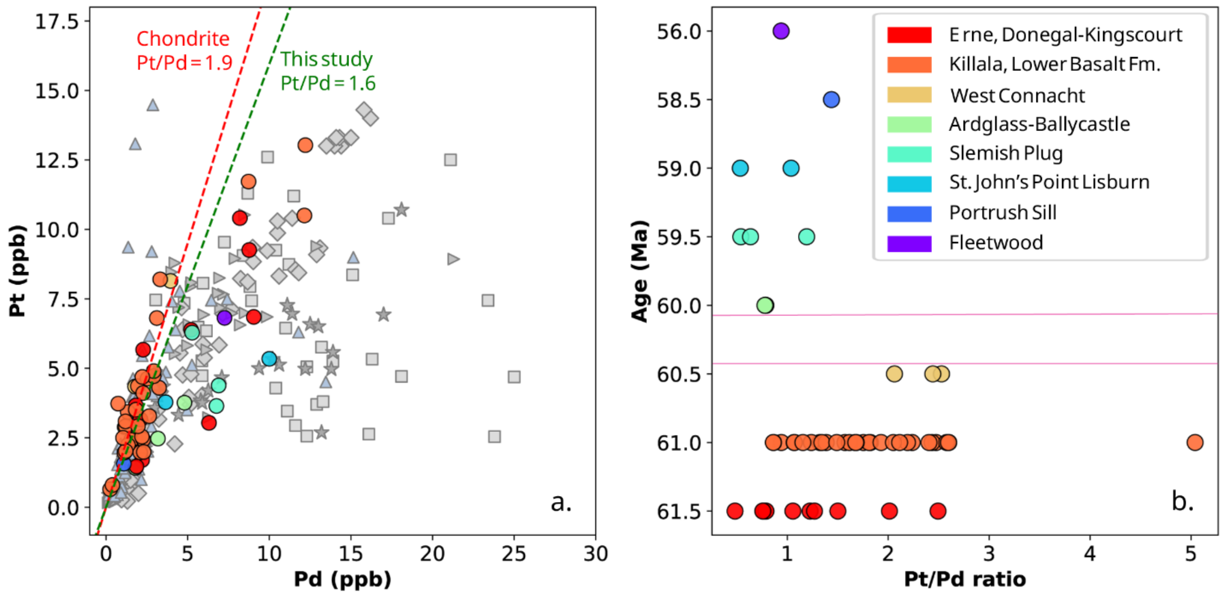

Figure 11 Pt/Pd ratios in NAIP deposits. Undepleted mantle contains approximately chondritic proportions of PGE (Carlson, 2005). Therefore, comparing sample ratios to chondritic values provides insight into the PGE fertility or depletion of the mantle source. a) Pt versus Pd for all NAIP deposits. Samples from this study are in colour (See legend) and literature data are represented in grey (see legend in Fig. 9). Data sources as in Figure 5. b) Pt/Pd ratios in this study with time (Ma). Older samples (Pre/during Lower Basalt Formation) are represented with red-orange hues and younger samples (During/after Upper Basalt Formation) are represented with green-blue-purple hues. The sample swarm/location within this study is denoted in the legend. Pink lines indicate the interbasaltic period between extrusion of Upper and Lower Basalts (Carter et al., 2024)

The Pt/Pd ratios of our samples range 0.4–5.04 with an average of 1.6 (Fig. 11a), spanning the range between older and younger NAIP centres reported in the literature data. There is structure within our dataset: older samples which formed at >61.4–60.5 Ma before/during eruption of the Lower Basalt Formation have an higher Pt/Pd ratios of ~1.85 (comparable to the Greenlandic and Scottish NAIP), whereas younger samples which formed at <60.5 Ma during/after eruption of the Upper Basalt Formation have a lower average Pt/Pd ratios of ~0.87 (comparable to offshore East Greenland; Fig. 11b;), trending towards modern Iceland. The proximity of magma generation to cratonic boundaries impacts the PGE ratios of primary (Griffin et al., 2013) with higher Pt/Pd ratios in older NAIP centres thought to record partial melting of the SCLM at the margin of the North Atlantic Craton and lower ratios in younger centres recording the absence of a SCLM component (pre-rift); for example, Hebridean magmas generated close to the cratonic keel have had more opportunity to incorporate Pt-enriched/metasomatized melt within ascending magmas

(Hughes et al., 2015c; Lindsay et al., 2021). Our data record the disappearance of this SCLM component in primary melts between the Upper and Lower Basalt Formation emplacement. The interbasaltic period between the Upper and Lower Basalt Formations marks a ~0.5 Myr near-hiatus in eruptive activity and correspond with a stabilisation and step-wise cooling of the proto-Icelandic plume (Fig. 11b; Cooper et al., 2020; Carter et al. 2024), and we suggest that this period marks a major geodynamic transition from intraplate plume-dominated magma generation to oceanic rifting-controlled petrogenesis (syn-rift). The time window between our oldest (e.g. Lower Basalt Formation, Erne dykes, Donegal-Kingscourt dykes) and youngest (e.g. Fleetwood and St. John's Point Lisburn dykes) samples spans ~6 Myr (Fig. 4e; Cooper and Tapster, 2025). Within this broader interval, our new data indicate that the critical transition from pre-rift SCLM-influenced magma generation to syn-rift melting that appears to have occurred during the interbasaltic period (<1 Myr), highlighting a shift in mantle conditions over a geologically short timescale (Fig. 4e, Fig. 11b).

5.8. Conclusions

Analysis of igneous centres on the island of Ireland provides new insights into precious metal behaviour and petrogenesis during a crucial phase of NAIP development. Our new digital maps show the distribution of seven discrete dyke swarms across the island of Ireland, demonstrating that some swarms originate from submarine centres in the North Atlantic but that the Erne dykes derive from onshore centres; a Southern Erne sub-swarm appears to originate from the Slieve Gullion and Carlingford central complexes, while a Northern Erne sub-swarm is concentrated around the Dromore High gravity anomaly suggesting and attests to sub-surface Palaeogene magmatism. The major element compositions of our dykes, minor intrusions and lava samples are broadly consistent with other NAIP centres, with major elements controlled by olivine and clinopyroxene crystallisation and chalcophile trace elements recording persistent sulphide saturation, even in our most mafic magmas. The PGE concentrations of magmas feeding our samples are elevated relative to background mantle values and Pt/Pd ratios are highly variable, recording a changing geodynamic environment. Igneous centres emplaced before and or during eruption of the Lower Basalt Formation have higher Pt/Pd ratios, whereas those which were emplaced during or after eruption of the Upper Basalt Formation have lower ratios. This transition records a major geodynamic shift in the interbasaltic period with older magmas recording a plume-dominated melting and inclusion of a SCLM mantle component as a result of their proximity to the North Atlantic craton, and later magmas recording rift-related melting and the absence of an SCLM component away from the cratonic margin. By integrating our results with existing absolute and relative dating of Northern Irish and Irish igneous centres, we show that the transition from pre- to syn-rift environments in the NAIP occurred within a geologically short timeframe.

5.9. Acknowledgements

This work emanated from a Master's by Research grant co-funded by the Geological Survey of Ireland and the Northern Irish Department of the Economy, a Trinity College Dublin Foundation Scholarship, and research jointly funded by Taighde Éireann – Research Ireland and Geological Survey Ireland under grant number 20/FFP-P/8895. XRF data collection was supported by the Geological Survey Ireland-funded Earth Surface Research Laboratory in Trinity College Dublin. Maura Morgan and Sarah Carty are thanked for their assistance in sample preparation, and Hilde Koch, Clara Siqueira and Carmela Tupaz are thanked for their assistance in XRF sample preparation and analysis.

5.10. References

Á HORNI, J., HOPPER, J. R., BLISCHKE, A., GEISLER, W. H., STEWART, M., MCDERMOTT, K., JUDGE, M., ERLENDSSON, Ö. & ÁRTING, U. 2017. Regional distribution of volcanism within the North Atlantic Igneous Province. *Geological Society, London, Special Publications,* 447**,** 105–125.

AMIS 2017. AMIS 0498: Certified Reference Material Platinum (PGM). Platreef Ore Bushveld Complex, South Africa. Certificate of Analysis Modderfontein, South Africa: A Division of Torre Analytical Services (Pty) Limited.

ANDERSEN, J. C. Ø., POWER, M. R. & MOMME, P. 2000. Platinum-Group Elements in the Palaeogene North Atlantic Igneous Province. *The Geology, Geochemistry, Mineralogy and Mineral Beneficiation of PGE,* 54**,** 637–667.

ANDERSEN, J. C. Ø., ROLLINSON, G. K., MCDONALD, I., TEGNER, C. & LESHER, C. E. 2017. Platinum-group mineralization at the margin of the Skaergaard intrusion, East Greenland. *Mineralium Deposita,* 52**,** 929–942.

ANDERSON, H., WALSH, J. J. & COOPER, M. R. 2016. Faults, intrusions and flood basalts: the Cenozoic structure of the north of Ireland. *In:* YOUNG, M. E. (ed.) *Unearthed: impacts of the Tellus surveys of the north of Ireland.* Dublin: Royal Irish Academy.

ANDERSON, H., WALSH, J. J. & COOPER, M. R. 2018. The development of a regional-scale intraplate strike-slip fault system; Alpine deformation in the north of Ireland. *Journal of Structural Geology,* 116**,** 47–63.

ANDERSON, P.E., COOPER, M.R., STEVENSON, C.T., HASTIE, A.R., HOGGETT, M., INMAN, J., MEIGHAN, I.G., HURLEY, C., REAVY, R.J., ELLAM, R.M. 2016 Zonation of the Newry Igneous Complex, Northern Ireland, based on geochemical and geophysical data, *Lithos*. doi: 10.1016/j.lithos.2016.05.009.

ANDERSON, P. E., STEVENSON, C. T., COOPER, M. R., MEIGHAN, I. G., HURLEY, C., REAVY, R. J., INMAN, J. & ELLAM, R. M. 2018. Refined model of incremental emplacement based on structural evidence from the granodioritic Newry igneous complex, Northern Ireland. *Geological Society of America Bulletin. GSA Bulletin*. 130 (5-6): 740-756.

BARNES, S.-J., MAIER, W. D. & ASHWAL, L. D. 2004. Platinum-group element distribution in the Main Zone and Upper Zone of the Bushveld Complex, South Africa. *Chemical Geology,* 208**,** 293–317.

BARNES, S.-J. & MANSUR, E. T. 2022. Distribution of Te, As, Bi, Sb, and Se in Mid-Ocean Ridge Basalt and Komatiites and in Picrites and Basalts from Large Igneous Provinces: Implications for the Formation of Magmatic Ni-Cu-Platinum Group Element Deposits. *Economic Geology,* 117**,** 1919–1933.

BARNES, S. J., COUTURE, J. F., SAWYER, E. W. & BOUCHAIB, C. 1993. Nickel-Copper occurrences in the BA belt of Pontiac Sub province and the use of Cu-Pd ratios in interpreting PGE distributions. *Economic Geology,* 88**,** 1402–1418.

BARNES, S. J., CRUDEN, A. R., ARNDT, N. & SAUMUR, B. M. 2016. The mineral system approach applied to magmatic Ni–Cu–PGE sulphide deposits. *Ore Geology Reviews,* 76**,** 296–316.

BARNES, S. J., MUNGALL, J. E. & MAIER, W. D. 2015. Platinum group elements in mantle melts and mantle samples. *Lithos,* 232**,** 395–417.

BARNES, S. J. & RIPLEY, E. M. 2016. Highly siderophile and strongly chalcophile elements in magmatic ore deposits. *Reviews in Mineralogy and Geochemistry,* 81**,** 725–74.

BAXTER, S. 2008. *A Geological Field Guide to Cooley, Gullion, Mourne & Slieve Croob,* Dublin, Geological Survey of Ireland.

BONADIO, R., LEBEDEV, S., CHEW, D., XU, Y., FULLEA, J. AND MEIER, T. 2025. Volcanism and long-term seismicity controlled by plume-induced plate thinning. *Nature Communications*, *16*(1), p.7837.

BRITISH GEOLOGICAL SURVEY. 2008. *BGS Geology 625k*. [dataset] British Geological Survey. Available at: https://www.bgs.ac.uk/datasets/bgs-geology-625k/.

CARLSON, R.W., 2005. Application of the Pt–Re–Os isotopic systems tomantle geochemistry and geochronology. Lithos 82, 249–272.

CARTER, E. J., STOCK, M. J., BERESFORD-BROWNE, A., COOPER, M. R., RAINE, R. & FEREYROLLES, A. 2024. Volcanic tempo driven by rapid fluctuations in mantle temperature during large igneous province emplacement. *Earth and Planetary Science Letters,* 644.

CHAMBERS, L.M., PRINGLE, M.S., 2001. Age and duration of activity at the Isle of Mull Tertiary igneous centre, Scotland, and confirmation of the existence of subchrons during Anomaly 26r. Earth and Planetary Science Letters 193, 333–345.

CHEN, C., FORSTER, M. W., SHCHEKA, S. S., EZAD, I. S., SHEA, J. J., LIU, Y., JACOB, D. E. & FOLEY, S. F. 2025. Sulfide-rich continental roots at cratonic margins formed by carbonated melts. *Nature,* 637**,** 615–621.

COOPER, M. R., ANDERSON, H., WALSH, J. J., VAN DAM, C. L., YOUNG, M. E., EARLS, G. & WALKER, A. 2012. Palaeogene Alpine tectonics and Icelandic plume-related magmatism and deformation in Northern Ireland. *Journal of the Geological Society,* 169**,** 29–36.

COOPER, M. R., CROWLEY, Q. G., HOLLIS, S. P., NOBLE, S. R, & HENNEY, P. 2013. A U-Pb age for the Late Caledonian Sperrin Mountains minor intrusions suite in the north of Ireland: timing of slab break-off in the Grampian terrane and the significance of deep-seated, crustal lineaments. *Journal of the Geological Society, London.* 170, 603-614.

COOPER, M. R, CROWLEY, Q. G., HOLLIS, S. P., NOBLE, S. R., ROBERTS, S., CHEW, D. M., MERRIMAN, R. J., EARLS, G. & HERRINGTON, R. 2011. Age constraints and geochemistry of the Ordovician Tyrone Igneous Complex, Northern Ireland: implications for the Grampian orogeny. *Journal of the Geological Society, London, Vol.* 168; p. 837-850. doi: 10.1144/0016-76492010-164.COOPER, M. R. & TAPSTER, S. 2025. Mapping and geochronological constraints on intrusion of the Fleetwood Dyke Swarm onshore Northern Ireland. VMSG-MDSG Joint Conference, 2025 Dublin.

COOPER, M. R. & TAPSTER, S. 2025. Mapping and geochronological constraints on intrusion of the Fleetwood Dyke Swarm onshore Northern Ireland. VMSG-MDSG Joint Conference, 2025 Dublin.

COOPER, M. R., TAPSTER, S. & CONDON, D. 2020. Feeling the pulse? New high resolution U-Pb zircon geochronological constraints for the Northern Ireland sector of the North Atlantic Igneous Province. *EGU General Assembly 2020.* Online, 4–8 May 2020: EGU2020-8464.

DEWEY, J. F. 2000. Cenozoic tectonics of western Ireland. *Proceedings of the Geologists' Association,* 111**,** 291–306.

DICKIN, A.P. AND DURANT, G.P., 2002. The Blackstones Bank igneous complex: geochemistry and crustal context of a submerged Tertiary igneous centre in the Scottish Hebrides. *Geological Magazine*, *139* (2), pp.199-207.

GAGNEVIN, D., HAUGHTON, P. D., WHITING, L. & SAQQB, M. M. 2018. Geological and geophysical evidence for a mafic igneous origin of the porcupine arch, offshore Ireland. *Journal of the Geological Society,* 175**,** 210–228.

GEOFFROY, L., BERGERAT, F. & ANGELIER, J. 1996. Brittle tectonism in relation to the Palaeogene evolution of the Thulean/NE Atl domain: a study in Ulster. *Geological Journal,* 31**,** 259–269.

GEOLOGICAL SURVEY OF IRELAND. 2021. *Bedrock Geology 1:100,000 Ireland (ROI) ITM*. Dublin: Geological Survey of Ireland.

GEOLOGICAL SURVEY OF IRELAND. 2022. Tellus Merge-2022 airborne geophysical technical report. Dublin: Geological Survey of Ireland.

GEOLOGICAL SURVEY IRELAND AND GEOLOGICAL SURVEY OF NORTHERN IRELAND (2022) *Tellus geochemical survey: deeper topsoil ('S' horizon) multi-element maps for the northern half of Ireland*. Dublin: Geological Survey Ireland.

GEOLOGICAL SURVEY OF JAPAN (GSJ) (2024) *Geochemical Reference Standards Database*. Available at: https://gbank.gsj.jp/geostandards/welcome.html.

GEOLOGICAL SURVEY OF NORTHERN IRELAND (GSNI). 2005. *Tellus Rural Soil Survey: Regional S Soils – Fire Assay dataset*. [dataset] Geological Survey of Northern Ireland (Department for the Economy), Northern Ireland. Available at: https://admin.opendatani.gov.uk/dataset/rural-soil-survey/resource/e9a4568a-677d-419a-a2ce-31940900bbe9

GLADNEY, E.S., ROELANDTS, I., & GILLS, T.E. (1988) '1988 Compilation of elemental concentration data for CCRMP reference rock samples SY-2, SY-3, and MRG-1', *Geostandards and Geoanalytical Research*, 14(3), pp. 373–458. doi:10.1111/j.1751-908X.1990.tb00078.x.

GOODMAN, R. & SLOWLEY, E. 2005. Independent review of exploration interests of BelmoreResources Ltd.

GOUVEIA, M.A., PRUDÊNCIO, M.I., BARROS, J.S., MORGADO, L. AND CABRAL, J.M.P., 1994. Elemental concentration data for USGS geochemical exploration reference materials GXR-1 to GXR-4 and GXR-6. *Journal of radioanalytical and nuclear chemistry*, *179*(1), pp.165-172.

GRIFFIN, W. L., BEGG, G. C. & O'REILLY, S. Y. 2013. Continental-root control on the genesis of magmatic ore deposits. *Nature Geoscience,* 6**,** 905–910.

GROUP ELEVEN CORP. 2020. Group Eleven Identifies Anomalous Palladium, Nickel and Cobalt at Ballinalack Zinc Project, Ireland. Vancouver, Canada.

HANSEN, J., JERRAM, D. A., MCCAFFREY, K. & PASSEY, S. R. 2009. The onset of the North Atlantic Igneous Province in a rifting perspective. *Geological Magazine,* 146**,** 309–325.

HAO, H., CAMPBELL, I. H., ARCULUS, R. J. & PERFIT, M. R. 2021. Using precious metal probes to quantify mid-ocean ridge magmatic processes. *Earth and Planetary Science Letters,* 553.

HOFFMAN, E. L. & DUNN, B. 2002. Sample preparation and bulk analytical methods for PGE. *The Geology, Geochemistry, Mineralogy and Mineral Beneficiation of PGE,* 54**,** 1–11.

HOLLIS, S.P., COOPER, M.R., HERRINGTON, R.J., ROBERTS, S., EARLS, G., VERBEETEN, A.,PIERCEY, S.J., AND ARCHIBALD, S.M. 2015. Distribution, mineralogy and geochemistry of silica-iron exhalites and related rocks from the Tyrone Igneous Complex: Implications for VMS mineralization in Northern Ireland. *Journal of Geochemical Exploration* 159: 148-168.

HOLNESS M.B., GEIFMAN E., STOCK M.J., COOPER M.R., BECKWITH J., HUBER C., CHEW D., AND ANDERSEN J.C.Ø., 2025. A microstructural investigation of the Portrush Sill, County Antrim, Northern Ireland: constraints on sill thickness and evidence for crustal assimilation. Lithos.

HUBER, H., KOEBERL, C., MCDONALD, I., REIMOND,W.U., 2001. Geochemistry and petrology of Witwatersrand and Dwyka diamictites from South Africa: search for an extraterrestrial component. Geochimica et Cosmochimica Acta 65, 2007–2016.

HUGHES, H. S. R. 2015. *Temporal, lithospheric and magmatic process controls on ni, cu and platinum-group element (pge) mineralisation: A case study from scotland*. Doctoral Thesis, Cardiff University.

HUGHES, H. S. R., BOYCE, A. J., MCDONALD, I., DAVIDHEISER-KROLL, B., HOLWELL, D. A., MCDONALD, A. & OLDROYD, A. 2015a. Contrasting mechanisms for crustal sulphur contamination of mafic magma: evidence from dyke and sill complexes from the British Palaeogene Igneous Province. *Journal of the Geological Society,* 172**,** 443–458.

HUGHES, H. S. R., MCDONALD, I., BOYCE, A. J., HOLWELL, D. A. & KERR, A. C. 2016. Sulphide Sinking in Magma Conduits: Evidence from Mafic–Ultramafic Plugs on Rum and the Wider North Atlantic Igneous Province. *Journal of Petrology,* 57**,** 383–416.

HUGHES, H. S. R., MCDONALD, I., FAITHFULL, J. W., UPTON, B. G. J. & DOWNES, H. 2015b. Trace-element abundances in the shallow lithospheric mantle of the North Atlantic Craton margin: Implications for melting and metasomatism beneath Northern Scotland. *Mineralogical Magazine,* 79**,** 877–907.

HUGHES, H. S. R., MCDONALD, I., GOODENOUGH, K. M., CIBOROWSKI, T. J. R., KERR, A. C., DAVIES, J. H. F. L. & SELBY, D. 2014. Enriched lithospheric mantle keel below the Scottish margin of the North Atlantic Craton: Evidence from the Palaeoproterozoic Scourie Dyke Swarm and mantle xenoliths. *Precambrian Research,* 250**,** 97–126.

HUGHES, H. S. R., MCDONALD, I. & KERR, A. C. 2015c. Platinum-group element signatures in the North Atlantic Igneous Province: Implications for mantle controls on metal budgets during continental breakup. *Lithos,* 233**,** 89–110.

HURST, E. 1997. Renewal Report for Prospecting Licence 3843. BHP.
JONES, S.M. AND WHITE, N., 2003. Shape and size of the starting Iceland plume swell. *Earth and Planetary Science Letters*, *216*(3), pp.271-282.
KEAYS, R. R. & LIGHTFOOT, P. C. 2007. Siderophile and chalcophile metal variations in Tertiary picrites and basalts from West Greenland with implications for the sulphide saturation history of continental flood basalt magmas. *Mineralium Deposita,* 42**,** 319–336.
KENT, R. W. & FITTON, J. G. 2000. Mantle sources and melting dynamics in the British Palaeogene Igneous Province. *Journal of Petrology,* 41**,** 1023–1040.
LE BAS, M.J., LE MAITRE, R.W., STRECKEISEN, A., & ZANETTIN, B. 1986. A chemical classification of volcanic rocks based on the total alkali–silica diagram. *Journal of Petrology*, 27(3), 745–750. https://doi.org/10.1093/petrology/27.3.745
LIGHTFOOT, P. C., HAWKESWORTH, C. J., OLSHEFSKY, K., GREEN, T., DOHERTY, W. & KEAYS, R. R. 1997. Geochemistry of Tertiary tholeiites and picrites from Qeqertarssuaq (Disko Island) and Nuussuaq, West Greenland with implications for the mineral potential of comagmatic intrusions. *Contributions to Mineralogy and Petrology,* 128**,** 139–163.
LINDSAY, J. J., HUGHES, H. S. R., SMYTH, D., MCDONALD, I., BOYCE, A. J. & ANDERSEN, J. C. Ø. 2018. Distinct sulfur saturation histories within the Palaeogene Magilligan Sill, Northern Ireland: implications for Ni – Cu – platinum group element mineralisation in the North Atlantic Igneous Province. *Canadian Journal of Earth Sciences,* 56**,** 774–789.
LINDSAY, J. J., HUGHES, H. S. R., YEOMANS, C. M., ANDERSEN, J. C. Ø. & MCDONALD, I. 2021. A machine learning approach for regional geochemical data: Platinum-group element geochemistry vs geodynamic settings of the North Atlantic Igneous Province. *Geoscience Frontiers,* 12.
LONMIN PLC. 2018. Mineral Resource and Mineral Reserve Statement 2018. London. UK.
LUSTY, P. A. J. 2016. Critical metals for hightechnology applications: mineral exploration potential in the north of Ireland. *In:* YOUNG, M. E. (ed.) *Unearthed: impacts of the Tellus surveys of the north of Ireland.* Dublin: Royal Irish Academy.
LYLE, P. & PRESTON, J. 1993. Geochemistry and volcanology of the Tertiary basalts of the Giant's Causeway area, Northern Ireland. *Journal of the Geological Society,* 150**,** 109–120.
MACDONALD, R., BAGIŃSKI, B., UPTON, B. G. J., PINKERTON, H., MACINNES, D. A. & MACGILLIVRAY, J. C. 2018. The Mull Palaeogene dyke swarm: insights into the evolution of the Mull igneous centre and dyke-emplacement mechanisms. *Mineralogical Magazine,* 74**,** 601–622.
MAIER, W. D. 2005. Platinum-group element (PGE) deposits and occurrences: Mineralization styles, genetic concepts, and exploration criteria. *Journal of African Earth Sciences,* 41**,** 165–191.
MCDONALD, I., VILJOEN, K.S., 2006. Platinum-group element geochemistry of mantle eclogites: a reconnaissance study of xenoliths from the Orapa kimberlite, Botswana. Applied Earth Science 115, 81–93.

MITCHELL, W. (ed.) 2004. *Geology of Northern Ireland: our natural foundation*: Geological Survey of Northern Ireland.

MOHR, P. 1988. The Analcime-Olivine Dolerites of West Connacht, Ireland: Classification and Genetic. *Irish Journal of Earth Sciences,* 9**,** 133–140.

MOHR, P. 2000. Late Palaeozoic and Palaeocene magmatic intrusion levels in West Connacht and inferences for palaeotopography. *Proceedings of the Geologists' Association,* 111**,** 337–343.

MOMME, P., ÓSKARSSON, N. & KEAYS, R. R. 2003. Platinum-group elements in the Icelandic rift system: melting processes and mantle sources beneath Iceland. *Chemical Geology,* 196**,** 209–234.

MOMME, P., TEGNER, C., BROOKS, K. C. & KEAYS, R. R. 2002. The behaviour of platinum-group elements in basalts from the East Greenland rifted margin. *Contributions to Mineralogy and Petrology,* 143**,** 133–153.

MORRIS, P. 1974. A Tertiary Dyke System in South-West Ireland. *Proceedings of the Royal Irish Academy. Section B: Biological, Geological and Chemical Science,* 74**,** 179–184.

MUDD, G. M., JOWITT, S. M. & WERNER, T. T. 2018. Global platinum group element resources, reserves and mining - A critical assessment. *Sci Total Environ,* 622-623**,** 614–625.

MUSSETT, A. E., DAGLEY, P. & SKELHORN, R. R. 1988. Time and duration of activity in the British Tertiary Igneous Province. *Geological Society, London, Special Publications,* 39**,** 337–348.

NALDRETT, A.J., 1999. World-class Ni-Cu-PGE deposits: key factors in their genesis. *Mineralium deposita*, *34*(3), pp.227-240.

NIST 2014. Certificate of Analysis: Standard Reference Material® 2684c *In:* GONZALEZ, C. A. (ed.) *Bituminous Coal (Nominal Mass Fraction 3 % Sulfur)* Gaithersburg, MD 20899 National Institute of Standards & Technology.

O'CONNOR, J.M., STOFFERS, P., WIJBRANS, J.R., SHANNON, P.M. AND MORRISSEY, T., 2000. Evidence from episodic seamount volcanism for pulsing of the Iceland plume in the past 70 Myr. *Nature*, *408* (6815), pp.954-958.ORE RESEARCH & EXPLORATION PTY LTD. 2009. Certificate of analysis for PGE-Cu-Ni reference material OREAS 13b Victoria, Australia.

ORE RESEARCH & EXPLORATION PTY LTD. 2009. Certificate of analysis for PGE-Cu-Ni reference material OREAS 13b Victoria, Australia.

PASSMORE, E. 2009. *Feeding large eruptions: crystallisation, mixing and degassing in Icelandic magma chambers.* Doctoral Thesis, University of Edinburgh.

PEARSON, D.G., CANIL, D. AND SHIREY, S.B., 2003. Mantle samples included in volcanic rocks: xenoliths and diamonds. *Treatise on geochemistry*, *2*, p.568.

PHILIP, H., ECKHARDT, J. D. & PUCHELT, H. 2001. Platinum-group elements (PGE) in basalts of the seaward-dipping reflector sequence, SE Greenland coast. *Journal of Petrology,* 42**,** 407–432.

PRESTON, J. 1963. The Dolerite plug at Slemish, Co Antrim, Ireland. *Geological Journal,* 3**,** 301–314.

REAY, D.M., 2004. Chapter 22, Oil and Gas. in Mitchell, W.I. ed. The Geology of Northern Ireland - Our Natural Foundation (second edition): Belfast, Geological Survey of Northern Ireland, p. 273–290.

RITCHIE, J. D. & HITCHEN, K. 1996. Early Paleogene offshore igneous activity to the northwest of the UK and its relationship to the North Atlantic Igneous Province. *Geological Society, London, Special Publications,* 101**,** 63–78.

SARM. (2022). *Certificate of analysis: BE-N reference material (basalt)*. Service d'Analyses des Roches et des Minéraux, Centre de Recherches Pétrographiques et Géochimiques (CRPG-CNRS), Vandoeuvre-lès-Nancy, France.

SAUNDERS, A. D., FITTON, J. G., KERR, A. C., NORRY, M. J. & KENT, R. W. 1997. The North Atlantic Igneous Province. *Large Igneous Provinces: Continental, Oceanic, and Planetary Flood Volcanism,* 100**,** 45–93.

SAUNDERS, A. D., LARSEN, H. C. & FITTON, J. G. 1998. Magmatic development of the southeast Greenland Margin and evolution of the Iceland plume: geochemical constraints from Leg 152. *Proceedings of the Ocean Drilling Program, Scientific Results,* 152**,** 479–501.

SINGH, T. D., MANIKYAMBA, C., SUBRAMANYAM, K. S. V., GANGULY, S., KHELEN, A. C. & RAMAKRISHNA REDDY, N. 2018. Mantle heterogeneity, plume-lithosphere interaction at rift controlled ocean-continent transition zone: Evidence from trace-PGE geochemistry of Vempalle flows, Cuddapah Basin, India. *Geoscience Frontiers,* 9**,** 1809–1827.

SHAW, J.I., TORVELA, T., COOPER, M.R, LESLIE, A.G., CHAPMAN, R.J., 2022. A progressive model for the development of the Cavanacaw Au–Ag–Pb vein deposit, Northern Ireland, and implications for the evolution and metallogeny of the Grampian Terrane. Journal of Structural Geology, 161. 104637. ISSN 0191-8141.

SMYTH, D. 2014. Lonmin Plc exploration in Northern Ireland – the contribution of mineral exploration to new observations in regional geology. *Mineral Deposits Studies Group 38th Annual Meeting,* Univeristy of Southampton.

TEGNER, C., SALMONSEN, L. P., HOLNESS, M. B., LESHER, C. E., HUMPHREYS, M. C. S., THY, P. & NIELSEN, T. F. D. 2023. A whole-rock data set for the Skaergaard intrusion, East Greenland. *GEUS Bulletin,* 53.

USGS (2022) *BCR-2 Geochemical Reference Material Information Sheet*. United States Geological Survey. Available at: https://www.usgs.gov/media/files/bcr-2-geochemical-reference-material-information-sheet-0

WILKINSON, C. M., GANERØD, M., HENDRIKS, B. W. H. & EIDE, E. A. 2016. Compilation and appraisal of geochronological data from the North Atlantic Igneous Province (NAIP). *Geological Society, London, Special Publications,* 447**,** 69–103.

Chapter 6

6. Conclusion

6.1. Evaluation of Aims and Objectives

The project has successfully achieved its primary objective, producing the first comprehensive PGE survey of mafic deposits in Northern Ireland and Ireland. We have produced a high-quality open-access geochemical dataset and compared it to literature data within the North Atlantic, helping us to understand mantle plume dynamics during the Palaeogene. We have furthered our understanding of dyke propagation and their chemical characteristics, spatially and temporally.

Objective 1

We have successfully compiled sixty-seven Palaeogene samples within our study and analysed them for major and trace elements. Furthermore, fifty-five samples were analysed for PGE to verify their PGE enrichment. Sample collection included twenty-nine samples from fieldwork alongside thirty-eight existing/archival samples. Data on twenty-six samples from the Antrim Lava Group supplemented our investigation.

H1: We hypothesised that PGE abundances would be elevated above mantle (MORB) concentrations. The results confirmed PGE concentrations in Irish and Northern Irish samples were indeed elevated relative to MORB, which reflects background mantle PGE abundance. Therefore, the hypothesis can be accepted.

H2: We hypothesised that the most mafic samples would have the highest PGE abundances; however, the PGE in the samples of this investigation did not strongly increase with increasing mafic content (Supplementary Material Fig. S10). The ΣPGE content of deposits peaked around 9 wt% MgO and decreased on either side of this. Therefore, we can reject this hypothesis.

H3: We hypothesised that older deposits would have higher Pt/Pd ratios than younger deposits. This was proven to be true and demonstrates a rapid transitional environment within the Irish and Northern Irish deposits. We accept this hypothesis.

Objective 2

Our second objective was met by quantitatively comparing the data in our study to literature data from the NAIP lavas (Greenland, Iceland and Scotland). This enabled us to demonstrate a spatial and temporal relationship of plume-driven deposits. We investigated important influences such as fractional crystallisation and S-saturation on the geochemistry of deposits, demonstrating the evolving nature of Palaeogene plume-mantle dynamics.

H4: We proposed that Irish and Northern Irish data would plot closely to Scottish data, as well as early formed Greenlandic deposits. There was a much larger spread of data than expected. In most cases, the Irish and Northern Irish samples overlapped well with all NAIP samples and showed variation across elemental trends, e.g., clustering close to Icelandic deposits for TiO_2, or overlapping well with Scottish deposits for Fe_2O_3. Chalcophile and Lithophile elements showed broad agreement with NAIP data, however, small anomalous subgroups provided insight into contrasting fractionation and saturation processes. Our data did align well with Scottish Pt and Pd values; however, West and East Greenland did not follow the same trends. Overall, I would reject this hypothesis; the geochemical characteristics of the Northern Irish and Irish deposits highlight an intermediate or transitional component of the NAIP, following some older trends as expected, but also aligning close to younger trends across different elements.

H5: We predicted that the Pt/Pd ratios of Irish and Northern Irish deposits would be close to chondritic (1.9). The results of this investigation have revealed that older extrusive samples (LBF) are very close to chondritic (1.853), older intrusive samples are slightly lower than chondritic (1.581), while younger intrusive samples are much lower (0.866). Overall, the data exhibit a transitional trend from older deposits close to chondritic, similar to data from West Greenland and Scotland, while younger deposits follow a declining Pt/Pd trend, close to Offshore East Greenland and Icelandic data. In light of this, we can accept the hypothesis for older samples and reject it for younger samples. This temporal shift enhances our understanding of changing mantle dynamics.

Objective 3

Lastly, this work has successfully updated digital maps of Palaeogene dykes in Ireland, Northern Ireland, the Isle of Man and offshore across the Irish Sea. Improving digital mapping capabilities using the updated Tellus geophysical dataset enabled strategic representative sampling of dyke swarms across the island and provided a foundation to interpret potential origin zones.

H6: We proposed that at least one dyke swarm would originate offshore. Our results have provided strong evidence for two swarms originating in North Atlantic seamounts. The Donegal-Kingscourt swarm aligns along strike with the Anton Dohrn and the Hebrides

Terrace, with ages of both submarine central complexes suggested to broadly coincide with emplacement of the dyke swarm. The St. John's Point Lisburn swarm also presents a case for an offshore origin in the Blackstones Bank complex, on account of orientation and broadly aligned age constraints. Overall, I would accept this hypothesis, however, more stringent geochronological data would be needed to further evaluate all propagation networks.

H7: Finally, we hypothesised that there is a greater density of dykes on the west Coast of Ireland than currently mapped. We can accept this hypothesis as a great array of dykes belonging to the Killala group that have been identified on the north coast of Mayo and across to the west coast. Additionally, the West Connacht dyke swarm has been digitally mapped and expanded upon, with many continuations offshore on the southwest coast of Galway. The dyke mapping exercise has been a great success; therefore, we can accept this hypothesis.

6.2. Summary and Future Work

To summarise our project, we have placed the first constraints on the PGE abundance of the Palaeogene mantle feeding Irish and Northern Irish volcanism, verifying its enrichment relative to MORB. We have found a correlation between the timing of magmatic activity and the PGE budget of the ascending plume magmas. This has identified Northern Ireland and Ireland as a transitional environment within the BIPIP and the broader NAIP. We have suggested this transition is linked with changing plume dynamics as the North Atlantic began to open, as well as the proximity of melting regions to SCLM. We have also produced an enhanced digital map of Palaeogene dyke-related magnetic anomalies and investigated potential onshore and offshore origins. Finally, our results suggest that the onshore Northern

Irish and Irish Palaeogene deposits are S-saturated and have segregated their sulphides prior to emplacement/extrusion. This suggests that earlier lava sequences, lateral magma conduits or deep staging chambers may hold concentrations of PGE. Considering these results, it is possible that mineralisation may be located offshore, close to the origins of dyke propagation, or within deep feeder networks below the ALG. Deep staging chambers such as Carlingford may also hold concentrations of PGE in layered sequences.

The results of this study are informative and set the foundation for further mineral exploration within Ireland and Northern Ireland. However, certain constraints have affected the scope of the research. Firstly, we did not include any data on the Upper Basalt Formation of the ALG; the data provided from the Cardiff group only focused on the Lower Basalt Formation from exploration drill cores. To fully understand the effects of timing and changing geodynamic environment on the PGE abundances, it would have been better to include younger extrusive samples in this comparison. Additionally, our samples lacked geochemical data on the rare-earth elements (REE). Including REE data would have allowed for further comparison with NAIP deposits and could have provided insight into magma source characteristics and mantle composition. Lastly, our samples from the GSNI archive were chosen to ensure representation of each swarm; however, as we extended our dyke mapping exercise, it revealed that the spatial distribution of samples is not representative of swarm extent, and we are missing potentially critical samples from the northwest of Northern Ireland and Ireland.

Despite the limitations, the positive outcomes of this study highlight numerous opportunities for future work in the region. Enhanced dyke mapping has provided a foundation to investigate prospective coastal zones in the north and northwest. Investigating fault zones and zones of dyke reorientation presents an opportunity to track potential mineralisation pathways. Furthermore, upon release of the full Tellus geophysical dataset – set to be released by December 2025 – a full map of dyke-related anomalies could be produced, including high-resolution mapping of the Dingle dyke system. This would be an interesting opportunity to further consider the plume's influence on the orientation of dyke swarms and investigate the relationship of Palaeogene dykes in the southwest of Ireland.

Additionally, this study could encourage further research into geochemical surveys along the length of dyke systems. This would present an opportunity for a better understanding of the changing geochemical properties of dykes as they propagate, providing potential insight into origin zones. Cu/Pd ratios would be especially interesting here as they could track S-saturation events along the length of a system, monitoring potential conduit-hosted mineralisation across the region. Lastly, this research has also highlighted the potential for further investigation into Irish layered intrusions, such as Carlingford, as prospective areas for Ni-Cu-PGE mineralisation. Verifying the initial PGE enrichment of older ascending plume magmas creates scope for investigating deep-staging chambers for potential mineralisation.

In conclusion, this study has highlighted the exciting future for Ni-Cu-PGE exploration in Ireland, Northern Ireland and surrounding offshore areas. Producing the first comprehensive geochemical and PGE survey of Palaeogene deposits has verified the original mantle enrichment of the proto-Icelandic plume feeding volcanism and establishes a strong foundation for continued exploration efforts in this field. It is hoped that this work will help de-risk future exploration efforts while contributing valuable data to both industry and academic research.

7. References

AMIS 2017. AMIS 0498: Certified Reference Material Platinum (PGM). Platreef Ore Bushveld Complex, South Africa. Certificate of Analysis Modderfontein, South Africa: A Division of Torre Analytical Services (Pty) Limited.

ANDERSEN, J. C. Ø., POWER, M. R. & MOMME, P. 2000. Platinum-Group Elements in the Palaeogene North Atlantic Igneous Province. *The Geology, Geochemistry, Mineralogy and Mineral Beneficiation of PGE,* 54**,** 637–667.

ANDERSON, H., WALSH, J. J. & COOPER, M. R. 2016. Faults, intrusions and flood basalts: the Cenozoic structure of the north of Ireland. *In:* YOUNG, M. E. (ed.) *Unearthed: impacts of the Tellus surveys of the north of Ireland.* Dublin: Royal Irish Academy.

ANDERSON, H., WALSH, J. J. & COOPER, M. R. 2018. The development of a regional-scale intraplate strike-slip fault system; Alpine deformation in the north of Ireland. *Journal of Structural Geology,* 116**,** 47–63.

ARNASON, J. G. & BIRD, D. K. 2000. A gold-and platinum-mineralized layer in gabbros of the Kap Edvard Holm Complex: Field, petrologic, and geochemical relations. *Economic Geology,* 95**,** 945–970.

BARNES, S. J., COUTURE, J. F., SAWYER, E. W. & BOUCHAIB, C. 1993. Nickel-Copper occurrences in the BA belt of Pontiac Sub province and the use of Cu-Pd ratios in interpreting PGE distributions. *Economic Geology,* 88**,** 1402–1418.

BARNES, S. J., CRUDEN, A. R., ARNDT, N. & SAUMUR, B. M. 2016. The mineral system approach applied to magmatic Ni–Cu–PGE sulphide deposits. *Ore Geology Reviews,* 76**,** 296–316.

BARNES, S. J., LE VAILLANT, M., GODEL, B. & LESHER, C. M. 2019. Droplets and Bubbles: Solidification of Sulphide-rich Vapour-saturated Orthocumulates in the Norilsk-Talnakh Ni–Cu–PGE Ore-bearing Intrusions. *Journal of Petrology,* 60**,** 269–300.

BARNES, S. J., MUNGALL, J. E. & MAIER, W. D. 2015. Platinum group elements in mantle melts and mantle samples. *Lithos,* 232**,** 395–417.

BARNES, S. J., NALDRETT, A. J. & GORTON, M. P. 1985. The origin of the fractionation of platinum-group elements in terrestrial magmas. *Chemical Geology,* 53**,** 303–323.

BARNES, S. J. & RIPLEY, E. M. 2016. Highly siderophile and strongly chalcophile elements in magmatic ore deposits. *Reviews in Mineralogy and Geochemistry,* 81**,** 725–74.

BUCHANAN, D. L. 1985. The Economic Potential of the Layered Mafic Rocks of the Carlingford Complex, Ireland Investigator:. Westland Exploration Ltd.

CARTER, E. J., STOCK, M. J., BERESFORD-BROWNE, A., COOPER, M. R., RAINE, R. & FEREYROLLES, A. 2024. Volcanic tempo driven by rapid fluctuations in mantle temperature during large igneous province emplacement. *Earth and Planetary Science Letters,* 644.

CHEN, C., FORSTER, M. W., SHCHEKA, S. S., EZAD, I. S., SHEA, J. J., LIU, Y., JACOB, D. E. & FOLEY, S. F. 2025. Sulfide-rich continental roots at cratonic margins formed by carbonated melts. *Nature,* 637**,** 615–621.

COE, K. 1969. The Geology of the Minor Intrusions of West Cork, Ireland. *Proceedings of the Geologists' Association,* 80**,** 441–457.

COOPER, M. R., ANDERSON, H., WALSH, J. J., VAN DAM, C. L., YOUNG, M. E., EARLS, G. & WALKER, A. 2012. Palaeogene Alpine tectonics and Icelandic plume-related magmatism and deformation in Northern Ireland. *Journal of the Geological Society,* 169**,** 29–36.

COOPER, M. R. & TAPSTER, S. Mapping and geochronological constraints on intrusion of the Fleetwood Dyke Swarm onshore Northern Ireland. VMSG-MDSG Joint Conference, 2025 Dublin.

GROUP ELEVEN CORP. 2020. Group Eleven Identifies Anomalous Palladium, Nickel and Cobalt at Ballinalack Zinc Project, Ireland. Vancouver, Canada.

DEWEY, J. F. 2000. Cenozoic tectonics of western Ireland. *Proceedings of the Geologists' Association,* 111**,** 291–306.

EUROPEAN COMMISSION. 2017. Study on the review of the list of Critical Raw Materials. Criticality Assessments. Brussels: Deloitte Sustainability, British Geological Survey, Bureau de Recherches Géologiques et Minières, Netherlands Organisation for Applied Scientific Research.

EUROPEAN COMMISSION. 2024. RMIS Dashboard. Brussels.

EUROPEAN COMMISSION. 2020. Study on the EU's list of Critical Raw Materials (2020): Final Report. Luxembourg.

GOVERNMENT OF IRELAND. 2022. Policy Statement on Mineral Exploration and Mining. Critical Raw Materials for the Circular Economy Transition. *In:* DEPARTMENT OF COMMUNICATIONS, C. A. A. E. (ed.). Dublin.

GRIFFIN, W. L., BEGG, G. C. & O'REILLY, S. Y. 2013. Continental-root control on the genesis of magmatic ore deposits. *Nature Geoscience,* 6**,** 905–910.

GUNN, A. G., LUSTY, P. A. J., SHAW, R., HOLBROOK, H. & D, R. 2020. Raw materials for decarbonisation: The potential for platinum-group metals and nickel in the UK. British Geological Survey.

HOFFMAN, E. L. & DUNN, B. 2002. Sample preparation and bulk analytical methods for PGE. *The Geology, Geochemistry, Mineralogy and Mineral Beneficiation of PGE,* 54**,** 1–11.

HOLNESS, M.B., ANDERSEN, J.C.Ø., NAMUR, O. AND NIELSEN, T.F. 2024. Are Microstructures in Plutonic Rocks Primary or Secondary? A Re-examination of the Metasomatism Hypothesis for the Roof-Sourced Autoliths in the Skaergaard Intrusion. *Journal of Petrology*, *65*(2), p.egae001.

HUGHES, H. S. R., BOYCE, A. J., MCDONALD, I., DAVIDHEISER-KROLL, B., HOLWELL, D. A., MCDONALD, A. & OLDROYD, A. 2015a. Contrasting mechanisms for crustal sulphur contamination of mafic magma: evidence from dyke and sill complexes from the British Palaeogene Igneous Province. *Journal of the Geological Society,* 172**,** 443–458.

HUGHES, H. S. R., MCDONALD, I., BOYCE, A. J., HOLWELL, D. A. & KERR, A. C. 2016a. Sulphide Sinking in Magma Conduits: Evidence from Mafic–Ultramafic Plugs on Rum and the Wider North Atlantic Igneous Province. *Journal of Petrology,* 57**,** 383–416.

HUGHES, H. S. R., MCDONALD, I., FAITHFULL, J. W., UPTON, B. G. J. & LOOCKE, M. 2016b. Cobalt and precious metals in sulphides of peridotite xenoliths and inferences concerning their distribution according to geodynamic environment: A case study from the Scottish lithospheric mantle. *Lithos,* 240-243**,** 202–227.

HUGHES, H. S. R., MCDONALD, I., GOODENOUGH, K. M., CIBOROWSKI, T. J. R., KERR, A. C., DAVIES, J. H. F. L. & SELBY, D. 2014. Enriched lithospheric mantle keel below the Scottish margin of the North Atlantic Craton: Evidence from the Palaeoproterozoic Scourie Dyke Swarm and mantle xenoliths. *Precambrian Research,* 250**,** 97–126.

HUGHES, H. S. R., MCDONALD, I. & KERR, A. C. 2015b. Platinum-group element signatures in the North Atlantic Igneous Province: Implications for mantle controls on metal budgets during continental breakup. *Lithos,* 233**,** 89–110.

HURST, E. 1997. Renewal Report for Prospecting Licence 3843. BHP.

KIRSTEIN, L. A. & TIMMERMAN, M. J. 2000. Evidence of the proto-Iceland plume in northwestern Ireland at 42 Ma from helium isotopes. *Journal of the Geological Society,* 157**,** 923–928.

LINDSAY, J. J., HUGHES, H. S. R., YEOMANS, C. M., ANDERSEN, J. C. Ø. & MCDONALD, I. 2021. A machine learning approach for regional geochemical data: Platinum-group element geochemistry vs geodynamic settings of the North Atlantic Igneous Province. *Geoscience Frontiers,* 12.

LONG, C. B., MCCONNELL, B. J., ALSOP, G. I., O'CONNOR, P. I., CLARINGBOLD, K. & CRONIN, C. 1999. *Geology of South Donegal: A geological description of South*

Donegal, to accompany the Bedrock Geology 1:100,000 Scale Map Series, Sheet 3 and part of Sheet 4, South Donegal. Geological map series of Ireland 1 : 100,000, no. Sheet 3 and part of sheet 4, Geological Survey of Ireland.
LORAND, J. P., LUGUET, A. & ALARD, O. 2008. Platinum-Group Elements: A New Set of Key Tracers for the Earth's Interior. *Elements,* 4**,** 247–252.
LUSTY, P. A. J. 2016. Critical metals for hightechnology applications: mineral exploration potential in the north of Ireland. *In:* YOUNG, M. E. (ed.) *Unearthed: impacts of the Tellus surveys of the north of Ireland.* Dublin: Royal Irish Academy.
MAIER, W. D. 2003. The Concentration of the Platinum-Group Elements in South African Komatiites: Implications for Mantle Sources, Melting Regime and PGE Fractionation during Crystallization. *Journal of Petrology,* 44**,** 1787–1804.
MAIER, W. D. 2005. Platinum-group element (PGE) deposits and occurrences: Mineralization styles, genetic concepts, and exploration criteria. *Journal of African Earth Sciences,* 41**,** 165–191.
MAIER, W. D. & GROVES, D. I. 2011. Temporal and spatial controls on the formation of magmatic PGE and Ni–Cu deposits. *Mineralium Deposita,* 46**,** 841–857.
MAIER, W. D., ROELOFSE, F. & BARNES, S. J. 2003. The Concentration of the Platinum-Group Elements in South African Komatiites: Implications for Mantle Sources, Melting Regime and PGE Fractionation during Crystallization. *Journal of Petrology,* 44**,** 1787–1804.
MAKKONEN, H. V., HALKOAHO, T., KONNUNAHO, J., RASILAINEN, K., KONTINEN, A. & EILU, P. 2017. Ni-(Cu-PGE) deposits in Finland–geology and exploration potential. *Ore Geology Reviews,* 90**,** 667–690.
MOHR, P. 1982. Tertiary Dolerite Intrusions of West-Central Ireland. *Proceedings of the Royal Irish Academy. Section B: Biological, Geological and Chemical Science,* 82**,** 53–82.
MOHR, P. 1987. The Cill Ala Dike Swarm, Cos Sligo and Mayo: Physical Parameters. *The Irish Naturalists' Journal,* 22**,** 326–334.
MOHR, P. 1988. The Analcime-Olivine Dolerites of West Connacht, Ireland: Classification and Genetic. *Irish Journal of Earth Sciences,* 9**,** 133–140.
MOHR, P. 2000. Late Palaeozoic and Palaeocene magmatic intrusion levels in West Connacht and inferences for palaeotopography. *Proceedings of the Geologists' Association,* 111**,** 337–343.
MOHR, P., HUNT, J., RIEKSTINS, H. & KENNAN, P. S. 2018. Distinguishing dolerite dike populations in post-grampian Connemara. *Irish Journal of Earth Sciences,* 36**,** 1–16.

MOMME, P., TEGNER, C., BROOKS, K. C. & KEAYS, R. R. 2002. The behaviour of platinum-group elements in basalts from the East Greenland rifted margin. *Contributions to Mineralogy and Petrology,* 143**,** 133–153.

MOORE, K. R., MOLES, N. R. & LUSTY, P. A. J. 2016. A natural labratory for critical metals investigations in the Mourne Mountains granites. *In:* YOUNG, M. E. (ed.) *Unearthed: impacts of the Tellus surveys of the north of the north of Ireland.* Dublin: Royal Irish Academy.

MOORE, K. R., MOLES, N. R., ROLLINSON, G. K. & LUSTY, P. A. J. 2023. Mechanisms for concentrating critical metals in granitic complexes: insights from the Mourne Mountains, Northern Ireland. *Geoenergy,* 1**,** 1–28.

MORRIS, P. 1974. A Tertiary Dyke System in South-West Ireland. *Proceedings of the Royal Irish Academy. Section B: Biological, Geological and Chemical Science,* 74**,** 179–184.

MUDD, B. G. M. 2012a. Sustainability Reporting and the Platinum Group Metals: A Global Mining Industry Leader? *Platinum Metals Review,* 56**,** 2–19.

MUDD, G. M. 2012b. Key trends in the resource sustainability of platinum group elements. *Ore Geology Reviews,* 46**,** 106–117.

MUDD, G. M., JOWITT, S. M. & WERNER, T. T. 2018. Global platinum group element resources, reserves and mining - A critical assessment. *Sci Total Environ,* 622-623**,** 614–625.

NEAVE, D. A. & PUTIRKA, K. D. 2017. A new clinopyroxene-liquid barometer, and implications for magma storage pressures under Icelandic rift zones. *American Mineralogist,* 102**,** 777–794.

NIELSEN, T. F. D., ANDERSEN, J. C. Ø., HOLNESS, M. B., KEIDING, J. K., RUDASHEVSKY, N. S., RUDASHEVSKY, V. N., SALMONSEN, L. P., TEGNER, C. & VEKSLER, I. V. 2015. The Skaergaard PGE and Gold Deposit: the Result of in situ Fractionation, Sulphide Saturation, and Magma Chamber-scale Precious Metal Redistribution by Immiscible Fe-rich Melt. *Journal of Petrology,* 56**,** 1643–1676.

NIST 2014. Certificate of Analysis: Standard Reference Material® 2684c *In:* GONZALEZ, C. A. (ed.) *Bituminous Coal (Nominal Mass Fraction 3 % Sulfur)* Gaithersburg, MD 20899 National Institute of Standards & Technology.

ORE RESEARCH & EXPLORATION PTY LTD. 2009. Certificate of analysis for PGE-Cu-Ni reference material OREAS 13b Victoria, Australia.

PASSMORE, E. 2009. *Feeding large eruptions: crystallisation, mixing and degassing in Icelandic magma chambers.* Doctoral Thesis, University of Edinburgh.

POWER, M. R., PIRRIE, D. & ANDERSEN, J. C. Ø. 2003. Diversity of platinum-group element mineralization styles in the North Atlantic Igneous Province: new evidence from Rum, UK. *Geological Magazine,* 140**,** 499–512.

PRACHT, M., WRIGHT, G., O'CONNOR, P., CLARINGBOLD, K. & WARREN, W. P. 1996. *Geology Of Dingle Bay A Geological Description To Accompany The Bedrock Geology 1:100,000 Map Series, Sheet 20, Dingle Bay*, Geological Survey of Ireland.

PRESTON, J. 1967. The Blind Rock Dyke, Co. Donegal. *The Irish Naturalists' Journal,* 15**,** 286–293.

RESPONSIBLE MINING FOUNDATION & INVESTMENT, COLUMBIA CENTER ON SUSTAINABLE INVESTMENT. 2020. Mining and the SDGs: A 2020 status update.

SAUNDERS, A. D., FITTON, J. G., KERR, A. C., NORRY, M. J. & KENT, R. W. 1997. The North Atlantic Igneous Province. *Large Igneous Provinces: Continental, Oceanic, and Planetary Flood Volcanism,* 100**,** 45–93.

SINGH, T. D., MANIKYAMBA, C., SUBRAMANYAM, K. S. V., GANGULY, S., KHELEN, A. C. & RAMAKRISHNA REDDY, N. 2018. Mantle heterogeneity, plume-lithosphere interaction at rift controlled ocean-continent transition zone: Evidence from trace-PGE geochemistry of Vempalle flows, Cuddapah Basin, India. *Geoscience Frontiers,* 9**,** 1809–1827.

STEPHENSON, M. H., LUDDEN, J., MCKINLEY, J. M., NATARAJAN, I., NASH, S., LEARY, D., SHI, Y. & WANG, C. 2023. The need for joined-up thinking in critical raw materials research. *Geoenergy,* 1.

White Paper. 2016. Mapping mining to the Sustainable Development Goals: An atlas. New York: Columbia Center on Sustainable Investment; Sustainable Development Solutions Network; United Nations Development Programme; World Economic Forum.

WILLIAMSON, M.-C. & SAUMUR, B. M. 2019. Introduction to the Special issue of the Canadian Journal of Earth Sciences, “Magmatic and metallogenic processes associated with large igneous provinces”. *Canadian Journal of Earth Sciences,* 56**,** v–vi.

8. Appendix

Supplementary Material

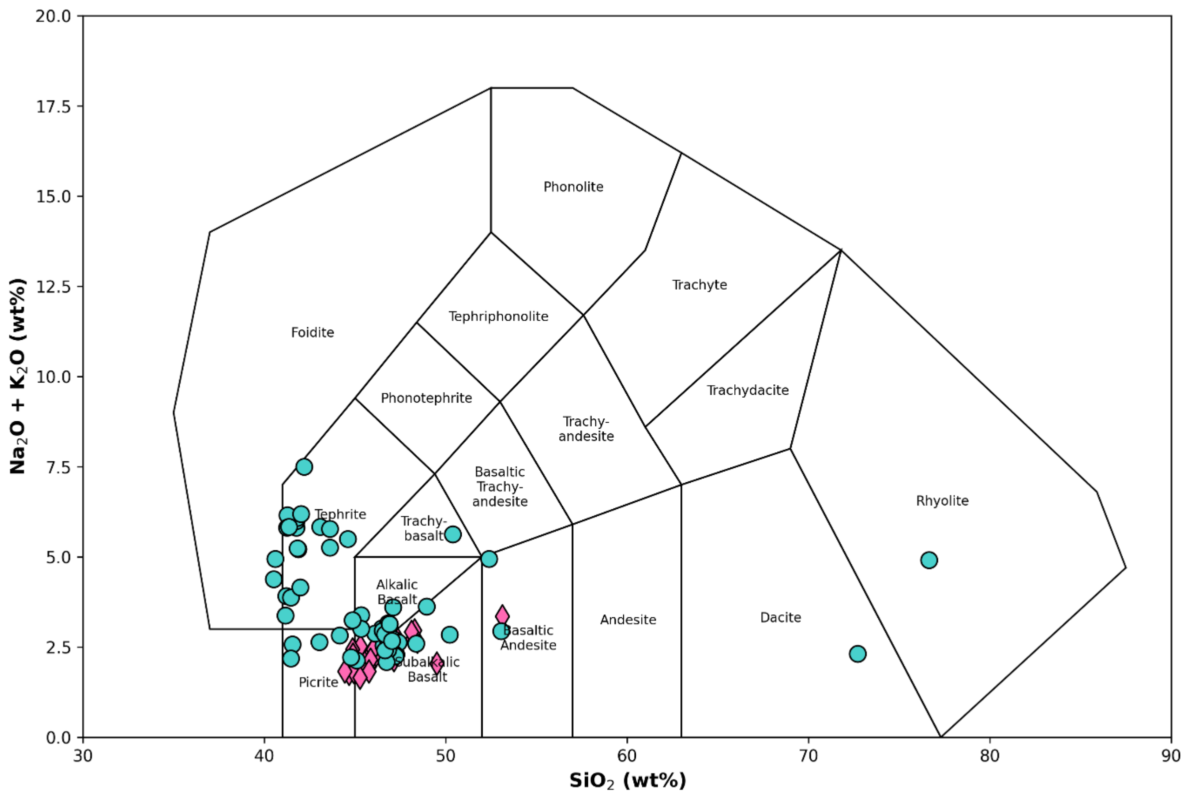

Figure 12 Supplementary Material Figure S6 Total Alkali Silica diagram showing the classification of volcanic samples within this study (after Le Bas et al., 1986). Dykes and minor intrusions represented as teal circles and ALG samples represented as pink diamonds (See legend in Fig. 4).

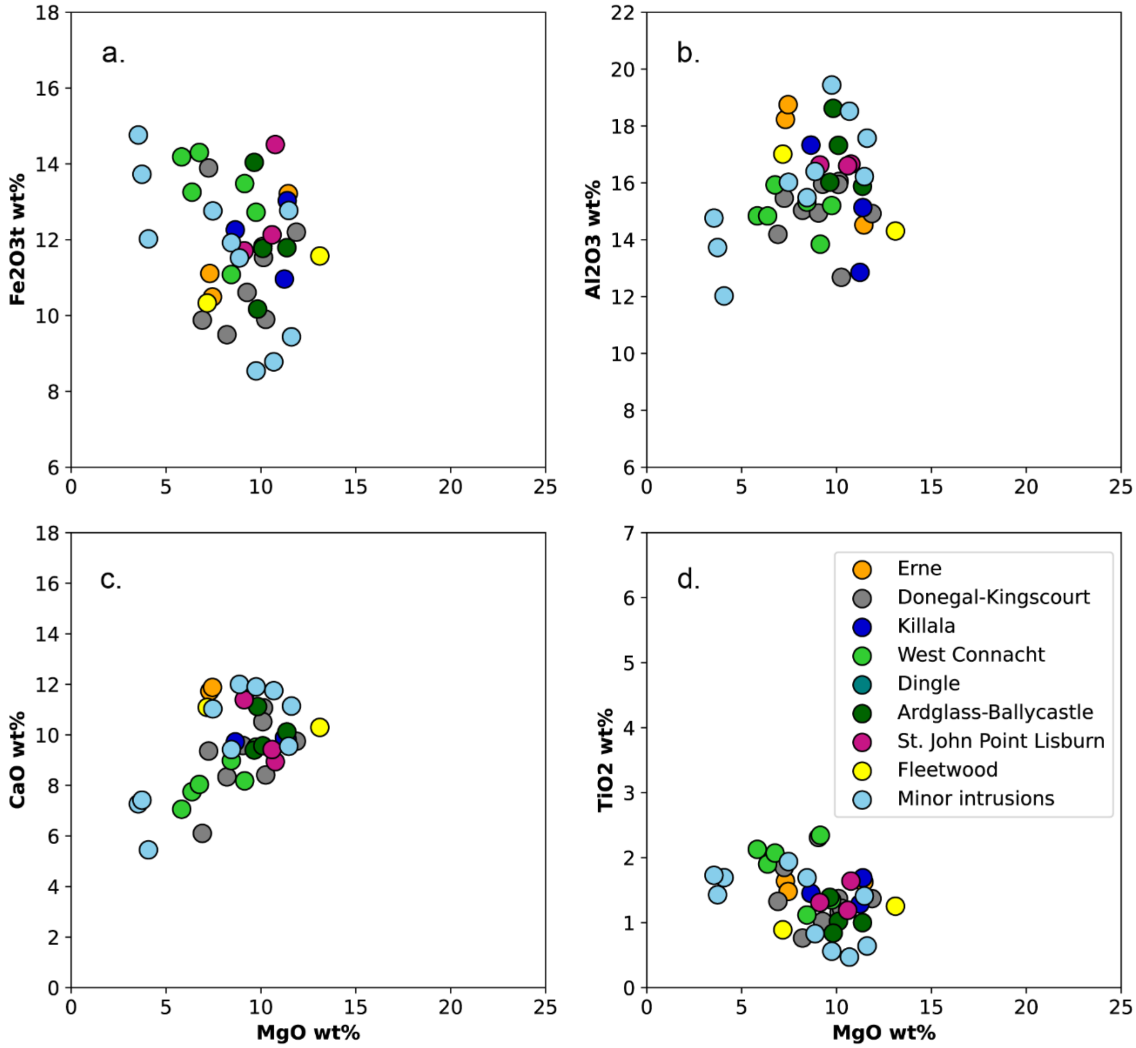

Figure 13 Supplementary Material Figure S7 Major element plots for intrusive samples within Northern Ireland and Ireland. a) Fe_2O_3, b) Al_2O_3, c) CaO, d) TiO_2. Dykes are categorised according to swarm (See Fig. 3a). Minor intrusions comprise Portrush sill, Magilligan Sill, Slemish plug and Carlingford cone sheets.

Supplementary Material D

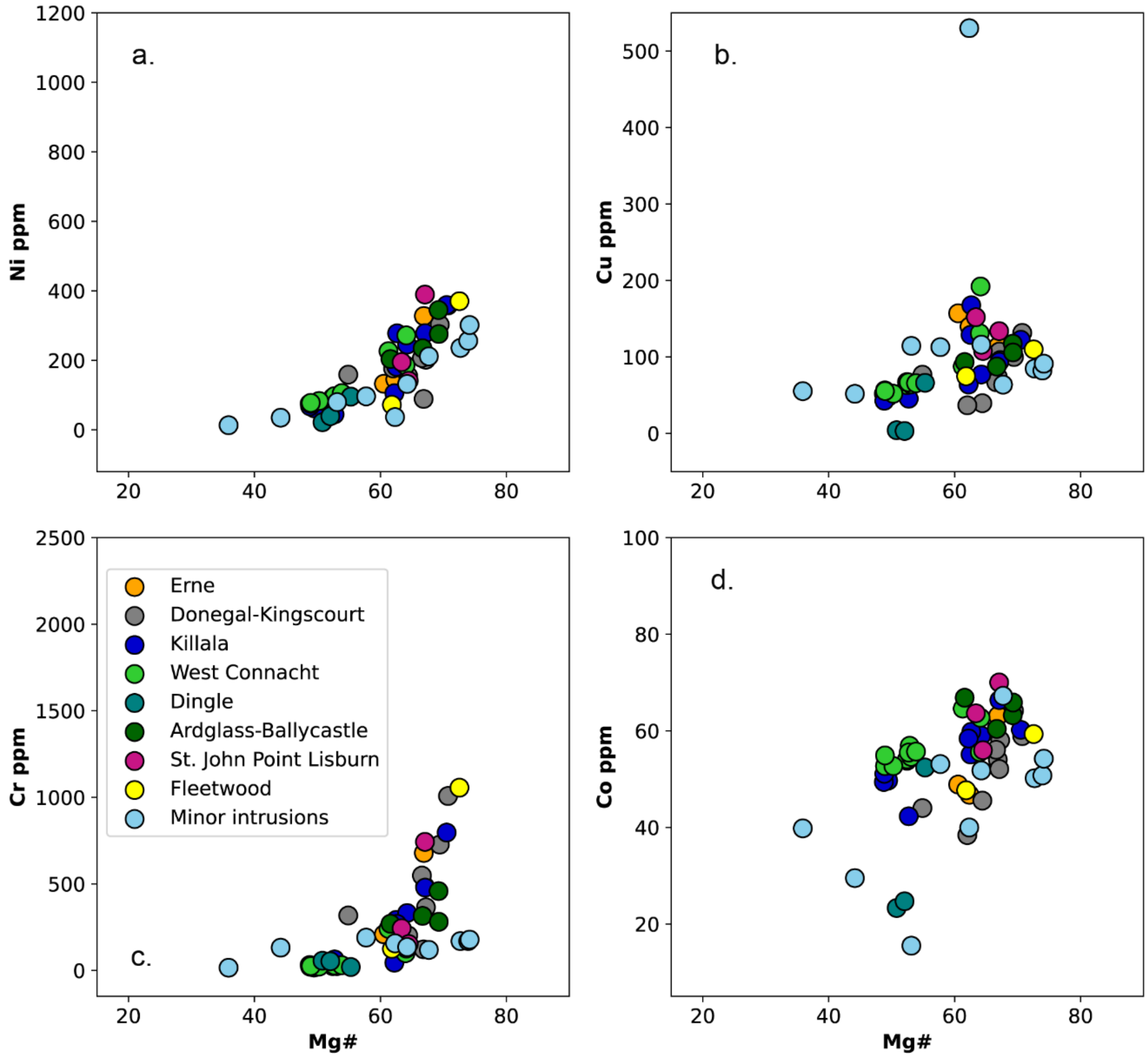

Figure 14 Supplementary Material Figure S8 Chalcophile element plots for intrusive samples within Northern Ireland and Ireland. a) Ni, b) Cu, c) Cr, d) Co. Dykes are categorised according to swarm (See Fig. 3a). Minor intrusions comprise Portrush sill, Magilligan Sill, Slemish plug and Carlingford cone sheets.

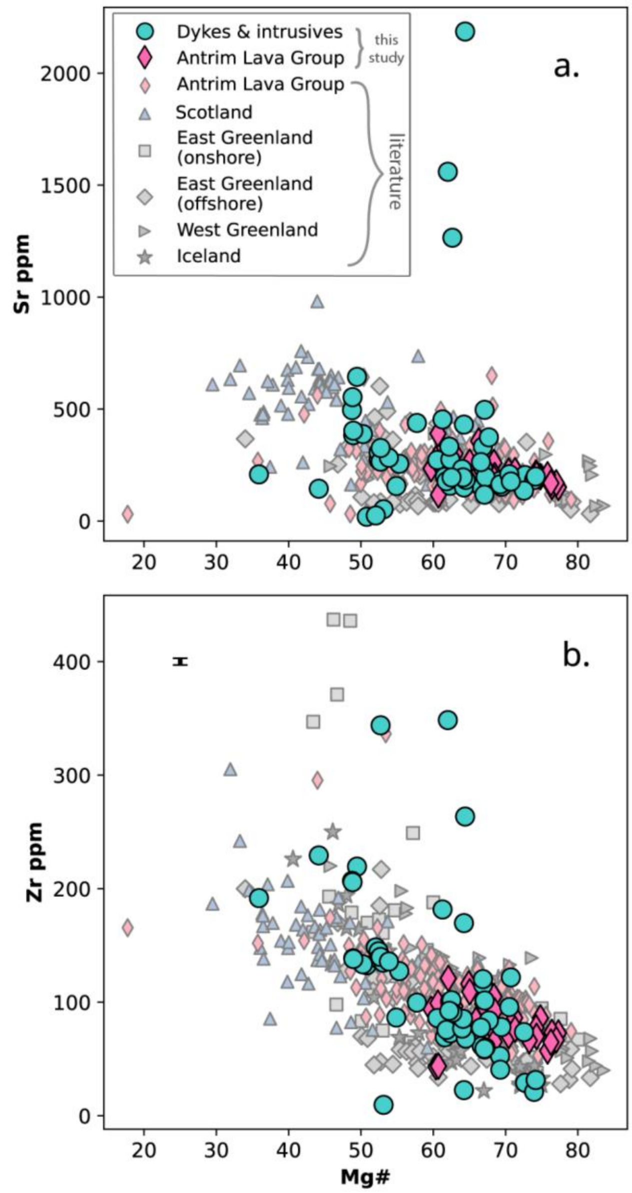

Figure 15 Supplementary Material Figure S9 Lithophile element binary plots against Mg# for NAIP volcanics. a) Sr, b) Zr.

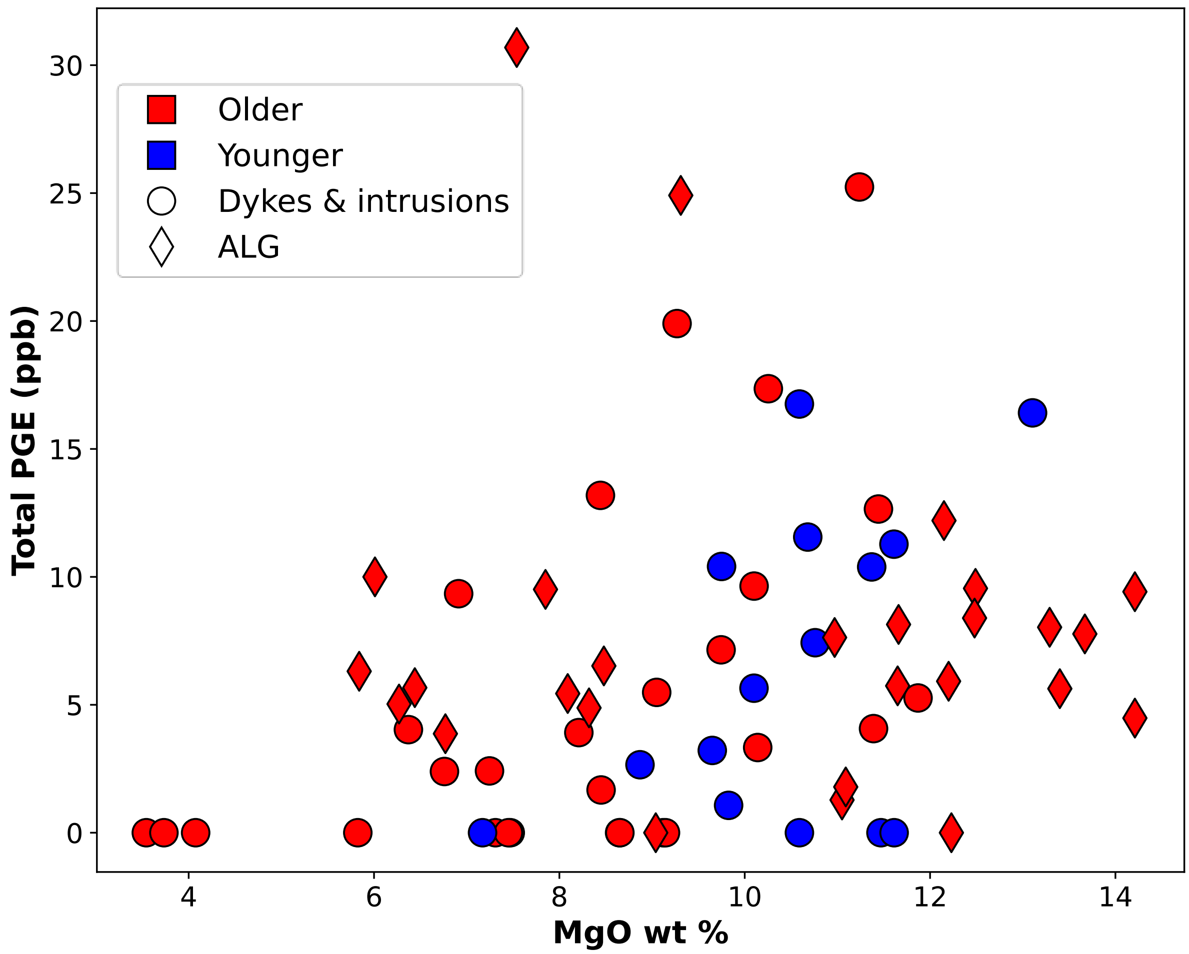

Figure 16 Supplementary Material Figure S10 Total PGE abundance (ppb) for all Northern Irish and Irish samples in this study. Samples categorised by extrusion or emplacement period. The older period contains samples from the lower basalt formation (ALG), Erne, Donegal-Kingscourt, West Connacht and Dingle dyke swarms and Carlingford cone sheets. The younger period comprises Ardglass-Ballycastle, St. John's Point Lisburn, Fleetwood, Portrush sill, Magilligan sill and Slemish plugs. No strong correlation is identified between total MgO (wt %) – a measure of mafic content- and ΣPGE content. Neither is a strong correlation between ΣPGE content and age observed, however the five the highest ΣPGE content do belong to samples from the older period. Data coloured according to age of extrusion/emplacement and markers according to sample type (ALG or Dykes and minor intrusions) – see legend.

Supplementary Material Table S1
Results of Total Sulphur Analysis

Sample Name	Total Sulphur	Mass Fraction
	g/g	%
24-WIT-01	0.000814	0.08
24-WIT-02	0.000825	0.08
24-WIT-03	0.001168	0.12
24-WIT-04	0.001126	0.11
24-WIT-07	0.001347	0.13
24-WIT-08	0.001533	0.15
24-WIT-09	0.001119	0.11
24-WIT-10	0.001180	0.12
24-WIT-12	0.000992	0.10
24-WIT-13	0.000949	0.09
24-WIT-14	0.001048	0.10
24-WIT-15	0.001079	0.11
24-WIT-16	0.000990	0.10
24-WIT-17	0.001165	0.12
24-WIT-18	0.001275	0.13
24-WIT-19	0.001403	0.14
24-WIT-20	0.001151	0.12
24-WIT-21	0.001437	0.14
24-WIT-22	0.001012	0.10
24-WIT-23	0.001820	0.18
24-WIT-24	0.001260	0.13
24-WIT-25	0.002407	0.24
24-WIT-26	0.001199	0.12
24-WIT-28	0.001700	0.17
24-WIT-29	0.001505	0.15
24-WIT-30c	0.000876	0.09
24-WIT-30d	0.000881	0.09
24-WIT-31	0.005267	0.53
24-WIT-32	0.000858	0.09
24-PM-01	0.001032	0.10
Typical 1σ error		-10.07%

Supplementary Material Table S2
Results of Passmore (2009) geochemical statistical significance – Homogeneity and Sample Preparation

PGE±Au analysis results

Sample Name	*MRC 404*	*MRC 464*	*MRC 510*	*MRC 613*	*A1007505*	*MRC 404 D1*	*MRC 404 D2*	*MRC 404 D3*	*MRC 404 D4*
Batch	1	1	1	1	1	2a	2a	2a	2a
Type	Sample	Sample	Sample	Sample	Sample	Repeat	Repeat	Repeat	Repeat
Ir	< 1.000	< 1.000	< 1.000	< 1.000	< 1.000	< 1.000	< 1.000	< 1.000	< 1.000
Ru	1.873	1.415	< 1.000	< 1.000	< 1.000	2.558	2.336	2.175	2.196
Rh	< 1.000	< 1.000	< 1.000	< 1.000	< 1.000	< 1.000	< 1.000	< 1.000	< 1.000
Pt	9.257	5.342	< 1.000	4.383	2.416	10.372	9.826	9.86	9.481
Pd	8.77	9.999	< 1.000	6.895	< 1.000	8.842	8.288	8.304	7.878
Au	3.217	2.045	< 1.000	1.592	< 1.000	2.271	2.542	2.693	2.112

Sample Name	*MRC 464 D*	*MRC 510 D*	*MRC 613 D*	*A1007505 D*	*24-D-01*	*24-D-02*	*24-D-03*	*24-D-04*
notes					MRC 404 duplicate	MRC 464 duplicate	MRC 613 duplicate	A100750 duplicate
Batch	2a	2a	2a	2a	2b	2b	2b	2b
Type	Duplicate	Duplicate	Duplicate	Duplicate	Duplicate	Duplicate	Duplicate	Duplicate
Ir	< 1.000	< 1.000	< 1.000	< 1.000	< 1.000	< 1.000	< 1.000	< 1.000
Ru	4.096	2.232	2.165	1.567	3.296	3.845	2.046	1.435
Rh	< 1.000	< 1.000	< 1.000	< 1.000	< 1.000	< 1.000	< 1.000	< 1.000
Pt	5.745	< 1.000	5.083	2.439	12.692	7.196	7.19	2.99
Pd	10.191	< 1.000	8.212	< 1.000	8.339	9.506	8.264	< 1.000
Au	2.339	< 1.000	1.996	< 1.000	3.018	2.862	2.72	1.013

Geochemical variation calculations (See Passmore (2009) for equations)

Element	*n*	*min*	*max*	$\bar{X}$	*So (whole)*	*So (repeats)*	*Sr*	*St*	*St/Sr*
Ir	0	0	0						

Ru	14	1.415	4.096	2.31625	0.820573	0.83024	0.1763	0.801411	4.545729
Rh	0	0	0						
Pt	15	2.416	12.692	9.88475	3.1459	3.206769	0.367192	3.124397	8.508883
Pd	12	6.895	10.191	8.328	3.072028	0.9212	0.395336	3.046484	7.70606
Au	13	1.013	3.217	2.4045	0.844892	0.605093	0.261736	0.803329	3.069234

Element	*P%*	*V%*	*c (0.05)*	*c (0.01)*	S_{rs}	S_{rp}	S_h	S_{t*}	S_{t*}/S_{rs}
Ir			0.351846	0.114832					
Ru	7.611428	34.59949	0.351846	0.114832	0.592474	0.1763	0.565635	0.567728	0.958234
Rh			0.351846	0.114832					
Pt	3.714736	31.60826	0.351846	0.114832	1.05095	0.367192	0.984716	2.965163	2.821411
Pd	4.747072	36.58122	0.351846	0.114832	0.482051	0.395336	0.27583	3.033972	6.293883
Au	10.88525	33.40938	0.351846	0.114832	0.51794	0.261736	0.446941	0.667519	1.288796

Geochemical significance levels

	Significance	*f*	*c*	*f/c*	*f/c-1*	*Threshold*
Maclennan et al 2003	0.99	9	2.087901	4.31055	3.31055	1.819492
	0.95	9	3.325113	2.706675	1.706675	1.306398
Passmore 2009	0.99	7	1.239042	5.649525	4.649525	2.156276
	0.95	7	2.16735	3.229751	2.229751	1.493235
Morrison	0.99	3	0.114832	26.12517	25.12517	5.012501
	0.95	3	0.351846	8.52645	7.52645	2.743438
	0.93	3	0.448739	6.685405	5.685405	2.384409

Pt variation plot

1:1 graph	*Platinum*	
	Pt (x)	**P (y)**
2 SD	0	0
0.734385	1	1
	2	2
	3	3
	4	4
	5	5
	6	6
	7	7
	8	8
	9	9
	10	10
	11	11
	12	12
1 Vs 2a	**1**	**2a**
MRC 404	9.257	9.88475
MRC 464	5.342	5.745
MRC 613	4.383	5.083
A1007505	2.416	2.439
1 Vs 2b	**1**	**2b**
MRC 404	9.257	12.692
MRC 464	5.342	7.196
MRC613	4.383	7.19
A1007505	2.416	2.99
2a Vs 2b	**2a**	**2b**
MRC 404D	9.88475	12.692
MRC 464D	5.745	7.196
MRC 613D	5.083	7.19
A1007505 D	2.439	2.99

Pd variation plot

1:1 graph	*Palladium*	
	Pd (x)	**Pd (y)**
2 SD	0	0

0.790672	1	1
	2	2
	3	3
	4	4
	5	5
	6	6
	7	7
	8	8
	9	9
	10	10
	11	11
	12	12
1 Vs 2a	**1**	**2a**
MRC 404	8.77	8.328
MRC 464	9.999	10.191
MRC 613	6.895	8.212
1 Vs 2b	**1**	**2b**
MRC 404	8.77	8.339
MRC 464	9.999	9.506
MRC 613	6.895	8.264
2a Vs 2b	**2a**	**2b**
MRC 404 D	8.328	8.339
MRC 464 D	10.191	9.506
MRC 613 D	8.212	8.264

Ru variation plot

1: graph	*Ruthenium*	
	Ru (x)	**Ru (y)**
2 SD	0	0
0.352599	1	1
	2	2
	3	3
	4	4
	5	5
1 Vs 2a	**1**	**2a**
MRC 404	1.873	2.31625
MRC 464	1.415	2.196

MRC 613	1	2.165
A1007505	1	1.567
1 Vs 2b	**1**	**2b**
MRC 404	1.873	3.296
MRC 464	1.415	3.845
MRC613	1	2.046
A1007505	1	1.435
2a Vs 2b	**2a**	**2b**
MRC 404D	2.31625	3.296
MRC 464D	2.196	3.845
MRC 613D	2.165	2.046
A1007505 D	1.567	1.435

Au variation plot

1:1 graph	*Gold*	
	Au (x)	**Au (y)**
2 SD	0	0
0.523472	1	1
	2	2
	3	3
	4	4
	5	5
1 Vs 2a	**1**	**2a**
MRC 404	3.217	2.4045
MRC 464	2.045	2.339
MRC 613	1.592	1.996
A1007505	1	1
1 Vs 2b	**1**	**2b**
MRC 404	3.217	3.018
MRC 464	2.045	2.862
MRC613	1.592	2.72
A1007505	1	1.013
2a Vs 2b	**2a**	**2b**
MRC 404D	2.4045	3.018

MRC 464D	2.339	2.862
MRC 613D	1.996	2.72
A1007505 D	1	1.013

Chi-square calculations

	probability	*df*	*chi*
Passmore 2009	0.99	7	1.239042
	0.95	7	2.16735
Maclennan 2003	0.99	9	2.087901
	0.95	9	3.325113
Morrison	0.99	3	0.114832
	0.95	3	0.351846
	0.93	3	0.448739

Supplementary Material Table S3
Results of Major Element Analysis

Sample name	***Swarm***	***SiO_2***	***TiO_2***	***Al_2O_3***	***Fe_2O_3t***	***MgO***	***CaO***	***Na_2O***	***K_2O***	***Mg #***
		wt %	wt %	wt %	wt %	wt %	wt %	wt %	wt %	
A1007507	Erne	45.10	1.62	14.52	13.22	11.44	9.59	1.95	0.18	66.89
A1007505	Donegal-Kingscourt	45.34	1.85	15.46	13.89	7.25	9.36	3.02	0.37	54.89
A1007506	Donegal-Kingscourt	53.06	0.76	15.03	9.50	8.21	8.34	2.11	0.84	66.86
MRC404	Donegal-Kingscourt	48.37	1.02	15.95	10.61	9.27	11.76	2.35	0.25	67.09
MRC407	Erne	46.48	1.64	18.23	11.11	7.31	11.73	2.73	0.29	60.55
MRC462	St. John's Point Lisburn	44.77	1.64	16.66	14.51	10.76	8.94	2.03	0.19	63.37
MRC464	St. John's Point Lisburn	46.65	1.19	16.60	12.13	10.59	9.42	2.64	0.22	67.07
MRC467	Sill	48.95	1.69	15.48	11.92	8.45	9.42	3.03	0.60	62.32
MRC471	Sill	46.82	1.94	16.02	12.76	7.47	11.03	2.60	0.56	57.73
MRC472	Ardglass-Ballycastle	46.56	1.00	15.88	11.79	11.37	10.12	2.30	0.24	69.23
MRC475	Ardglass-Ballycastle	46.11	1.39	16.02	14.04	9.65	9.40	2.64	0.24	61.59
MRC482	Ardglass-Ballycastle	47.11	1.02	17.32	11.77	10.10	9.57	2.53	0.19	66.69
MRC483	Erne	46.51	1.48	18.75	10.49	7.45	11.88	2.68	0.27	62.36
MRC496	Fleetwood	50.22	0.89	17.01	10.33	7.17	11.09	2.31	0.54	61.82

MRC507	Donegal-Kingscourt	43.08	2.31	14.94	11.67	9.05	9.58	4.49	1.34	64.40
MRC510	Killala	46.90	1.45	17.33	12.26	8.65	9.72	2.79	0.35	62.21
MRC513	Killala	45.33	1.69	15.13	13.03	11.39	9.81	2.87	0.14	67.10
MRC517	Donegal-Kingscourt	47.27	1.16	16.05	11.53	10.14	11.07	2.09	0.20	67.23
MRC521	Sill	47.39	0.83	16.40	11.52	8.87	12.00	2.41	0.22	64.24
MRC523	Plug	47.20	0.56	19.44	8.54	9.75	11.90	2.13	0.16	72.70
MRC558	Donegal-Kingscourt	46.79	1.37	14.92	12.20	11.87	9.75	2.30	0.25	69.42
MRC574	St. John's Point Lisburn	46.91	1.31	16.63	11.71	9.12	11.39	2.36	0.16	64.50
MRC607	Sill	44.86	1.41	16.22	12.77	11.47	9.55	2.96	0.29	67.69
MRC612	Plug	47.23	0.47	18.52	8.78	10.68	11.75	2.06	0.19	73.94
MRC613	Plug	46.81	0.64	17.57	9.44	11.61	11.14	2.22	0.20	74.15
22CCCI.35	Cone Sheet	50.38	1.69	12.02	12.02	4.08	5.45	2.70	2.93	44.16
22CCI.23	Cone Sheet	52.38	1.73	14.76	14.76	3.54	7.27	3.28	1.67	35.89
22CCI.6	Cone Sheet	47.10	1.43	13.73	13.73	3.47	7.42	2.46	1.15	53.13
MRC622	Fleetwood	46.74	1.25	14.31	11.57	13.11	10.30	1.84	0.25	72.54
MRC490	Ardglass-Ballycastle	46.64	0.84	18.62	10.17	9.83	11.12	2.27	0.15	69.27
MRC552	Donegal-Kingscourt	47.04	1.37	15.95	11.82	10.10	10.52	2.37	0.30	66.59
24-PM-01	West Connacht (IBF)	41.21	2.13	14.84	14.19	5.83	7.06	3.65	0.27	48.93

24-PM-02	West Connacht (IBF)	41.56	1.12	15.32	11.08	8.44	8.98	2.36	0.22	63.99
24-PM-04	West Connacht (CI)	41.45	1.90	14.84	13.25	6.37	7.75	3.67	0.20	52.86
24-PM-05	West Connacht (CM)	41.17	2.34	13.84	13.48	9.15	8.18	2.97	0.41	61.28
24-WIT-01	Dingle	72.71	0.44	7.92	4.98	2.20	0.16	1.86	0.45	50.79
24-WIT-02	Dingle	76.65	0.46	8.26	5.33	2.48	0.17	4.81	0.11	52.05
24-WIT-04	Dingle	43.61	1.89	15.91	13.35	7.08	8.09	4.99	0.27	55.30
24-Wit-08	West Connacht (CM)	43.04	1.35	15.20	12.72	9.75	9.52	2.48	0.16	64.11
24-WIT-10	West Connacht (CI)	44.60	2.07	15.93	14.30	6.76	8.04	5.25	0.25	52.44
24-WIT-12	West Connacht (CI)	43.62	2.03	15.62	14.01	6.62	8.18	5.52	0.25	52.44
24-WIT-14	West Connacht (CI)	41.86	1.93	14.98	13.53	6.56	7.89	4.97	0.24	53.08
24-WIT-15	West Connacht (CI)	41.83	1.92	14.92	13.37	6.38	7.97	5.03	0.20	52.70
24-WIT-16	West Connacht (CI)	41.76	1.90	14.87	13.42	6.72	7.80	5.61	0.20	53.87
24-WIT-17	West Connacht (CI)	41.77	2.02	15.25	13.79	5.98	7.08	5.76	0.24	50.27
24-WIT-18	West Connacht (CI)	41.82	2.12	15.12	14.19	5.83	6.96	5.85	0.24	48.94
24-WIT-19	Killala	41.27	2.94	14.80	13.93	5.84	6.84	5.85	0.31	49.45
24-WIT-20	Killala	41.26	2.70	14.47	14.11	5.75	7.56	5.51	0.30	48.76

24-WIT-21	Killala	41.98	1.43	14.36	11.41	8.16	9.94	4.01	0.15	62.53
24-WIT-22	Killala	41.36	2.60	14.64	13.91	5.69	7.50	5.56	0.27	48.83
24-WIT-23	Killala	40.61	2.15	13.53	13.36	10.29	6.64	4.62	0.33	64.24
24-WIT-25	Killala	42.03	2.71	13.09	14.03	6.70	6.05	5.23	0.96	52.71
24-WIT-28	Killala	40.51	1.58	14.17	12.20	8.77	10.18	4.24	0.14	62.64
24-WIT-29	Killala	41.46	1.29	12.85	10.96	11.24	9.89	2.02	0.16	70.51
24-WIT-30d	Inver Dyke	42.20	1.33	14.19	9.88	6.91	6.10	5.54	1.96	62.01
24-WIT-32	Blind Dyke	44.14	1.22	12.68	9.90	10.26	8.41	2.03	0.80	70.73
ANT 9.75	Lower Basalt	46.08	1.41	12.90	11.12	12.49	11.29	1.88	0.34	74.82
ANT 35.55	Lower Basalt	45.76	1.25	12.57	10.88	14.21	10.09	1.70	0.28	77.30
ANT 54.20	Lower Basalt	44.67	1.21	12.62	10.90	13.67	9.35	1.58	0.18	76.40
ANT 61.40	Lower Basalt	45.30	1.26	13.57	10.62	11.65	10.68	2.07	0.45	74.22
ANT 70.05	Lower Basalt	44.85	1.24	13.20	10.95	12.20	10.55	1.99	0.44	74.28
ANT 80.00	Lower Basalt	45.92	1.24	13.51	10.53	13.40	9.67	1.97	0.41	77.01
ANT 89.90	Lower Basalt	44.88	1.20	13.04	10.96	13.29	10.68	1.90	0.39	75.80
ANT 101.70	Lower Basalt	45.83	1.25	13.52	11.40	14.21	9.99	1.94	0.35	76.27
NIRE-01-08-0006	Lower Basalt	47.36	1.39	15.68	11.87	9.04	9.29	2.28	0.43	66.27
NIRE-03/08-0004	Lower Basalt	45.02	1.23	11.69	14.01	12.23	7.09	1.80	0.29	67.83
NIRE-09/08-	Lower Basalt	45.52	1.86	14.49	13.33	11.05	8.87	1.83	0.24	68.39

0001 (59)										
NIRE-08/08-0002	Lower Basalt	46.01	1.65	16.68	12.46	7.85	6.46	1.91	0.53	62.08
NIRE-01/08-0003	Lower Basalt	46.43	1.54	16.07	11.97	8.48	8.42	2.18	0.58	64.90
NIRE-03/14-0001	Lower Basalt	48.43	1.55	15.01	11.96	6.77	10.13	2.36	0.29	59.69
NIRE-11/08-0001	Lower Basalt	49.51	1.08	13.89	10.18	9.31	9.56	1.88	0.17	70.43
NIRE-02/08-0001	Lower Basalt	53.11	1.31	16.90	10.32	5.84	8.87	3.11	0.24	60.36
NIRE-03/08-0003	Lower Basalt	44.92	1.44	13.18	12.72	12.48	7.22	1.53	0.29	71.26
NIRE-03/08-0002	Lower Basalt	45.84	1.61	13.98	12.94	10.97	7.90	1.83	0.32	68.49
NIRE-01/08-0005	Lower Basalt	46.37	1.38	15.61	11.22	8.32	8.04	2.29	0.62	65.91
NIRE-04/08-0002	Lower Basalt	44.43	1.30	13.83	11.90	11.66	8.07	1.49	0.34	71.31
NIRE-01/08-0002	Lower Basalt	46.62	1.41	15.27	11.35	8.09	8.78	2.17	0.66	65.04
NIRE-09/08-0001 (120)	Lower Basalt	48.28	1.72	16.48	10.39	6.27	10.87	2.58	0.39	63.01
NIRE-03/08-0001	Lower Basalt	48.18	1.97	16.42	9.28	6.01	11.96	2.56	0.18	66.81

MBC49	Lower Basalt	45.76	0.96	17.93	11.93	7.54	7.69	1.73	0.10	60.71
NIRE-05/08-0002	Lower Basalt	45.26	1.54	13.76	13.00	11.09	8.32	1.49	0.17	68.42
NIRE-04/08-0001	Lower Basalt	47.15	1.17	13.63	11.32	12.15	9.44	1.89	0.25	73.28
08/08-0001	Lower Basalt	48.10	1.39	14.99	11.01	6.44	10.26	2.30	0.62	60.64
Typical 1σ error (%)		0.26	-0.98	0.52	0.59	3.37	0.37	-3.76	1.26	

Supplementary Material Table S3
Results of Major Element Analysis (continued)

Sample name	*Mn3O4*	*P2O5*	*SO3*	*Cr2O3*	*SrO*	*ZrO2*	*BaO*	*NiO*	*CuO*
	wt %	wt %	wt %	wt %	wt %	wt %	wt %	wt %	wt %
A1007507	0.203	0.167	0.300	0.103	0.027	0.014	0.006	0.047	0.021
A1007505	0.227	0.244	0.143	0.016	0.037	0.014	0.043	0.014	0.013
A1007506	0.158	0.104	0.238	0.044	0.017	0.009	0.015	0.023	0.011
MRC404	0.180	0.070	0.000	0.070	0.000	0.010	0.010	0.030	0.010
MRC407	0.180	0.140	0.100	0.030	0.030	0.010	0.010	0.020	0.020
MRC462	0.210	0.110	0.100	0.030	0.020	0.010	0.010	0.030	0.020
MRC464	0.210	0.090	0.100	0.130	0.010	0.010	0.010	0.060	0.020
MRC467	0.130	0.150	0.100	0.030	0.010	0.010	0.010	0.010	0.070
MRC471	0.190	0.360	0.100	0.030	0.050	0.010	0.050	0.010	0.010
MRC472	0.190	0.090	0.100	0.080	0.010	0.010	0.250	0.050	0.010

MRC475	0.200	0.160	0.100	0.040	0.010	0.010	0.010	0.030	0.010
MRC482	0.170	0.100	0.100	0.050	0.010	0.010	0.010	0.030	0.010
MRC483	0.170	0.130	0.100	0.040	0.030	0.010	0.010	0.020	0.020
MRC496	0.240	0.110	0.050	0.020	0.010	0.010	0.010	0.010	0.010
MRC507	0.180	1.260	0.100	0.030	0.260	0.050	1.660	0.020	0.010
MRC510	0.210	0.140	0.100	0.010	0.030	0.010	0.080	0.020	0.010
MRC513	0.200	0.150	0.100	0.070	0.050	0.010	0.010	0.040	0.010
MRC517	0.210	0.100	0.100	0.060	0.010	0.010	0.010	0.030	0.010
MRC521	0.200	0.050	0.100	0.020	0.010	0.010	0.010	0.020	0.010
MRC523	0.150	0.070	0.100	0.020	0.010	0.010	0.010	0.030	0.010
MRC558	0.190	0.110	0.100	0.120	0.010	0.010	0.010	0.040	0.010
MRC574	0.200	0.090	0.100	0.020	0.010	0.010	0.010	0.020	0.010
MRC607	0.190	0.140	0.100	0.020	0.040	0.010	0.010	0.030	0.010
MRC612	0.150	0.040	0.100	0.030	0.010	0.010	0.010	0.040	0.010
MRC613	0.160	0.070	0.100	0.030	0.020	0.010	0.010	0.040	0.010
22CCCI.35	0.315	0.292	0.003	0.016	0.015	0.030	0.047	0.004	0.016
22CCI.23	0.262	0.289	0.145	0.004	0.018	0.024	0.044	0.004	0.004
22CCI.6	0.223	0.179	0.024	0.003	0.009	0.014	0.030	0.003	0.003
MRC622	0.219	0.100	0.052	0.198	0.005	0.010	0.010	0.052	0.010
MRC490	0.152	0.060	0.051	0.051	0.010	0.010	0.010	0.040	0.010
MRC552	0.196	0.110	0.052	0.093	0.031	0.010	0.010	0.031	0.005
24-PM-01	0.194	0.239	0.042	0.004	0.032	0.015	0.000	0.014	0.008

24-PM-02	0.185	0.116	0.068	0.014	0.019	0.007	-0.003	0.023	0.020
24-PM-04	0.192	0.241	0.026	0.002	0.024	0.017	0.003	0.014	0.009
24-PM-05	0.193	0.267	0.045	0.032	0.046	0.023	-0.004	0.038	0.012
24-WIT-01	0.030	0.118	0.007	0.005	-0.001	0.017	-0.001	0.005	-0.001
24-WIT-02	0.045	0.124	0.072	0.006	0.000	0.020	-0.007	0.006	0.000
24-WIT-04	0.195	0.226	0.099	0.003	0.022	0.015	0.015	0.013	0.011
24-Wit-08	0.204	0.128	0.066	0.019	0.017	0.008	0.000	0.038	0.031
24-WIT-10	0.225	0.264	0.091	0.001	0.025	0.018	-0.001	0.014	0.009
24-WIT-12	0.199	0.246	0.081	0.002	0.029	0.017	0.003	0.013	0.010
24-WIT-14	0.192	0.233	0.059	0.004	0.026	0.016	0.001	0.014	0.008
24-WIT-15	0.195	0.237	0.110	0.001	0.020	0.016	0.004	0.012	0.009
24-WIT-16	0.190	0.233	0.080	0.000	0.021	0.014	0.000	0.013	0.009
24-WIT-17	0.188	0.229	0.114	0.002	0.036	0.016	-0.002	0.012	0.006
24-WIT-18	0.195	0.242	0.108	0.002	0.036	0.016	0.002	0.012	0.006
24-WIT-19	0.192	0.372	0.109	0.001	0.060	0.028	0.053	0.008	0.007
24-WIT-20	0.200	0.364	0.090	0.003	0.044	0.026	0.013	0.010	0.009
24-WIT-21	0.192	0.166	0.186	0.038	0.013	0.010	0.000	0.025	0.020
24-WIT-22	0.195	0.357	0.115	0.001	0.052	0.022	0.005	0.009	0.005
24-WIT-23	0.175	0.292	0.224	0.050	0.042	0.021	0.014	0.034	0.014

24-WIT-25	0.163	0.975	0.200	0.006	0.031	0.043	0.042	0.006	0.005
24-WIT-28	0.158	0.176	0.288	0.035	0.130	0.013	0.002	0.036	0.025
24-WIT-29	0.177	0.158	0.046	0.111	0.023	0.010	-0.001	0.047	0.018
24-WIT-30d	0.163	0.975	0.026	0.031	0.148	0.041	0.099	0.023	0.005
24-WIT-32	0.159	0.146	0.010	0.137	0.010	0.013	0.008	0.047	0.023
ANT 9.75	0.165	0.123							
ANT 35.55	0.147	0.111							
ANT 54.20	0.141	0.115							
ANT 61.40	0.185	0.119							
ANT 70.05	0.185	0.122							
ANT 80.00	0.157	0.124							
ANT 89.90	0.159	0.114							
ANT 101.70	0.168	0.119							
NIRE-01-08-0006	0.155	0.185							
NIRE-03/08-0004	0.160	0.151							
NIRE-09/08-0001 (59)	0.189	0.164							
NIRE-08/08-0002	0.169	0.189							
NIRE-01/08-0003	0.267	0.181							
NIRE-03/14-0001	0.146	0.187							
NIRE-11/08-0001	0.158	0.131							

NIRE-02/08-0001	0.171	0.176							
NIRE-03/08-0003	0.233	0.211							
NIRE-03/08-0002	0.222	0.216							
NIRE-01/08-0005	0.161	0.166							
NIRE-04/08-0002	0.163	0.149							
NIRE-01/08-0002	0.183	0.186							
NIRE-09/08-0001 (120)	0.144	0.192							
NIRE-03/08-0001	0.319	0.193							
MBC49	0.103	0.111							
NIRE-05/08-0002	0.142	0.117							
NIRE-04/08-0001	0.166	0.138							
08/08-0001	0.177	0.177							
Typical 1σ error (%)	1.62	4.21	0.67	0.03	0.017	0.045	0.032	0.01	0.006

Supplementary Material Table S4
Results of Trace Element Analysis

Sample name	Co	Ni	Cu	Cr	La	Ce	Sr	Y	Zr
	ppm	ppm	ppm	ppm	ppm	ppm	ppm	ppm	ppm
A1007507	63.10	327.70	113.60	678.50	7.10	13.00	237.50	33.90	115.40
A1007505	44.00	159.00	76.70	317.50	10.80	19.70	156.40	26.50	86.50
A1007506	54.00	89.00	73.70	121.80	14.80	23.00	332.70	39.20	120.40
MRC404	52.08	202.48	106.87	484.13	3.93	9.13	169.05	22.17	58.39
MRC407	48.88	132.66	156.99	208.65	5.19	13.70	272.68	28.30	86.11
MRC462	63.63	195.06	151.88	243.77	2.13	6.79	190.84	27.88	82.58
MRC464	70.01	389.41	133.68	742.67	2.62	6.60	117.81	22.29	59.03
MRC467	39.98	36.83	529.92	156.28	6.28	14.65	157.79	26.20	100.63
MRC471	53.11	96.45	112.77	189.72	9.72	23.44	438.11	27.86	99.70
MRC472	63.22	344.75	117.23	458.37	3.20	7.67	179.81	22.01	52.67
MRC475	66.85	203.74	93.28	269.50	3.12	8.48	197.17	23.96	69.13
MRC482	60.39	234.87	87.41	315.21	3.51	8.29	150.26	19.80	61.45
MRC483	46.75	145.37	139.65	263.94	4.83	12.30	275.24	26.23	72.70
MRC496	47.69	72.10	74.69	124.88	13.10	25.00	177.95	37.57	75.70
MRC507	45.54	155.21	39.43	202.58	94.15	148.14	2185.77	24.56	263.55
MRC510	58.41	105.40	63.84	44.60	6.79	16.46	332.29	24.32	92.47
MRC513	66.35	278.41	93.55	478.59	3.64	11.90	496.65	24.93	101.56
MRC517	58.04	202.05	95.79	364.65	4.96	12.03	196.04	25.37	60.09
MRC521	51.79	132.07	116.00	134.89	2.32	5.58	150.02	16.29	22.62

MRC523	50.18	235.78	84.74	169.55	2.27	5.63	205.45	14.40	29.06
MRC558	64.16	302.81	99.89	726.76	4.64	12.15	153.28	26.78	78.13
MRC574	55.99	141.30	107.67	152.31	2.21	6.98	184.01	26.29	68.00
MRC607	67.25	211.45	63.68	118.73	6.03	16.48	373.98	17.87	83.96
MRC612	50.75	256.34	82.14	169.82	1.39	3.58	183.40	11.50	21.06
MRC613	54.23	301.56	91.14	178.12	2.14	5.75	199.08	15.39	31.50
22CCCl.35	29.50	35.10	51.70	131.60	45.30	89.90	144.40	68.20	229.30
22CCl.23	39.80	13.40	55.20	15.80	30.00	55.40	208.40	59.90	191.70
22CCl.6	15.50	80.00	114.40		51.30		52.90	142.60	9.60
MRC622	59.32	370.30	109.87	1055.78	3.88	10.82	136.06	21.45	73.73
MRC490	65.86	275.92	105.84	280.91	2.44	6.31	164.28	18.49	40.62
MRC552	56.07	206.90	66.85	547.91	5.17	13.64	263.24	27.36	77.71
24-PM-01	52.70	74.80	56.20	23.50	10.20	16.50	383.60	43.10	138.70
24-PM-02	55.60	185.80	130.90	99.60	4.70	13.40	232.20	32.80	76.80
24-PM-04	56.90	89.70	64.50	30.20	8.60	18.90	281.10	42.30	139.30
24-PM-05	64.60	226.50	87.50	240.40	8.60	22.90	453.90	35.30	181.70
24-WIT-01	23.30	21.90	4.10	56.10	6.70	15.20	19.10	15.00	132.60
24-WIT-02	24.70	39.40	3.10	53.00	4.80	9.00	25.00	14.50	148.30
24-WIT-03	52.40	94.80	63.50	14.70	7.70	11.30	285.80	38.40	124.70
24-WIT-04	52.40	95.70	66.10	19.70	6.10	10.40	255.70	39.00	127.40
24-WIT-07	64.40	315.60	186.40	112.40	5.80	7.30	203.10	35.20	82.00
24-Wit-08	62.70	271.90	192.10	126.60	4.20	3.70	195.00	35.60	85.40

24-WIT-09	53.80	90.40	67.70	26.40	7.20	18.10	256.20	41.60	139.30
24-WIT-10	53.80	93.30	63.10	24.80	9.30	12.80	273.70	43.70	144.90
24-WIT-12	54.10	88.70	67.10	28.00	8.90	9.30	306.40	41.60	138.00
24-WIT-13	51.60	96.30	62.90	22.50	6.40	12.40	398.60	39.30	125.00
24-WIT-14	54.60	92.30	64.00	24.80	9.10	16.20	294.90	40.30	134.90
24-WIT-15	55.50	97.10	66.70	29.10	11.40	20.20	265.40	42.00	139.90
24-WIT-16	55.70	105.80	65.60	30.10	8.50	18.60	282.70	40.40	135.90
24-WIT-17	52.70	83.20	51.80	22.40	6.40	14.60	388.50	41.20	133.40
24-WIT-18	54.90	77.70	55.30	25.20	9.00	15.60	403.70	42.30	138.10
24-WIT-19	49.70	62.30	47.90	16.60	11.60	24.90	644.00	37.70	219.50
24-WIT-20	49.40	75.40	51.90	30.90	13.50	28.40	495.40	44.70	206.90
24-WIT-21	55.10	181.60	128.80	292.30	7.60	12.80	194.80	32.00	101.80
24-WIT-22	51.10	67.70	42.60	21.60	10.80	24.40	553.30	46.10	205.80
24-WIT-23	59.00	245.40	77.00	331.70	10.60	23.30	430.80	31.70	169.70
24-WIT-24	39.50	46.00	43.20	41.20	35.90	85.20	484.50	61.10	423.00
24-WIT-25	42.30	44.60	45.30	63.80	29.40	72.00	326.30	56.50	343.90
24-WIT-26	61.60	307.90	159.10	272.10	8.10	12.70	340.10	33.90	115.60
24-WIT-28	59.80	277.80	167.50	268.80	4.30	13.60	1265.20	32.80	90.80
24-WIT-29	60.20	359.00	122.40	796.40	7.30	11.00	209.10	29.20	95.80
24-WIT-30c	41.10	252.20	38.20	313.90	80.00	141.40	1521.60	30.40	333.30
24-WIT-30d	38.40	176.80	36.70	254.10	84.00	148.10	1559.60	31.40	348.50

24-WIT-31	14.70	51.50	32.20	73.50	34.90	58.40	1037.40	29.70	147.90
24-WIT-32	58.90	358.10	131.40	1007.60	13.00	24.10	176.70	34.30	121.90
ANT 9.75	55.29	268.90	446.27	1019.43	6.20	15.82	203.57	28.14	90.49
ANT 35.55	53.64	228.88	269.19	1005.99	4.59	12.31	152.23	22.94	71.36
ANT 54.20	62.03	196.01	110.98	1157.16	5.44	14.27	166.26	25.65	77.07
ANT 61.40	58.38	205.98	99.32	1047.24	6.20	16.13	223.84	27.29	82.05
ANT 70.05	59.09	187.04	331.11	965.72	5.61	14.94	215.13	26.29	73.96
ANT 80.00	53.92	150.67	353.19	820.63	5.06	13.52	172.05	25.14	70.58
ANT 89.90	57.28	186.06	307.28	1133.42	5.11	13.51	208.74	24.76	63.86
ANT 101.70	59.10	191.60	279.49	1141.82	4.47	12.16	169.55	25.38	67.71
NIRE-01-08-0006	55.03	243.54	140.47	374.64	8.48	20.36	369.10	29.89	118.15
NIRE-03/08-0004	90.07	857.05	61.87	1682.66	5.64	14.34	225.69	22.51	85.64
NIRE-09/08-0001 (59)	70.84	310.83	114.86	457.29	5.33	15.27	264.35	26.33	106.29
NIRE-08/08-0002	49.45	144.04	106.83	198.04	9.82	22.92	335.72	29.16	127.51
NIRE-01/08-0003	55.94	252.26	99.06	434.58	8.44	20.73	258.81	31.67	114.87
NIRE-03/14-0001	48.41	85.96	40.91	187.26	7.60	18.58	236.62	35.55	96.74
NIRE-11/08-0001	51.98	290.50	57.46	784.76	5.08	12.82	230.43	24.82	72.02

NIRE-02/08-0001	40.28	136.12	76.50	6.26	3.40	9.08	268.28	24.83	43.42
NIRE-03/08-0003	70.63	471.25	107.91	961.08	7.15	18.17	196.27	26.79	91.78
NIRE-03/08-0002	65.05	422.14	83.66	863.23	6.59	17.14	212.37	24.33	94.99
NIRE-01/08-0005	49.19	202.20	106.94	254.20	7.59	18.82	247.03	27.73	87.78
NIRE-04/08-0002	62.07	398.32	110.03	673.33	6.75	17.66	237.65	27.22	82.97
NIRE-01/08-0002	50.04	109.38	81.24	212.89	9.38	22.24	272.53	31.97	114.98
NIRE-09/08-0001 (120)	55.03	67.76	127.49	187.30	6.49	16.71	303.67	29.97	98.95
NIRE-03/08-0001	35.38	91.38	65.68	268.56	7.22	17.54	241.66	31.23	102.40
MBC49	61.97	478.70	99.83	705.11	2.16	5.73	124.35	23.03	46.01
NIRE-05/08-0002	82.78	758.55	113.64	714.39	4.05	11.13	198.74	26.98	70.57
NIRE-04/08-0001	59.56	372.30	103.66	1123.37	4.21	11.26	174.63	25.22	68.05
08/08-0001	49.84	83.24	66.27	157.61	9.25	21.16	409.23	29.74	104.44
Typical 1σ error (%)	10.72	75.58	63.58	94.64	19.94	11.30	1.93	23.57	5.63

Supplementary Material Table S4
Results of Trace Element Analysis (continued)

Sample name	*Li*	*Mg*	*Al*	*P*	*Ca*	*V*	*Ga*	*As*	*Se*
	ppm	ppm	ppm	ppm	ppm	ppm	ppm	ppm	ppm
A1007507						284.30	17.60	5.00	-1.40
A1007505						198.90	16.00	5.10	-1.80
A1007506						294.30	20.90	3.20	-2.40
MRC404	7.78	55128.92	78162.84	306.30	79775.17	265.61	13.71	0.30	1.75
MRC407	5.97	43913.11	89410.59	652.60	81617.80	281.40	13.49	0.59	0.50
MRC462	21.82	61235.66	77446.80	328.38	56917.20	298.04	13.23	0.55	1.71
MRC464	32.38	61154.40	78126.74	417.54	61639.29	213.79	12.57	0.61	0.50
MRC467	15.73	46300.97	69348.59	757.02	59207.01	282.78	15.28	2.35	0.50
MRC471	7.11	45118.38	79088.15	1490.72	73911.06	318.27	16.24	0.15	0.50
MRC472	19.67	65993.22	76249.92	406.91	68368.62	228.35	11.30	3.60	0.50
MRC475	8.43	60638.08	81909.55	674.07	68897.59	208.00	13.68	0.15	0.50
MRC482	49.36	59215.37	83651.32	409.47	60977.68	188.71	11.44	1.60	3.79
MRC483	5.39	44735.79	92097.10	360.78	80396.54	279.31	15.97	0.15	0.50
MRC496	44.08	40815.81	80995.10	388.06	71506.66	232.69	15.28	22.94	0.50
MRC507	47.33	54657.32	72302.99	4642.59	62928.12	159.29	13.08	2.41	0.50
MRC510	47.84	52254.27	86244.22	532.15	68115.37	278.74	14.41	0.60	0.50
MRC513	23.46	69111.14	75605.28	551.33	66719.98	268.44	14.36	0.15	1.63
MRC517	36.79	60799.89	78817.18	406.82	77152.08	256.55	12.62	0.53	0.50
MRC521	5.10	52360.93	80166.26	214.79	83388.84	219.09	11.62	0.15	0.50

MRC523	2.00	58753.08	94219.85	376.96	77087.72	171.23	12.26	0.15	0.50
MRC558	10.96	70227.91	70508.99	453.49	64293.01	260.67	15.01	0.15	0.50
MRC574	11.21	56068.42	81802.62	478.29	75082.93	297.61	16.65	0.15	0.50
MRC607	6.89	68179.59	77283.65	558.01	59021.80	224.44	14.15	0.15	0.50
MRC612	2.00	62813.47	88803.34	274.67	76209.17	161.05	12.50	0.15	0.50
MRC613	2.00	68043.42	83385.37	323.53	70872.69	178.29	12.19	0.15	1.20
22CCCI.35						205.40	25.40	2.40	-2.10
22CCI.23						366.30	23.20	4.50	-1.60
22CCI.6						28.40	1.50	-2.30	53.20
MRC622	30.10	73497.53	65496.39	366.07	63573.74	246.74	13.70	0.81	0.50
MRC490	12.97	62032.80	95519.13	247.06	81724.07	203.24	13.73	0.41	0.50
MRC552	7.61	57484.14	72421.37	327.43	65472.47	261.31	13.66	0.15	1.54
24-PM-01						213.50	19.80	6.00	-2.00
24-PM-02						244.30	18.40	0.40	-1.90
24-PM-04						217.70	19.10	3.20	-2.00
24-PM-05						260.20	19.00	0.30	-2.00
24-WIT-01						68.80	12.00	4.60	-1.40
24-WIT-02						67.10	11.20	5.20	-1.30
24-WIT-03						197.70	17.80	4.30	-1.20
24-WIT-04						201.80	17.90	2.70	-1.70
24-WIT-07						251.40	18.20	3.00	-1.60

24-Wit-08		267.20	17.90	1.70	-1.10
24-WIT-09		213.60	18.70	3.10	-1.60
24-WIT-10		208.20	18.50	-0.70	-1.80
24-WIT-12		216.50	18.40	4.20	-2.10
24-WIT-13		220.40	18.00	2.80	-1.70
24-WIT-14		211.10	19.70	5.00	-3.00
24-WIT-15		213.60	20.00	2.50	-2.10
24-WIT-16		205.90	19.80	3.30	-2.10
24-WIT-17		200.60	19.90	6.00	-1.60
24-WIT-18		215.00	20.10	1.70	-2.40
24-WIT-19		261.70	20.50	5.70	-2.70
24-WIT-20		243.90	17.60	1.70	-1.40
24-WIT-21		287.60	18.60	2.10	-1.90
24-WIT-22		229.10	18.50	1.30	-2.40
24-WIT-23		268.70	18.20	3.20	-2.20
24-WIT-24		239.60	24.50	4.10	-2.30
24-WIT-25		287.00	22.50	3.60	-2.00
24-WIT-26		288.60	19.50	3.60	-2.50
24-WIT-28		272.80	18.90	2.70	-0.80
24-WIT-29		258.40	16.80	1.80	-1.60

24-WIT-30c		107.00	20.60	8.00	-0.50
24-WIT-30d		120.70	20.40	8.00	-0.80
24-WIT-31		131.00	16.40	4.70	-0.90
24-WIT-32		247.50	18.50	1.80	-2.30
ANT 9.75			15.45		
ANT 35.55			13.57		
ANT 54.20			15.22		
ANT 61.40			16.44		
ANT 70.05			15.43		
ANT 80.00			14.01		
ANT 89.90			14.28		
ANT 101.70			14.80		
NIRE-01-08-0006			20.75		
NIRE-03/08-0004			14.86		
NIRE-09/08-0001 (59)			19.61		
NIRE-08/08-0002			21.48		
NIRE-01/08-0003			19.95		

NIRE-03/14-0001		19.32
NIRE-11/08-0001		14.81
NIRE-02/08-0001		11.91
NIRE-03/08-0003		17.06
NIRE-03/08-0002		16.45
NIRE-01/08-0005		17.71
NIRE-04/08-0002		17.17
NIRE-01/08-0002		19.59
NIRE-09/08-0001 (120)		18.74
NIRE-03/08-0001		18.27
MBC49		15.90
NIRE-05/08-0002		18.07
NIRE-04/08-0001		15.53

08/08-0001							19.23
Typical 1σ error (%)	224.53	0.04	0.01	0.48	0.01	1.08	47.58

Supplementary Material Table S5
Results of PGE ± Au analysis

Sample name	***Swarm***	***Ir***	***Ru***	***Rh***	***Pt***	***Pd***	***Au***
		ppb	ppb	ppb	ppb	ppb	ppb
A1007507	Erne	< 1.000	1.060	< 1.000	6.384	5.208	2.265
A1007505	Donegal-Kingscourt	< 1.000	< 1.000	< 1.000	2.416	< 1.000	< 1.000
A1007506	Donegal-Kingscourt	< 1.000	< 1.000	< 1.000	1.702	2.211	< 1.000
MRC404	Donegal-Kingscourt	< 1.000	1.873	< 1.000	9.257	8.770	3.217
MRC407	Erne	< 1.000	< 1.000	< 1.000	< 1.000	< 1.000	1.311
MRC462	St. John's Point Lisburn	< 1.000	< 1.000	< 1.000	3.782	3.645	1.510
MRC464	St. John's Point Lisburn	< 1.000	1.415	< 1.000	5.342	9.999	2.045
MRC467	Sill	< 1.000	< 1.000	< 1.000	< 1.000	1.671	4.584
MRC471	Sill	< 1.000	< 1.000	< 1.000	< 1.000	< 1.000	2.677
MRC472	Ardglass-Ballycastle	< 1.000	1.823	< 1.000	3.761	4.804	3.775
MRC475	Ardglass-Ballycastle	< 1.000	< 1.000	< 1.000	1.417	1.799	< 1.000
MRC482	Ardglass-Ballycastle	< 1.000	< 1.000	< 1.000	2.472	3.177	2.113
MRC483	Erne	< 1.000	< 1.000	< 1.000	< 1.000	< 1.000	< 1.000
MRC496	Fleetwood	< 1.000	< 1.000	< 1.000	< 1.000	< 1.000	< 1.000
MRC507	Donegal-Kingscourt	< 1.000	< 1.000	< 1.000	3.664	1.821	1.665
MRC510	Killala	< 1.000	< 1.000	< 1.000	< 1.000	< 1.000	< 1.000

MRC513	Killala	< 1.000	< 1.000	< 1.000	1.972	2.097	< 1.000
MRC517	Donegal-Kingscourt	< 1.000	< 1.000	< 1.000	1.468	1.862	< 1.000
MRC521	Sill	< 1.000	< 1.000	< 1.000	1.567	1.090	3.911
MRC523	Plug	< 1.000	< 1.000	< 1.000	3.646	6.761	1.413
MRC558	Donegal-Kingscourt	< 1.000	< 1.000	< 1.000	3.161	2.106	< 1.000
MRC574	St. John's Point Lisburn	< 1.000	< 1.000	< 1.000	< 1.000	< 1.000	< 1.000
MRC607	Sill	< 1.000	< 1.000	< 1.000	< 1.000	< 1.000	< 1.000
MRC612	Plug	< 1.000	< 1.000	< 1.000	6.284	5.272	2.118
MRC613	Plug	< 1.000	< 1.000	< 1.000	4.383	6.895	1.592
22CCCI.35	Cone Sheet	< 1.000	< 1.000	< 1.000	< 1.000	< 1.000	< 1.000
22CCI.23	Cone Sheet	< 1.000	< 1.000	< 1.000	< 1.000	< 1.000	< 1.000
22CCI.6	Cone Sheet	< 1.000	< 1.000	< 1.000	< 1.000	< 1.000	< 1.000
24-D-05	Donegal-Kingscourt	< 1.000	< 1.000	< 1.000	10.405	8.198	2.042
MRC622	Fleetwood	1.040	2.337	< 1.000	6.815	7.258	2.103
MRC490	Ardglass-Ballycastle	< 1.000	< 1.000	< 1.000	1.070	< 1.000	< 1.000
MRC552	Donegal-Kingscourt	< 1.000	1.696	< 1.000	5.670	2.274	< 1.000
24-PM-01	West Connacht (IBF)	< 1.000	< 1.000	< 1.000	< 1.000	< 1.000	< 1.000
24-PM-02	West Connacht (IBF)	< 1.000	1.092	< 1.000	8.144	3.950	< 1.000
24-PM-04	West Connacht (CI)	< 1.000	< 1.000	< 1.000	2.887	1.142	< 1.000
24-PM-05	West Connacht (CM)	< 1.000	< 1.000	< 1.000	< 1.000	< 1.000	< 1.000
24-WIT-02	Dingle	< 1.000	< 1.000	< 1.000	1.009	< 1.000	2.075
24-WIT-04	Dingle	< 1.000	< 1.000	< 1.000	< 1.000	< 1.000	< 1.000

24-WIT-08	West Connacht (CM)	< 1.000	1.026	< 1.000	4.344	1.779	< 1.000
24-WIT-10	West Connacht (CI)	< 1.000	< 1.000	< 1.000	2.393	< 1.000	< 1.000
24-WIT-12	West Connacht (CI)	< 1.000	< 1.000	< 1.000	1.493	< 1.000	< 1.000
24-WIT-14	West Connacht (CI)	< 1.000	< 1.000	< 1.000	1.256	< 1.000	< 1.000
24-WIT-15	West Connacht (CI)	< 1.000	< 1.000	< 1.000	1.246	< 1.000	< 1.000
24-WIT-16	West Connacht (CI)	< 1.000	< 1.000	< 1.000	< 1.000	< 1.000	< 1.000
24-WIT-17	West Connacht (CI)	< 1.000	< 1.000	< 1.000	< 1.000	< 1.000	< 1.000
24-WIT-19	Killala	< 1.000	1.222	< 1.000	4.360	1.949	< 1.000
24-WIT-20	Killala	< 1.000	< 1.000	< 1.000	8.201	3.316	< 1.000
24-WIT-21	Killala	< 1.000	< 1.000	< 1.000	< 1.000	< 1.000	< 1.000
24-WIT-22	Killala	< 1.000	< 1.000	< 1.000	< 1.000	< 1.000	< 1.000
24-WIT-23	Killala	< 1.000	< 1.000	< 1.000	1.965	1.120	< 1.000
24-WIT-25	Killala	< 1.000	1.679	1.240	6.810	3.108	< 1.000
24-WIT-28	Killala	< 1.000	< 1.000	< 1.000	< 1.000	< 1.000	1.048
24-WIT-29	Killala	< 1.000	< 1.000	< 1.000	13.030	12.209	2.441
24-WIT-30c	Inver Dyke	< 1.000	< 1.000	< 1.000	3.038	6.304	< 1.000
24-WIT-32	Blind Dyke	< 1.000	1.456	< 1.000	6.850	9.048	1.870
ANT 9.75	Lower Basalt	0.48	0.93	0.35	4.30	3.25	2.86
ANT 35.55	Lower Basalt	0.64	1.05	0.32	4.63	2.54	0.65
ANT 54.20	Lower Basalt	0.50	1.00	0.26	3.28	2.65	4.18
ANT 61.40	Lower Basalt	0.45	0.74	0.20	2.48	1.79	2.79
ANT 70.05	Lower Basalt	0.46	0.83	0.21	2.92	1.20	1.98
ANT 80.00	Lower Basalt	0.48	0.89	0.20	2.42	1.54	1.49
ANT 89.90	Lower Basalt	0.48	0.69	0.25	4.11	2.27	1.03
ANT 101.70	Lower Basalt	0.22	0.39	0.15	2.24	1.34	0.93

NIRE-09/08-0001 (59)	Lower Basalt	0.03	0.22	0.08	0.65	0.25	1.92
NIRE-08/08-0002	Lower Basalt	0.19	0.86	0.73	4.72	2.92	3.27
NIRE-01/08-0003	Lower Basalt	0.35	0.84	0.51	3.43	1.33	8.68
NIRE-03/14-0001	Lower Basalt	0.09	0.24	0.28	2.02	1.20	4.45
NIRE-11/08-0001	Lower Basalt	1.38	1.70	0.62	11.72	8.73	4.50
NIRE-02/08-0001	Lower Basalt	0.07	1.26	0.22	2.44	2.28	3.28
NIRE-03/08-0003	Lower Basalt	0.85	1.75	0.44	2.54	2.20	1.11
NIRE-03/08-0002	Lower Basalt	0.63	1.23	0.40	2.92	1.96	1.76
NIRE-01/08-0005	Lower Basalt	0.10	0.96	0.25	2.50	1.04	2.78
NIRE-04/08-0002	Lower Basalt	0.24	2.13	0.32	3.51	1.82	1.54
NIRE-01/08-0002	Lower Basalt	0.24	0.40	0.27	3.73	0.74	5.58
NIRE-09/08-0001 (120)	Lower Basalt	0.12	0.18	0.40	3.09	1.19	25.95
NIRE-03/08-0001	Lower Basalt	0.34	1.21	0.46	4.90	2.92	3.38
MBC49	Lower Basalt	2.32	2.66	1.41	10.50	12.15	4.87
NIRE-05/08-0002	Lower Basalt	0.08	0.36	0.10	0.80	0.39	0.50
NIRE-04/08-0001	Lower Basalt	1.33	2.79	0.47	4.69	2.22	1.59
08/08-0001	Lower Basalt	0.09	1.02	0.23	1.99	2.31	2.47
Typical 1σ error (%)		0.32	9.01	5.46	4.25	5.56	7.11